symmetry

MDPI

Article

Business Management Improvement Enterprise Development Optimization Algorithm for Numerical Optimization and Its Application

Liyun Deng [1,*,†] and Antong Li [2,†]

[1] Faculty of Humanities and Social Sciences, Yanbian University, Yanji 133300, China
[2] Faculty of Business, Lingnan University, Hong Kong, China; liantong@ln-edu.hk
* Correspondence: dengliyun@ybu-edu.cn
† These authors contributed equally to this work.

Abstract

Complex optimization problems are widely encountered in engineering design, intelligent manufacturing, communication systems, and wireless sensor network deployment. However, the original Enterprise Development Optimization Algorithm (EDOA) still suffers from insufficient population diversity, weak search guidance, and limited adaptability in balancing exploration and exploitation when solving high-dimensional and multimodal optimization problems. To address these issues, this paper proposes a Multi-Strategy Improved Enterprise Development Optimization Algorithm (MIEDOA). First, a Strategic Diversification Initialization (SDI) strategy is developed by integrating Sobol sequence sampling, random initialization, and Gaussian perturbation to improve the diversity and distribution quality of the initial population. Second, an Organizational Synergy Learning (OSL) mechanism is introduced to enhance search guidance through the collaborative utilization of elite information, population mean information, and peer interaction. Third, an Adaptive Governance with Feedback Regulation (AGFR) strategy is designed to dynamically regulate the exploration–exploitation behavior according to the current population fitness state. The proposed MIEDOA is evaluated on the CEC2017 and CEC2020 benchmark suites and compared with representative EDOA variants, CEC winner algorithms, and other advanced optimization methods. The experimental results indicate that MIEDOA generally achieves competitive performance in terms of solution quality, convergence behavior, and robustness across different benchmark scenarios. In addition, strategy effectiveness analysis, parameter sensitivity analysis, and statistical tests further provide evidence supporting the effectiveness of the proposed strategies. Finally, MIEDOA is applied to a three-dimensional wireless sensor network deployment problem. The results suggest that the proposed algorithm can obtain competitive deployment solutions and satisfactory coverage performance under different node scales, demonstrating its potential applicability to practical engineering optimization problems.

Keywords: metaheuristic algorithms; enterprise development optimization algorithm; numerical optimization; wireless sensor network deployment

Check for updates

Academic Editor: Yirui Wang

Received: 10 May 2026
Revised: 1 June 2026
Accepted: 8 June 2026
Published: 23 June 2026

Copyright: © 2026 by the authors. Licensee MDPI, Basel, Switzerland. This article is an open access article distributed under the terms and conditions of the Creative Commons Attribution (CC BY) license.

1. Introduction

With the rapid advancement of science and technology, complex optimization problems have become increasingly prevalent across a wide range of domains, including engineering design [1], intelligent manufacturing [2], communication systems [3], energy

management [4], and data analytics [5]. These problems are often characterized by high dimensionality, strong nonlinearity, multimodality, and intricate constraints, leading to highly irregular and non-convex search spaces. Moreover, in many real-world scenarios, multiple conflicting objectives, dynamic environments, and uncertain parameters further increase the difficulty of obtaining optimal solutions. As problem scale and complexity continue to grow, traditional optimization methods based on gradient information or deterministic rules are often inadequate, as they typically rely on assumptions such as continuity, differentiability, and convexity, which are rarely satisfied in practical applications [6,7]. Consequently, these methods are prone to becoming trapped in local optima or suffering from excessive computational cost when dealing with large-scale and complex problems. Therefore, developing efficient, robust, and adaptive optimization algorithms capable of handling such challenges has become a critical research focus in modern computational intelligence and engineering optimization fields.

Meta-heuristic algorithms have garnered widespread attention due to their flexibility, simplicity, and powerful global search capabilities. Unlike traditional optimization methods, meta-heuristic algorithms do not rely on gradient information and are capable of obtaining satisfactory near-optimal solutions within limited computational resources [8,9]. In recent years, numerous representative algorithms have emerged and have been successfully applied in fields such as numerical optimization [10], engineering design [11], image processing [12], energy scheduling [13], path planning [14], and wireless sensor network deployment [15]. Typical examples include Particle Swarm Optimization (PSO) [16], Genetic Algorithm (GA) [17], Ant Colony Optimization (ACO) [18], the Grey Wolf Optimizer (GWO) [19], as well as emerging methods such as the Bounty Hunter Optimizer (BHO) [20], the Detective Behavior Algorithm (DBA) [21], and the Farthest Better or Nearest Worse Optimizer (FBNWO) [22]. Braik et al. proposed the Coriolis Force Tornado Optimizer (TOC), a metaheuristic algorithm designed for engineering design and industrial optimization problems [23]. The reported results indicate that TOC achieves competitive solution quality and global search performance compared with several existing optimizers. Experimental results demonstrate that this optimizer outperforms other competing optimizers in terms of both solution quality and global optimality. To address the problems of photovoltaic model parameter identification and the tuning of fractional-order proportional-integral-derivative controllers, Xiao et al. proposed a novel Artificial Lemming Algorithm inspired by biological mechanisms [24]. The research results demonstrate the competitive advantages and immense potential of the ALA in real-world engineering applications. These methods have demonstrated immense potential in addressing complex optimization tasks.

Despite possessing the aforementioned advantages, existing meta-heuristic algorithms still face several common challenges. First, the quality of the initial population directly impacts search efficiency and ultimate optimization accuracy. A randomly generated population may result in an uneven distribution of individuals within the search space, thereby undermining global exploration capabilities. Second, many algorithms suffer from insufficient search guidance during the iterative process. Although random perturbations and population collaboration help enhance diversity, they often lack clear directional guidance, consequently leading to slow convergence speeds. Third, maintaining a balance between exploration and exploitation remains a major challenge. Excessive exploration may reduce convergence efficiency, while excessive exploitation is prone to triggering premature convergence, causing the algorithm to become trapped in local optima. Therefore, many studies have focused on improving existing metaheuristic algorithms by modifying their search mechanisms, adaptive control strategies, or population update rules to better address specific optimization problems and improve overall performance.

For instance, Yu et al. developed a device-agnostic energy estimation model based on multimodal energy-consumption factors to evaluate the computational energy cost of optimization algorithms [25]. This model was incorporated into GA, DE, and PSO for three-dimensional UAV path planning, providing a basis for carbon-aware algorithm evaluation and computational resource allocation. Experimental results demonstrate that, following the adoption of optimization algorithms that account for CFER, CO_2 emissions were reduced by 45.91%, 28.28%, and 59.14%, respectively. This contributes to facilitating carbon-aware evaluation and algorithm selection, as well as the adaptive allocation of computational budgets within green artificial intelligence systems. To address the problem of 3D drone path planning, Xie et al. proposed a multi-strategy improved RIME optimization algorithm [26]. By incorporating piecewise mapping, an elite pool exploration strategy, and sine-cosine functions, the algorithm's performance was significantly enhanced. Experiments conducted across three distinct scenarios demonstrated that the improved algorithm achieved a performance increase of approximately 30% compared to the original algorithm. In the field of wireless sensor deployment, Lu et al. proposed an improved Secretary bird Optimization Algorithm by integrating a Gaussian Cuckoo mutation mechanism and a smooth exploitation strategy [27]. The proposed algorithm demonstrates faster convergence speeds and higher accuracy across 23 benchmark functions as well as a newly designed wireless sensor deployment problem, achieving significant results.

The Enterprise Development Optimization Algorithm (EDOA) is a recently proposed population-based metaheuristic algorithm inspired by the actual development processes of enterprises [28]. This algorithm simulates the evolutionary process of candidate solutions through four key enterprise activities: tasks, structure, technology, and personnel. Each of these activities corresponds to a distinct optimization behavior, collectively establishing a fundamental framework for exploration and exploitation within EDOA. However, the original EDOA still exhibits certain limitations, which has prompted numerous researchers to undertake improvements aimed at enhancing its performance.

Therefore, Zhao et al. proposed LMEDO to improve the performance of EDOA in terms of premature convergence and the balance between exploration and exploitation [29]. LMEDO introduces a time-phase switching strategy, an economy-driven guided learning mechanism, and a spatial-selectivity-based screening strategy. Its effectiveness was validated through engineering design optimization problems. Cai et al. proposed MSEDO, a multi-strategy variant of EDOA, to improve population diversity and exploration capability [30]. By incorporating multiple search strategies into the EDOA framework, MSEDO enhances the algorithm's ability to solve constrained engineering optimization problems. To estimate photovoltaic model parameters, Li et al. proposed a multi-strategy enhanced Enterprise Evolution Optimization Algorithm (MEED), which integrates a hybrid initialization strategy combining chaotic mapping and adversarial learning, a parameter update mechanism based on historical trends, and a mirror-reflection boundary control strategy. Simulation results demonstrate that MEED provides an efficient and reliable optimization framework for the estimation of photovoltaic model parameters, as well as for other complex engineering optimization problems [31].

Although LMEDO, MSEDO, MEED, and the proposed MIEDOA all aim to improve the optimization performance of EDOA, their mathematical designs and modified components are different. LMEDO mainly improves EDOA through time-phase switching and guided learning, MSEDO focuses on multi-strategy fusion to enhance population diversity and search capability, and MEED emphasizes historical-trend-based parameter updating and boundary control. In contrast, MIEDOA reconstructs three specific components of the original EDOA framework: population initialization, structure activity, and activity switching mechanism.

Specifically, the proposed SDI strategy is not merely a random initialization enhancement, but a hybrid initialization model that explicitly combines low-discrepancy global coverage, stochastic sampling, and local Gaussian perturbation to simultaneously improve uniformity and diversity. The OSL mechanism replaces the simple averaging operation in the original structure activity with a three-source collaborative learning model composed of elite guidance, population-level mean information, and peer interaction. Different from PSO-like velocity learning, OSL does not introduce an accumulated velocity term or personal historical best memory; instead, it directly reconstructs the structural cooperation behavior of EDOA in the solution space. Furthermore, AGFR differs from conventional time-dependent switching mechanisms by using the real-time fitness gap between the population average and the best individual to regulate the probability of exploration and exploitation. Therefore, the search behavior of MIEDOA is determined by the current population state rather than only by the iteration index.

Accordingly, the mathematical novelty of MIEDOA lies in the coordinated reconstruction of EDOA's key operational components: SDI improves the initial enterprise resource allocation, OSL redesigns organizational cooperation from single averaging to multi-source synergy, and AGFR changes the activity control mechanism from time-driven switching to feedback-driven adaptive governance. These mechanisms are embedded into the intrinsic activity structure of EDOA, rather than being independently stacked as generic operators.

Based on the above research, this paper proposes a Multi-Strategy Improved Enterprise Development Optimization Algorithm (MIEDOA). Unlike simple strategy stacking, the proposed algorithm reconstructs the original EDOA from the perspective of enterprise management mechanisms. Specifically, three complementary strategies are introduced. First, a Strategic Diversification Initialization (SDI) strategy is designed by combining Sobol sequence sampling, random initialization, and Gaussian perturbation to improve the distribution quality and diversity of the initial population. Second, an Organizational Synergy Learning (OSL) mechanism is developed to replace the simple averaging strategy of the original structure activity. By integrating elite guidance, population mean information, and peer learning, OSL enhances search directionality while maintaining population diversity. Third, an Adaptive Governance with Feedback Regulation (AGFR) strategy is proposed to dynamically adjust the exploration–exploitation behavior according to population fitness feedback, enabling the algorithm to adapt to different search states more effectively. Table 1 presents a comparison between the proposed MIEDOA and other EDOA variants.

Table 1. Comparison between EDOA Variants.

Algorithm	Initialization	Structure Learning	Search Regulation	Main Characteristic
EDOA	Random initialization	Mean averaging	Iteration-dependent switching	Original framework
LMEDO	Original	Economy-driven learning	Time-phase switching	Phase-based search
MSEDO	Multi-strategy initialization	Multi-strategy fusion	Fixed strategy cooperation	Diversity enhancement
MEED	Chaotic-opposition initialization	Historical-trend updating	Historical adaptation	Trend-guided evolution
MIEDOA	SDI	OSL	AGFR	Framework-level reconstruction

Compared with existing EDOA variants, the advantage of MIEDOA does not rely on introducing more search operators. Instead, MIEDOA simultaneously reconstructs three key components of the original EDOA framework, including initialization, structure activity, and activity switching control. LMEDO mainly improves the search process

through time-phase switching, MSEDO focuses on strategy fusion, and MEED emphasizes historical-trend adaptation. In contrast, MIEDOA establishes a coordinated interaction among SDI, OSL, and AGFR, enabling population diversity enhancement, directional learning, and exploration–exploitation regulation to be performed within a unified framework. This coordinated design contributes to improved convergence accuracy, robustness, and stability, as demonstrated by the experimental results on the CEC2017 and CEC2020 benchmark suites.

To comprehensively evaluate the performance of MIEDOA, this paper conducts numerical optimization experiments on the CEC2017 and CEC2020 benchmark suites. These benchmark functions include unimodal, multimodal, hybrid, and composite functions, which can effectively test the global exploration ability, local exploitation ability, convergence accuracy, and robustness of optimization algorithms. MIEDOA is compared with eleven advanced algorithms, including INFO, RUN, GRO, ESC, RIME, GKSO, RTH, FTO, BBO, IGWO, and the original EDOA. The experimental results are analyzed from multiple perspectives, including convergence curves, boxplot distributions, mean and standard deviation values, strategy effectiveness analysis, and statistical tests. The results show that MIEDOA achieves competitive or superior performance on most benchmark functions, demonstrating better convergence speed, optimization accuracy, and stability.

Furthermore, to verify the practical applicability of the proposed algorithm, MIEDOA is applied to the three-dimensional wireless sensor network deployment problem. Compared with two-dimensional deployment scenarios, 3D WSN deployment is more complex because sensor nodes must be reasonably distributed in a volumetric space to maximize coverage while reducing redundant deployment and coverage holes. In this study, a 3D deployment model is established, and experiments are conducted under different node scales. The experimental results demonstrate that MIEDOA can generate more uniform node distributions, achieve higher coverage quality, and maintain stable convergence performance. This further confirms the effectiveness and engineering potential of the proposed algorithm in solving practical deployment optimization problems.

The main contributions of this paper are summarized as follows:

(1) A Multi-Strategy Improved Enterprise Development Optimization Algorithm, named MIEDOA, is proposed to address the limitations of the original EDOA in population diversity, search guidance, and dynamic search regulation.
(2) A Strategic Diversification Initialization strategy is designed to improve the quality and spatial distribution of the initial population, thereby enhancing global exploration capability.
(3) An Organizational Synergy Learning mechanism is introduced to strengthen collaborative learning among individuals by combining elite guidance, population-level information, and peer interaction, which improves search directionality and convergence efficiency.
(4) An Adaptive Governance with Feedback Regulation strategy is developed to dynamically balance exploration and exploitation according to real-time fitness feedback, improving the adaptability and robustness of the algorithm.
(5) Extensive experiments on CEC2017 and CEC2020 benchmark functions, together with strategy effectiveness analysis and statistical tests, are conducted to verify the superiority of MIEDOA.
(6) The proposed algorithm is further applied to the 3D wireless sensor network deployment problem, demonstrating its strong applicability and effectiveness in practical engineering optimization scenarios.

The remainder of this paper is organized as follows. Section 2 introduces the original EDOA and presents the proposed MIEDOA in detail, including the three improvement

strategies and computational complexity analysis. Section 3 reports the numerical optimization experiments on the CEC2017 and CEC2020 benchmark suites. Section 4 applies MIEDOA to the 3D wireless sensor network deployment problem and analyzes the experimental results. Finally, Section 5 concludes the paper and discusses future research directions.

2. Multi-Strategy Improved Enterprise Development Optimization Algorithm

2.1. Original Enterprise Development Optimization Algorithm

The Enterprise Development Optimization Algorithm (EDOA) is a population-based metaheuristic inspired by the dynamic development process of enterprises. Unlike traditional swarm intelligence algorithms that are typically derived from natural behaviors, EDOA models the evolution of candidate solutions through four core enterprise activities, namely task, structure, technology, and people. These activities correspond to different optimization behaviors and collaboratively drive the search process.

In EDOA, each individual represents a potential solution, and the optimization process simulates the iterative evolution of enterprises under different operational mechanisms. The algorithm alternates among the four activities through a dynamic switching mechanism, thereby achieving a balance between global exploration and local exploitation.

2.1.1. Population Initialization

At the initial stage, EDOA randomly generates a population within the predefined search space:

$$x_i(0) = l + \text{rand}(0,1)\cdot(u - l) \tag{1}$$

where $x_i(0)$ denotes the initial position of the i-th individual, l and u represent the lower and upper bounds, respectively. This uniform initialization ensures that the population is well distributed across the search space, providing sufficient diversity for subsequent exploration.

2.1.2. Task Activity: Random Exploration Mechanism

The task activity simulates routine operational adjustments within an enterprise. In the optimization process, it mainly acts as a global exploration operator, which introduces new candidate solutions by randomly perturbing or reinitializing certain dimensions:

$$x_{new,n}(t) = l_n + \text{rand}(0,1)\cdot(u_n - l_n) \tag{2}$$

This mechanism increases population diversity and helps the algorithm escape from local optima. However, since it is largely random, it may lack effective search guidance in later stages.

2.1.3. Structure Activity: Population Cooperation Mechanism

The structure activity reflects the reorganization of enterprise structures. In EDOA, this behavior is modeled by allowing individuals to learn from a subset of randomly selected individuals, thereby forming a cooperative search pattern:

$$x_i^k(t-1) = \frac{1}{m}\sum_{j=1}^{m} x_{rand_j}(t-1) \tag{3}$$

$$x_i(t) = \frac{x_i(t-1) + x_i^k(t-1)}{2} \tag{4}$$

where $x_i^k(t-1)$ represents the structural center of selected individuals, and m denotes the number of individuals involved in the interaction. This operation enhances information

sharing within the population and guides individuals toward more promising regions. Nevertheless, the simple averaging strategy may weaken directional exploitation ability.

2.1.4. Structure Activity: Guided by the Global Best Solution

The technology activity models innovation and knowledge accumulation in enterprises. In this stage, individuals are guided by the global best solution, which acts as a knowledge leader:

$$\begin{aligned} x_{new}(t) = x_{best}(t-1) + k(x_{best}(t-1) - x_i(t-1)) \\ +\text{rand}(0,1)(x_{best}(t-1) - x_i(t-1)) \end{aligned} \tag{5}$$

where $x_{best}(t-1)$ denotes the current global best solution, and k is a control parameter. This mechanism strengthens local exploitation by directing individuals toward high-quality regions. However, excessive reliance on the global best may lead to premature convergence.

2.1.5. People Activity: Local Adjustment Mechanism

The people activity simulates collaboration and experience sharing among individuals. It focuses on refining solutions through localized interactions:

$$x_i^a(t-1) = \frac{1}{m}\sum_{j=1}^{m} x_{rand_j}(t-1) \tag{6}$$

$$d = \lfloor \text{rand}(0,1) \cdot n \rfloor + 1 \tag{7}$$

where d represents a randomly selected dimension. This mechanism allows partial updates of solutions, improving local search capability and maintaining flexibility in different dimensions.

2.1.6. Activity Switching Mechanism

To coordinate the four activities, EDOA introduces a dynamic switching mechanism controlled by:

$$c(t) = 3\left(1 - \frac{\text{rand}(0,1) \cdot t}{Max_{iter}}\right) \tag{8}$$

where t is the current iteration number and Max_{iter} is the maximum number of iterations. As the iteration progresses, the value of $c(t)$ gradually decreases, enabling the algorithm to transition from exploration-dominated behavior (task and structure activities) to exploitation-oriented behavior (technology and people activities).

This switching mechanism is critical for maintaining the balance between diversification and intensification throughout the optimization process.

2.1.7. Overall Characteristics of EDOA

From the perspective of search behavior, the four activities in EDOA can be summarized as:

(1) Task activity: strong exploration but weak guidance.
(2) Structure activity: cooperative search with limited directionality.
(3) Technology activity: strong exploitation guided by elite solutions.
(4) People activity: local refinement and adaptive adjustment.

Through the dynamic coordination of these components, EDOA achieves a certain balance between exploration and exploitation. However, due to the limitations of each mechanism (e.g., randomness, weak guidance, and over-reliance on the global best), there is still room for further improvement, which motivates the development of the proposed multi-strategy enhanced algorithm in the next section.

2.2. Multi-Strategy Improved Enterprise Development Optimization Algorithm (MIEDOA)

To address the limitations of the original EDOA, a Multi-Strategy Improved Enterprise Development Optimization Algorithm (MIEDOA) is proposed. Unlike conventional approaches that simply combine multiple strategies, this study performs a mechanism-level reconstruction inspired by enterprise management principles, where each strategy corresponds to a key managerial process. Specifically, three complementary strategies are introduced, namely strategic diversification, organizational synergy, and adaptive governance, to enhance exploration capability, decision quality, and dynamic control, respectively.

2.2.1. Strategic Diversification Initialization (SDI)

In enterprise management, diversified investment is widely adopted to mitigate risks and enhance system robustness. Inspired by this concept, a Strategic Diversification Initialization (SDI) strategy is proposed to improve the quality and distribution of the initial population. The initial population is generated using a hybrid diversification model:

$$X = \alpha X_{sobol} + (1-\alpha)X_{rand} + \beta \cdot \mathcal{N}(0,1) \tag{9}$$

where X_{sobol} denotes a low-discrepancy sequence, X_{rand} represents a uniformly distributed random population, and $\mathcal{N}(0,1)$ is the Gaussian perturbation. The parameters α and β control the balance between structured exploration and stochastic diversity. This strategy enhances the uniformity and diversity of the initial population, thereby providing a stronger foundation for subsequent optimization and improving global exploration capability. Figure 1 illustrates a schematic diagram of this strategy.

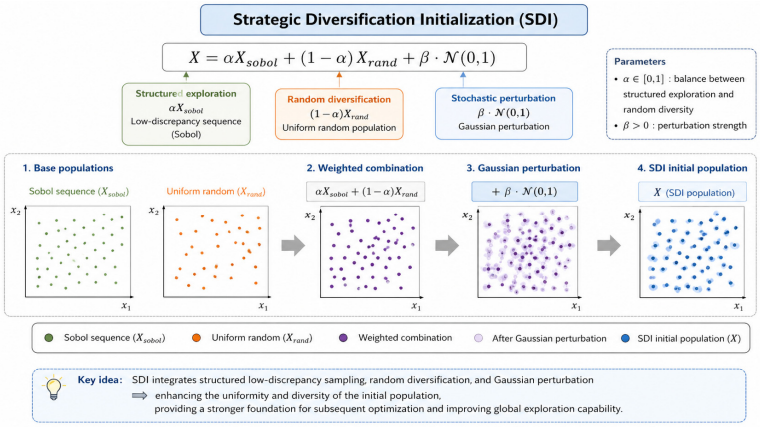


Figure 1. Schematic diagram of the strategic diversification initialization strategy.

2.2.2. Organizational Synergy Learning (OSL)

In modern enterprises, decision-making is often achieved through multi-level collaboration among executives, teams, and peers. To simulate this process, an Organizational Synergy Learning (OSL) mechanism is proposed to replace the simple averaging strategy in the original structure activity. The update rule is formulated as:

$$X_i^{new} = X_i + \lambda_1(X_{best} - X_i) + \lambda_2(X_{mean} - X_i) + \lambda_3(X_{peer} - X_i) \tag{10}$$

where X_{best} represents the global best solution, X_{mean} denotes the population mean, and X_{peer} is a randomly selected individual. The coefficients λ_1, λ_2, λ_3 are adaptive weights satisfying:

$$\lambda_1 + \lambda_2 + \lambda_3 = 1, \lambda_k \in [0,1] \tag{11}$$

where $\lambda_1(t) = 0.6\frac{t}{T} + 0.3\left(1 - \frac{t}{T}\right), \lambda_2(t) = 0.3, \lambda_3 = 1 - \lambda_1(t) - \lambda_2(t)$. This mechanism integrates elite guidance, collective intelligence, and peer learning, thereby enhancing search directionality and improving convergence efficiency while maintaining population diversity. Figure 2 illustrates a schematic diagram of this strategy.

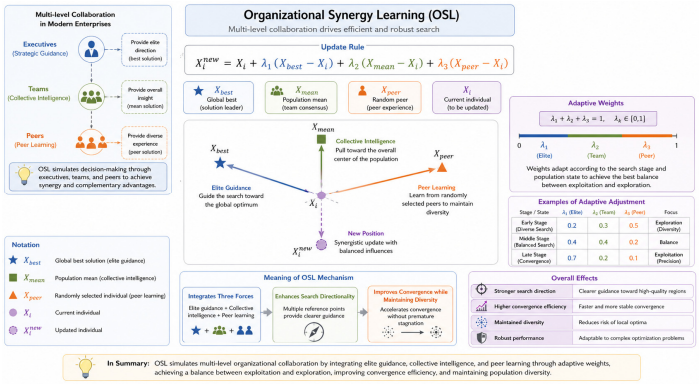


Figure 2. Schematic diagram of the organizational synergy learning.

2.2.3. Adaptive Governance with Feedback Regulation (AGFR)

In real-world enterprises, governance systems are not static; instead, they dynamically adjust decision-making intensity based on performance feedback. Inspired by this principle, an Adaptive Governance with Feedback Regulation (AGFR) strategy is proposed to replace the original activity switching mechanism.

Unlike traditional time-dependent control, this strategy introduces a fitness-feedback-driven regulation mechanism, defined as:

$$\delta(t) = \frac{f_{avg}(t) - f_{best}(t)}{\left|f_{avg}(t)\right|} \tag{12}$$

where $f_{avg}(t)$ and $f_{best}(t)$ denote the average and best fitness values of the population at iteration t respectively.

Based on $\delta(t)$, the exploration–exploitation balance is adaptively adjusted:

$$\omega(t) = \omega_{min} + (\omega_{max} - \omega_{min}) \cdot e^{-\eta \cdot \delta(t)} \tag{13}$$

where η is a sensitivity parameter. The update behavior is then governed as:

$$X_i(t+1) = \begin{cases} \text{Exploration strategy, if} rand < \omega(t) \\ \text{Exploitation strategy, otherwise} \end{cases} \tag{14}$$

Mechanism interpretation: It should be noted that $\delta(t)$ is not a direct population diversity measure. Instead, it represents a fitness-gap indicator that characterizes the relative difference between the population average fitness and the current best fitness. A large value of $\delta(t)$ indicates that the population is still widely distributed in the fitness space and that considerable performance differences exist among individuals. In contrast, a small value of $\delta(t)$ suggests that the population fitness values have become similar, implying a more converged search state. Accordingly, the adaptive governance factor $\omega(t)$ is designed as a fitness-feedback-driven regulation mechanism rather than a diversity-based control strategy. When $\delta(t)$ is large, the population still contains substantial fitness variation, and the algorithm gradually reduces the exploration probability in order to strengthen the utilization of promising search directions. Conversely, when $\delta(t)$ becomes small, the population approaches a converged state, and the regulation mechanism maintains a

relatively higher exploration probability to alleviate premature convergence and improve the chance of escaping local optima. Figure 3 illustrates a schematic diagram of this strategy.

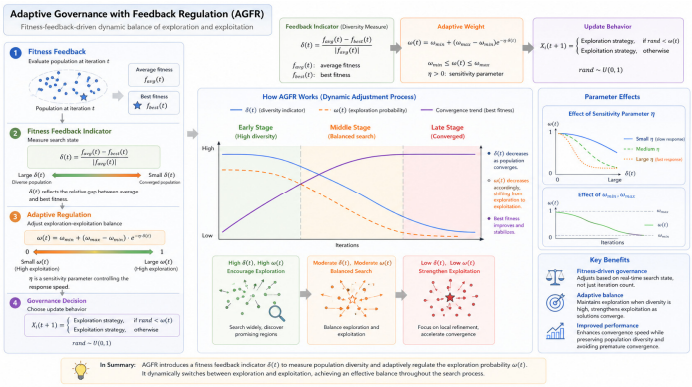


Figure 3. Schematic Diagram of the adaptive governance with feedback regulation.

2.2.4. Integrated Framework of MIEDOA

By integrating the above strategies, the proposed MIEDOA reconstructs the original EDOA framework into a more efficient and adaptive optimization system: SDI enhances the initial population distribution and exploration capability; OSL improves interaction quality and directional guidance; AGFR dynamically regulates the search process through feedback.

From a business management perspective, the optimization process can be interpreted as: "diversified resource allocation to collaborative decision-making to feedback-driven governance regulation".

Through this mechanism-level reconstruction, MIEDOA achieves a more effective balance between exploration and exploitation, resulting in improved convergence speed, solution accuracy, and robustness in complex optimization problems. The overall procedure of the proposed MIEDOA is summarized in Algorithm 1. First, the SDI strategy is employed to generate a diversified initial population. Then, AGFR dynamically controls the search behavior according to the population fitness feedback. During the iterative process, the OSL mechanism is used to enhance collaborative learning among individuals, while the original technology and people activities are retained for local refinement. Finally, a greedy selection strategy is adopted to preserve superior solutions. The pseudocode of the MIEDOA is outlined in Algorithm 1. Figure 4 illustrates the execution flowchart of MIEDOA. Table 2 illustrates the differences between MIEDOA and existing variants of EDOA.

Table 2. Feature-by-feature comparison between MIEDOA and existing EDOA variants.

Algorithm	Main Modified Component	Core Mechanism	Control Basis	Difference from MIEDOA
LMEDO	Search phase and guided learning	Time-phase switching, economy-driven learning, spatial screening	Iteration stage and search phase	Mainly relies on predefined phase division, while MIEDOA uses real-time fitness feedback to regulate search behavior.
MSEDO	Multiple search operators	Multi-strategy fusion for diversity and exploitation	Strategy combination	Focuses on combining several enhancement operators, while MIEDOA reconstructs specific EDOA components including initialization, structure activity, and switching control.
MEED	Parameter updating and boundary handling	Historical-trend-based updating and mirror-reflection boundary control	Historical information and boundary state	Emphasizes historical evolution and boundary correction, while MIEDOA focuses on population-state feedback and organizational synergy learning.
MIEDOA	Initialization, structure activity, and activity switching	SDI, OSL, and AGFR	Population distribution, elite–mean–peer synergy, and real-time fitness gap	Reconstructs the original EDOA framework from three corresponding enterprise-management mechanisms rather than simply adding external operators.

Algorithm 1: The pseudo-code of the MIEDOA

Input: Population size N, maximum iterations T, dimension D, lower bound lb, upper bound ub, objective function $f(\cdot)$.
Output: Best solution X_{best} and best fitness f_{best}

Initialize parameters $\alpha,\ \beta,\ \eta,\ \omega_{min},\ \omega_{max}$
Generate Sobol population X_{sobol}
Generate random population X_{rand}
Generate initial population by $X = \alpha X_{sobol} + (1-\alpha)X_{rand} + \beta \cdot \mathcal{N}(0,1)$
Apply boundary control to X_i
Calculate fitness value f_{X_i} for each individual
Determine the current best solution X_{best} and f_{best}
for $t = 1$ *to* T do
    Calculate the population mean solution X_{mean}
    Calculate the average fitness $f_{avg(t)}$
    Compute the feedback indicator $\delta(t)$
    Compute the adaptive governance factor $\omega(t)$
    for $i = 1$ *to* N do
        if $rand < \omega(t)$ then
            Randomly select dimension d
            Taskexploration
            $X_{i,d} = lb_d + rand(ub_d - lb_d)$
        else
            Randomly select X_{peer}
            Organizational Synergy Learning
            Generate adaptive weights $\lambda_1,\ \lambda_2,\ \lambda_3$
            $X_{i,new} = X_i + \lambda_1(X_{best} - X_i) + \lambda_2(X_{mean} - X_i) + \lambda_3(X_{peer} - X_i)$
        end if
        Technology/people refinement
        if $rand < 0.5$ then
            Update $X_{i,new}$ by $X_{i,new} = X_{best} + k(X_{best} - X_i) + rand(X_{best} - X_i)$
        else
            Randomly select m individuals
            Compute their average position X_a
            Randomly select dimension d
            People activity by $X_{i,new}(d) = X_a(d)$
        end if
        Apply boundary control by $X_{i,new} = \min(\max(X_{i,new}, lb), ub)$
        Calculate fitness $f(X_{i,new})$
        if $f(X_{i,new}) < f(X_i)$ then
            $X_i = X_{i,new}$
            $f(X_i) = f(X_{i,new})$
        end if
        if $f(X_i) < f_{best}$ then
            $X_{best} = X_i$
            $f_{best} = f(X_i)$
        end if
    end for
    Record f_{best} at iteration t
end for
return X_{best} and f_{best}

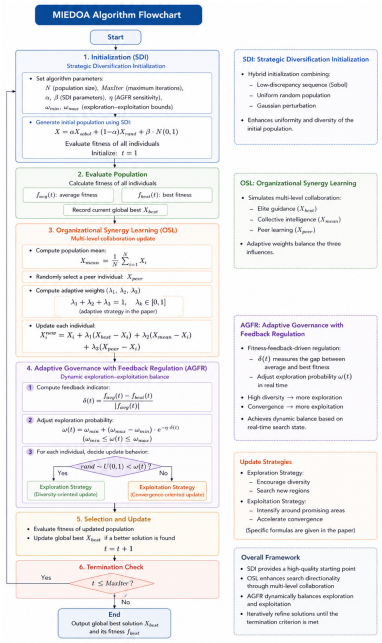


Figure 4. MIEDOA Execution Flowchart.

2.3. Computational Complexity Analysis of MIEDOA

The computational complexity of the proposed MIEDOA is analyzed in terms of the population size N, problem dimension D, and maximum number of iterations T. In the initialization stage, the Strategic Diversification Initialization (SDI) strategy generates the initial population through the combination of low-discrepancy sequences, random sampling, and Gaussian perturbation, resulting in a computational cost of $O(N{\cdot}D)$.

During the iterative optimization process, the main computational cost arises from fitness evaluation and position updating. Specifically, the evaluation of the objective function for all individuals incurs a cost of $O(N{\cdot}C_f)$, where C_f denotes the complexity of the fitness function. In addition, the Organizational Synergy Learning (OSL) mechanism requires the computation of the population mean and individual updates, which together contribute to the complexity of $O(N{\cdot}D)$ per iteration. The exploration and exploitation operations, including task-based random search, technology-driven updates, and people-based refinements, also involve vector operations with a total cost of $O(N{\cdot}D)$.

The Adaptive Governance with Feedback Regulation (AGFR) strategy introduces additional computations, including the calculation of average fitness and feedback indicators. However, these operations only require $O(N)$ time and therefore have a negligible impact on the overall complexity.

Combining all the above components, the total computational complexity of MIEDOA can be expressed as $O(T{\cdot}N{\cdot}(D + C_f))$. In most practical optimization problems, the fitness evaluation cost C_f dominates, and thus the overall complexity can be approximated as $O(T{\cdot}N{\cdot}C_f)$.

Overall, although MIEDOA introduces several additional strategies, these improvements only incur linear computational overhead and do not change the order of time complexity compared with the original EDOA and other classical population-based metaheuristic algorithms. Therefore, the proposed algorithm maintains computational efficiency while achieving enhanced optimization performance.

Table 3 presents a comparison of the average running times of MIEDOA and the original EDOA across various test sets; the experimental results are shown below.

Table 3 presents the average runtime comparison between the original EDOA and the proposed MIEDOA on different benchmark suites and dimensional settings. As can be

observed, MIEDOA requires slightly more computational time than EDOA across all test scenarios. This increase is mainly attributed to the additional computations introduced by the SDI, OSL, and AGFR mechanisms, including population-state feedback evaluation, collaborative learning operations, and diversified initialization.

Nevertheless, the increase in runtime remains relatively moderate in absolute terms. For example, under the CEC2017 benchmark suite, the additional runtime ranges from approximately 0.82 s to 2.53 s as the problem dimension increases from 30 to 100. Similarly, for the CEC2020 benchmark suite, the additional computational cost is less than 0.5 s in both dimensional settings. Considering that the proposed strategies substantially improve convergence behavior, solution quality, and robustness, the additional computational overhead can be regarded as acceptable. Furthermore, the overall computational complexity of MIEDOA remains in the same order as that of the original EDOA, indicating that the enhanced optimization performance is achieved without a significant sacrifice in computational efficiency.

Table 3. Runtime Comparison.

Algorithm/Test Set	**CEC2017**			**CEC2020**	
Dimension	30	50	100	10	20
EDOA	4.28	8.86	37.74	0.69	1.00
MIEDOA	5.10	10.22	40.27	0.95	1.46

3. Numerical Optimization Experiments and Detailed Analysis

In this section, to evaluate the performance of MIEDOA, we conducted numerical optimization experiments utilizing 40 test functions drawn from the CEC2017 and CEC2020 test suites. First, we provide a brief introduction to these two test suites; second, to enhance the reproducibility of our experiments, we present a detailed description of the comparative algorithms and their parameter settings. Subsequently, we conduct a comprehensive analysis of MIEDOA's performance across both test suites. Finally, to determine whether MIEDOA exhibits statistically significant differences compared to the other comparative algorithms, we perform a statistical analysis. The specific details are as follows.

3.1. Standard Benchmark Functions for Numerical Optimization

In the fields of numerical optimization and intelligent computation, the CEC2017 [32] and CEC2020 [33]. Benchmark Suites—released by the IEEE CEC (Congress on Evolutionary Computation) competition platform—serve as authoritative standard test sets that have been widely adopted for the performance evaluation and comparative analysis of various heuristic optimization algorithms. The CEC2017 test suite typically comprises diverse function types, including unimodal, multimodal, hybrid, and composite functions. These functions exhibit distinct characteristics regarding separability, rotatability, scale variation, and the distribution of local optima, thereby enabling a systematic assessment of an algorithm's global exploration and local exploitation capabilities across a variety of search environments. Building upon this foundation, the CEC2020 test suite further elevates problem complexity; by introducing stronger variable coupling, higher-dimensional nonlinear structures, and more intricate composition mechanisms, it renders the test functions more representative of real-world engineering optimization problems, thereby imposing more rigorous demands on an algorithm's robustness, convergence accuracy, and stability.

Owing to their high degree of standardization, strong reproducibility, and excellent fairness in comparative analysis, the CEC series of test sets have emerged as the mainstream benchmarking tools for evaluating the performance of heuristic algorithms, and are widely

utilized to validate the effectiveness and advanced nature of novel algorithms. Consequently, this paper selects the CEC2017 and CEC2020 test sets as the experimental platform to conduct a comprehensive evaluation of the proposed MIEDOA. Through a comparative analysis against various state-of-the-art optimization algorithms, the study verifies the algorithm's superior performance in addressing complex optimization problems across multiple dimensions, including convergence speed, solution accuracy, and result stability.

3.2. Competitor Algorithms and Parameter Setting

In this section, the performance of MIEDOA is comprehensively evaluated through comparisons with 11 state-of-the-art optimization algorithms, aiming to demonstrate its effectiveness and robustness. The algorithms used for comparison include weighted mean of vectors (INFO), Runge Kutta optimizer (RUN), Gold Rush Optimizer (GRO), Escape algorithm (ESC), rime optimization algorithm (RIME), Genghis Khan shark optimizer (GKSO), Red-tailed hawk algorithm (RTH), Fourier transform optimizer (FTO), Beaver behavior optimizer (BBO), Improved grey wolf optimizer (IGWO), and Enterprise Development Optimization Algorithm (EDOA). The parameter configurations of all compared algorithms are summarized in Table 4 for clarity and reproducibility.

Table 4. Parameter Settings for the Compared Algorithms.

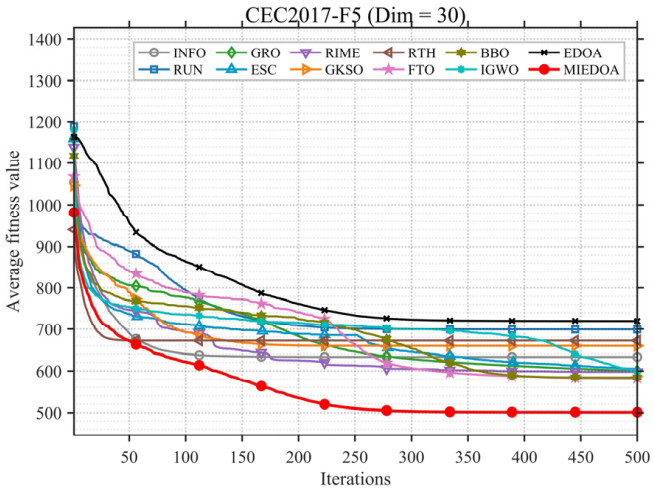
Algorithms	Parameter Name	Parameter Value	Population Size	Number of Iterations	Reference
INFO	e	1×10^{-25}	50	500	[34]
RUN	u	0.5	50	500	[35]
GRO	$sigma_initial$	2	50	500	[36]
ESC	a, b	0.15, 0.35	50	500	[37]
RIME	w	2	50	500	[38]
GKSO	h	0.1	50	500	[39]
RTH	A, r_0, r	15, 0.5, 1.5	50	500	[40]
FTO	$beta,\ alpha$	1.5, 0.1	50	500	[41]
BBO	v	0.25	50	500	[42]
IGWO	w	2	50	500	[43]
EDOA	--	--	50	500	[28]

3.3. Comparison of the CEC2017 Test Functions

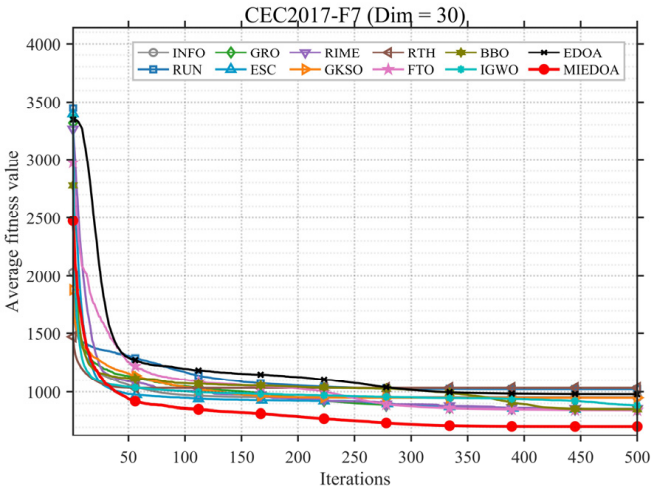
To evaluate the effectiveness of the proposed MIEDOA, we conducted extensive numerical experiments on the CEC2017 benchmark test suite. Based on the mean and standard deviation obtained from 30 independent runs, we compared the performance of MIEDOA against 11 state-of-the-art algorithms. To further assess the convergence characteristics of the algorithms, Figure 5 illustrates the convergence curves of MIEDOA and the comparison algorithms for selected test functions under two different dimensional settings. Furthermore, Figure 6 presents box plots depicting the distribution of results from the 30 independent runs, thereby providing a more comprehensive assessment of the stability and robustness of each algorithm. Additionally, Tables 5–7 summarize the detailed performance results of all 12 algorithms on the CEC2017 benchmark functions across three different dimensional settings. In these tables, "Mean" represents the average fitness value obtained from the 30 runs, while "Std" denotes the corresponding standard deviation, serving as an indicator of the algorithm's stability.

Figure 5 presents the convergence curves of the compared algorithms on the CEC2017 benchmark functions. It can be observed that MIEDOA generally exhibits a relatively fast convergence trend during the early search stages and maintains stable optimization behavior throughout the iterative process on many test functions. On several complex multimodal and hybrid functions, MIEDOA often reaches lower fitness values than some comparative algorithms, suggesting its capability to effectively utilize promising search

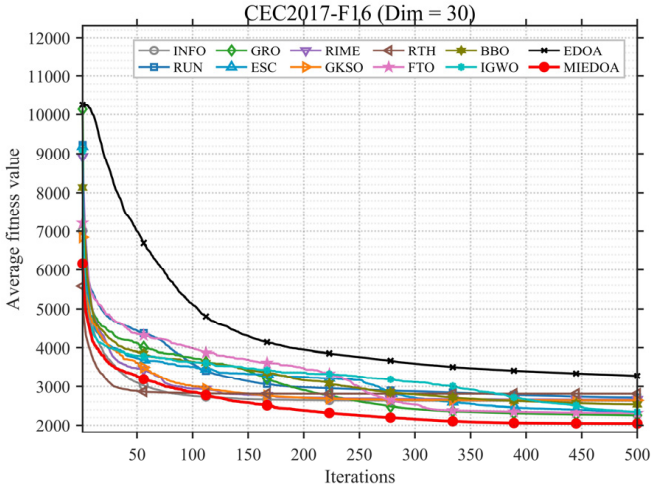
regions while maintaining search diversity. Although the performance differences vary across different benchmark functions, the overall convergence results indicate that MIEDOA provides competitive optimization performance and satisfactory search stability on the CEC2017 benchmark suite.



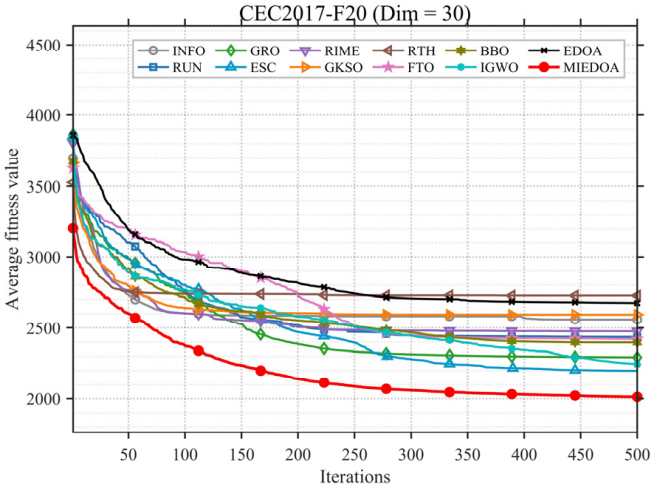
(**a**) CEC2017-F5 (Dim = 30)



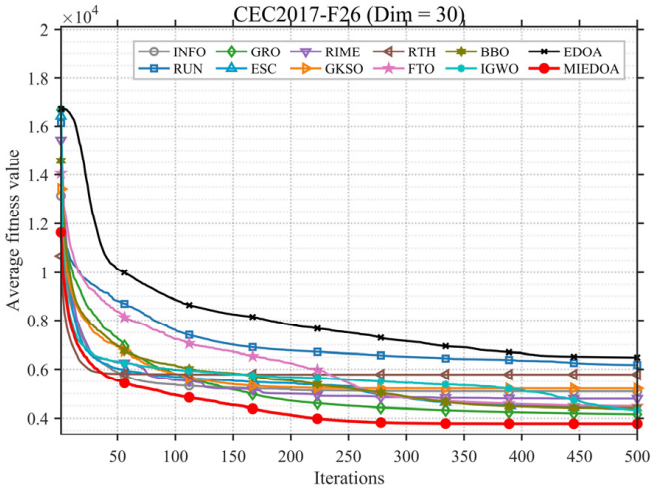
(**b**) CEC2017-F7 (Dim = 30)



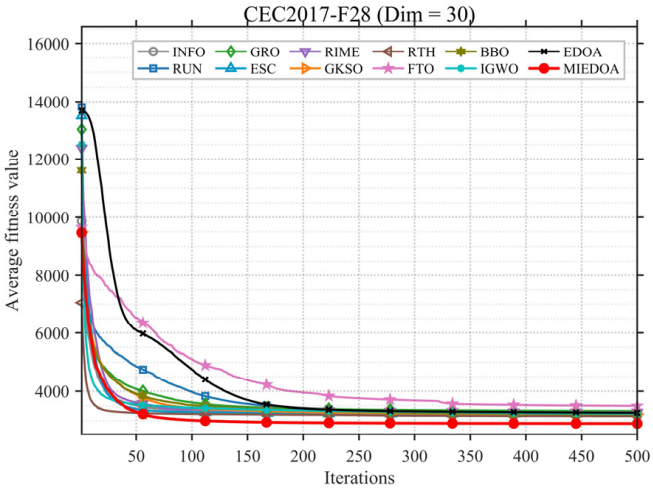
(**c**) CEC2017-F16 (Dim = 30)



(**d**) CEC2017-F20 (Dim = 30)

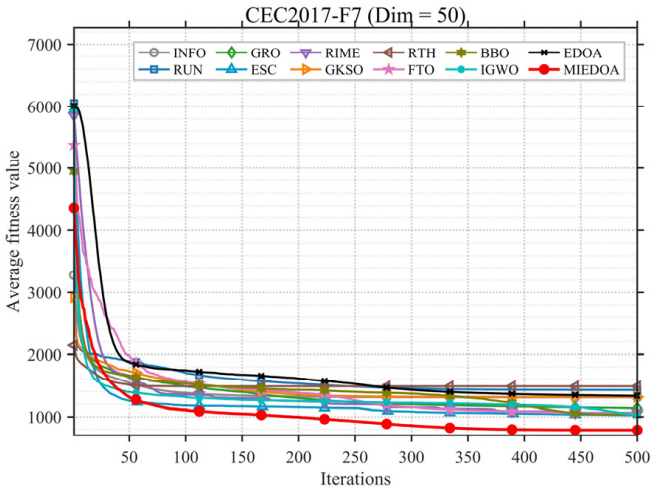


(**e**) CEC2017-F26 (Dim = 30)

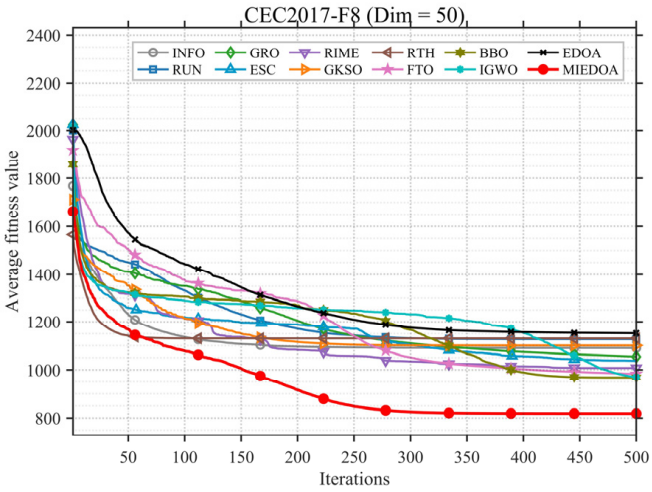


(**f**) CEC2017-F28 (Dim = 30)

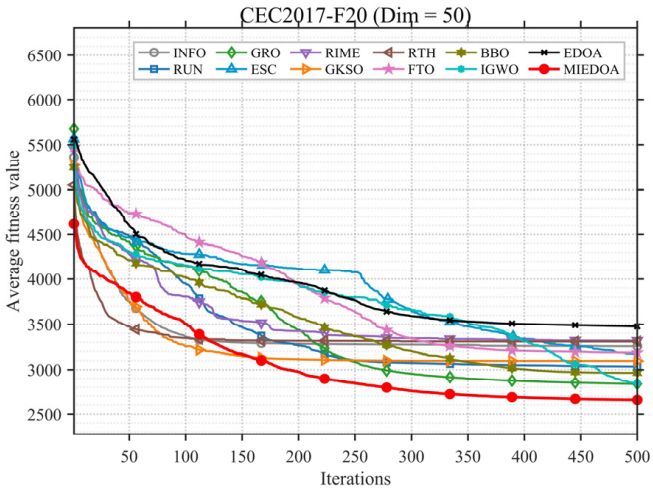
Figure 5. *Cont.*



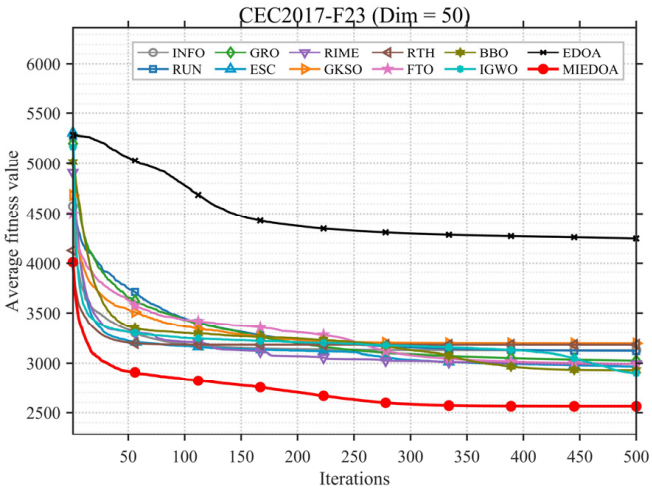
(**g**) CEC2017-F7 (Dim = 50)



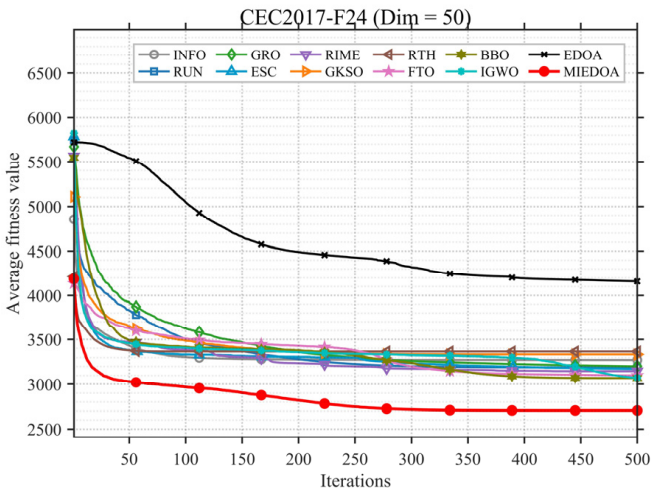
(**h**) CEC2017-F8 (Dim = 50)



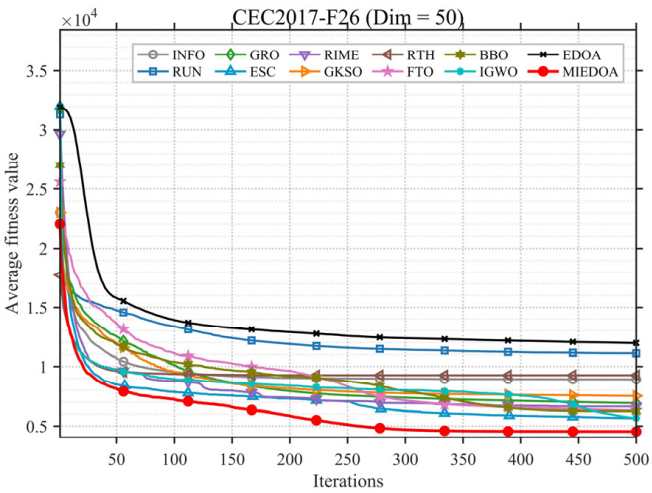
(**i**) CEC2017-F20 (Dim = 50)



(**j**) CEC2017-F23 (Dim = 50)

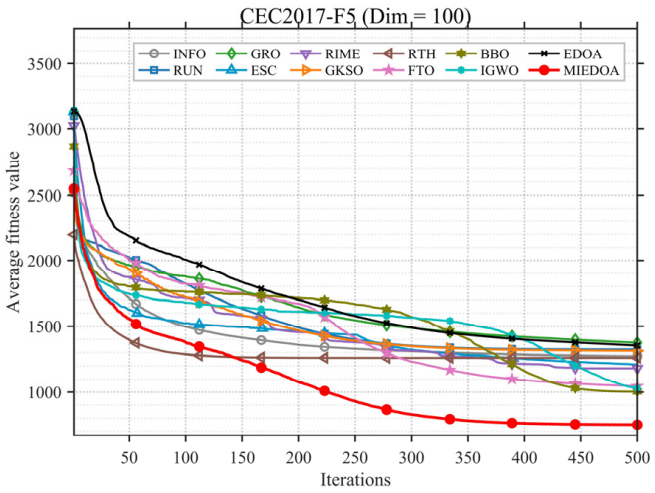


(**k**) CEC2017-F24 (Dim = 50)

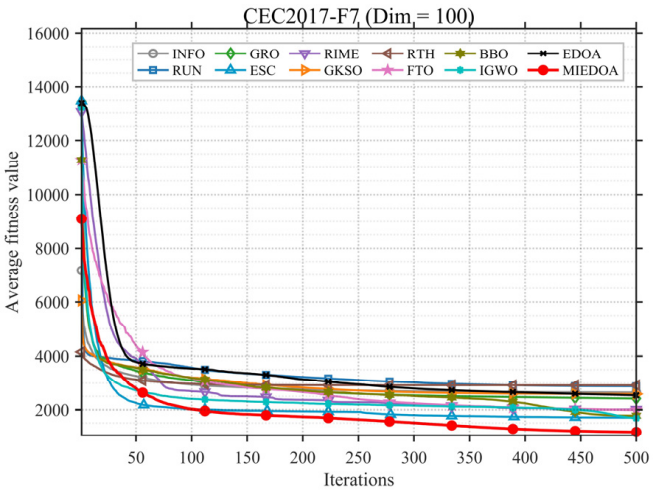


(**l**) CEC2017-F26 (Dim = 50)

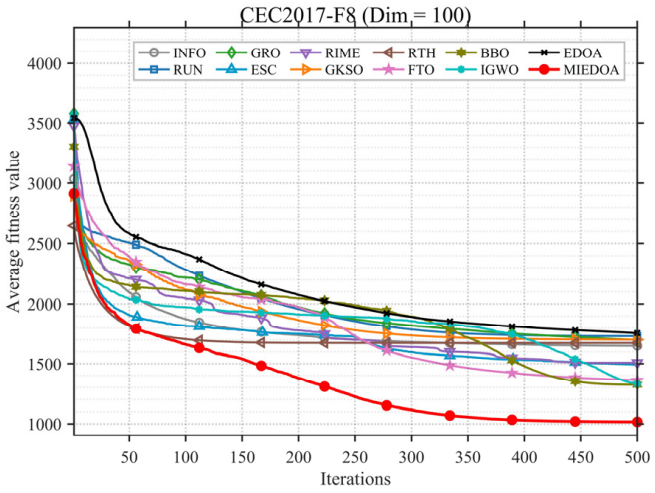
Figure 5. *Cont.*



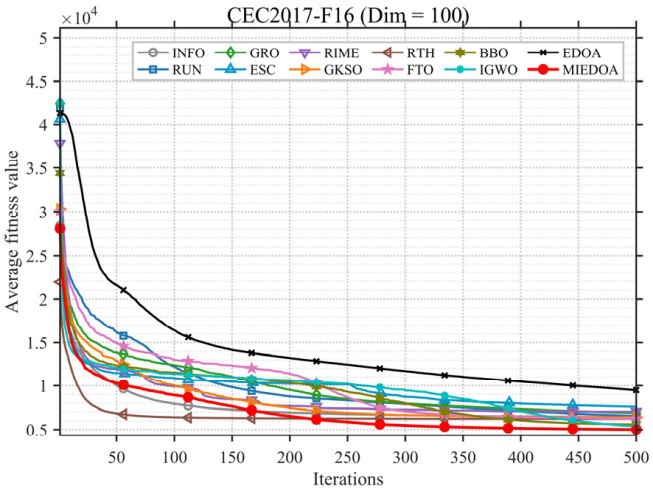
(**m**) CEC2017-F5 (Dim = 100)



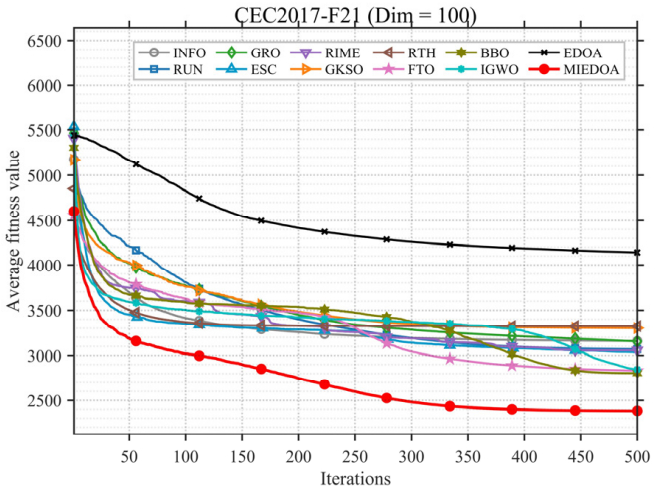
(**n**) CEC2017-F7 (Dim = 100)



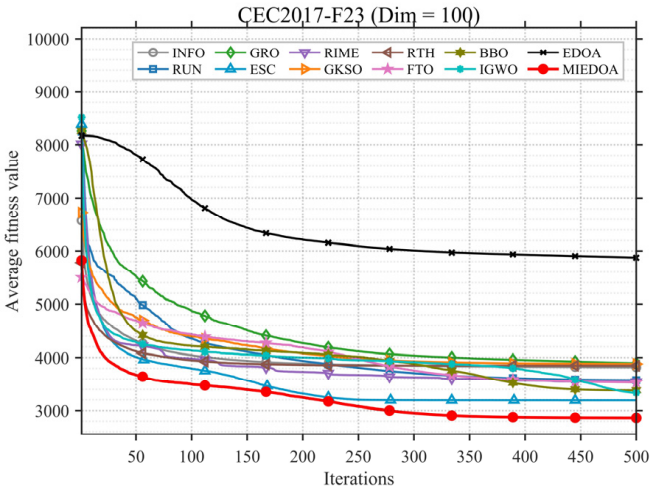
(**o**) CEC2017-F8 (Dim = 100)



(**p**) CEC2017-F16 (Dim = 100)

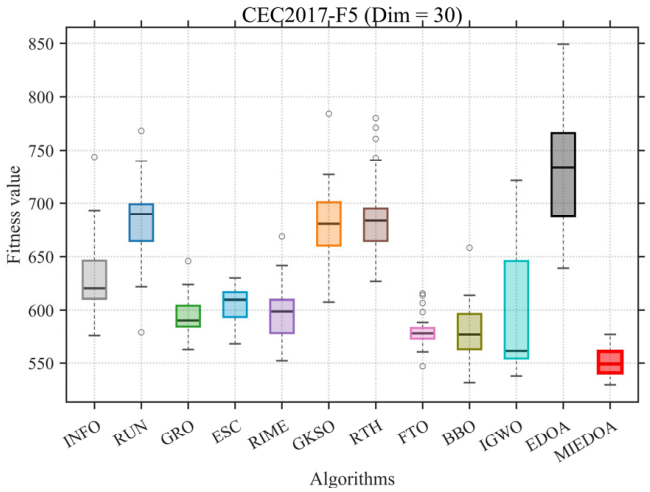


(**q**) CEC2017-F21 (Dim = 100)

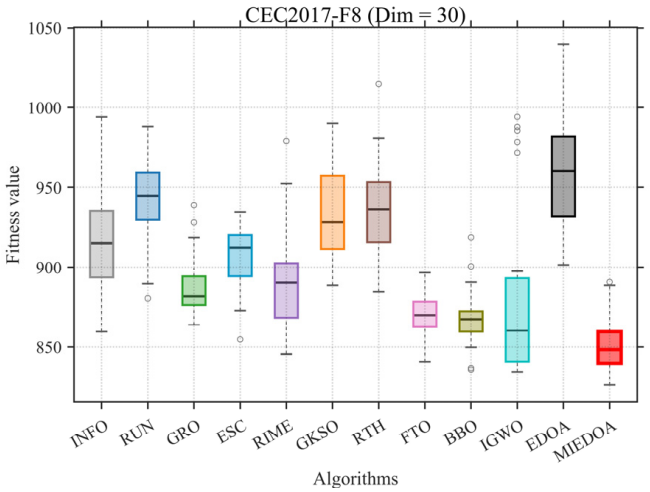


(**r**) CEC2017-F23 (Dim = 100)

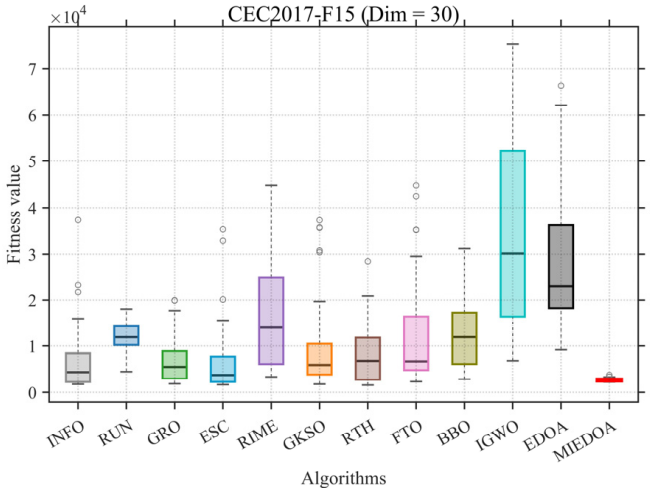
Figure 5. Convergence Behavior of Different Algorithms on the CEC2017 Benchmark Functions.



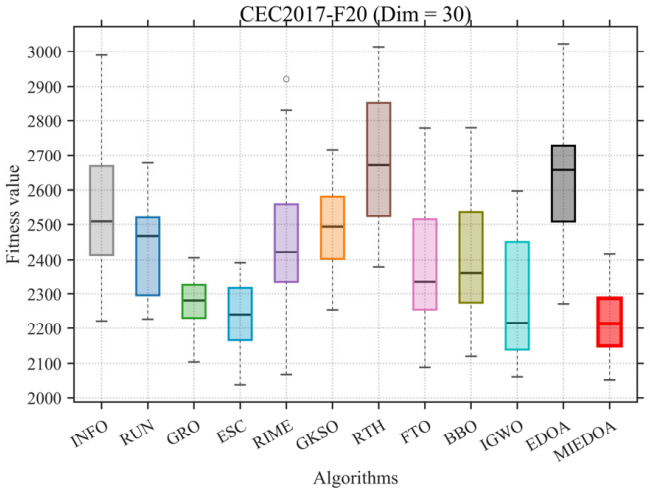
(**a**) CEC2017-F5 (Dim = 30)



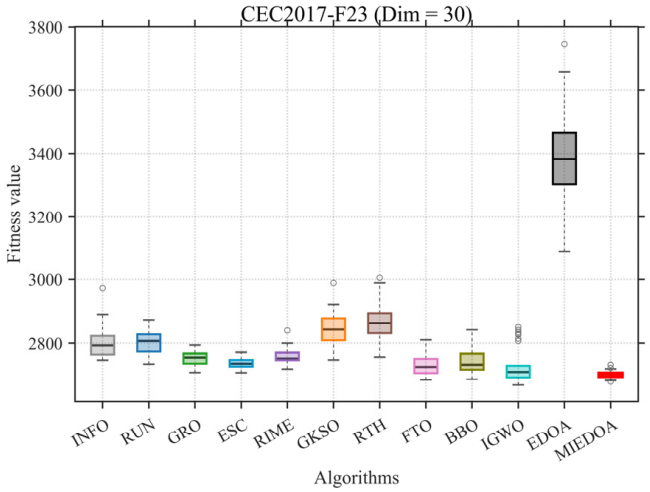
(**b**) CEC2017-F8 (Dim = 30)



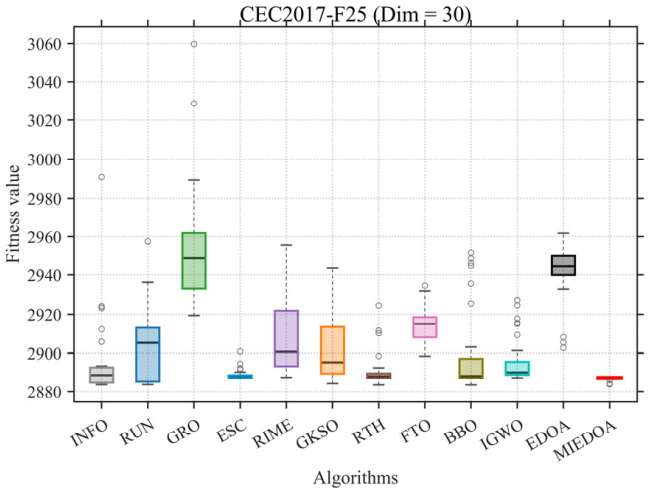
(**c**) CEC2017-F15 (Dim = 30)



(**d**) CEC2017-F20 (Dim = 30)

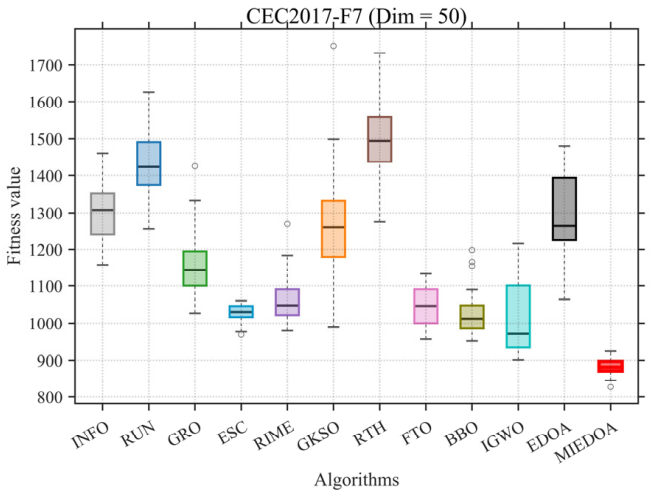


(**e**) CEC2017-F23 (Dim = 30)

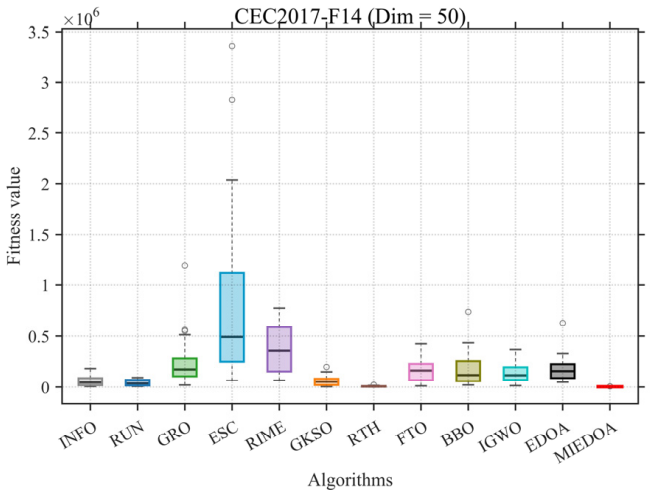


(**f**) CEC2017-F25 (Dim = 30)

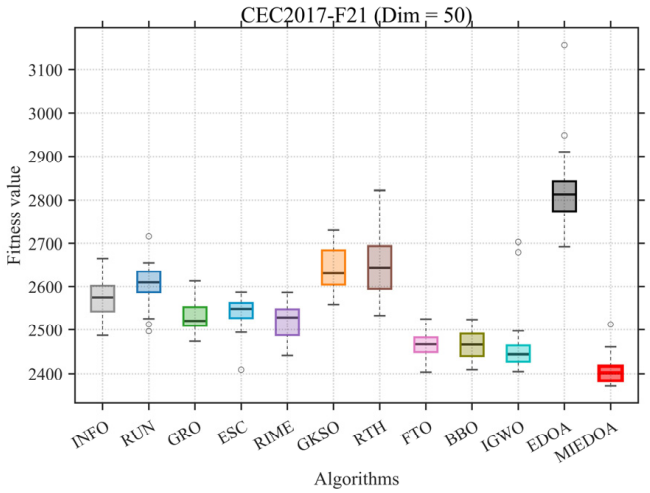
Figure 6. *Cont.*



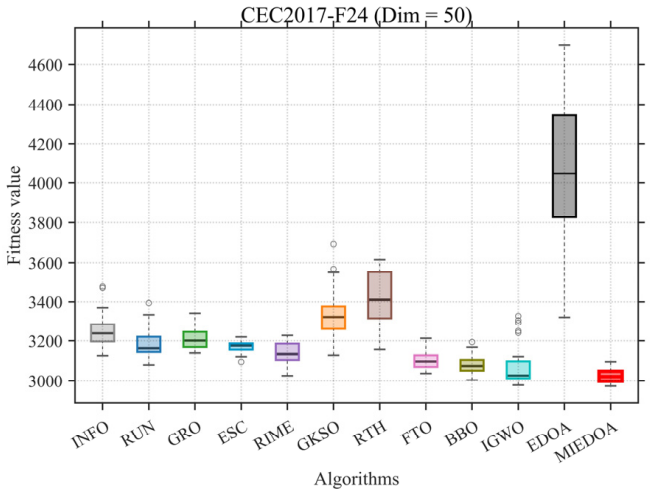
(**g**) CEC2017-F7 (Dim = 50)



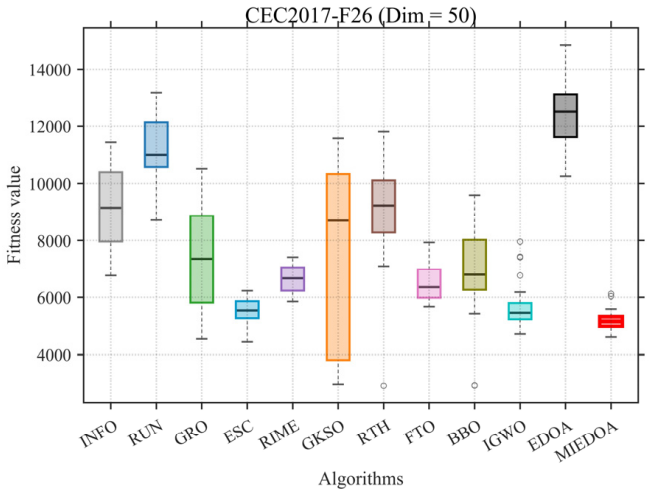
(**h**) CEC2017-F14 (Dim = 50)



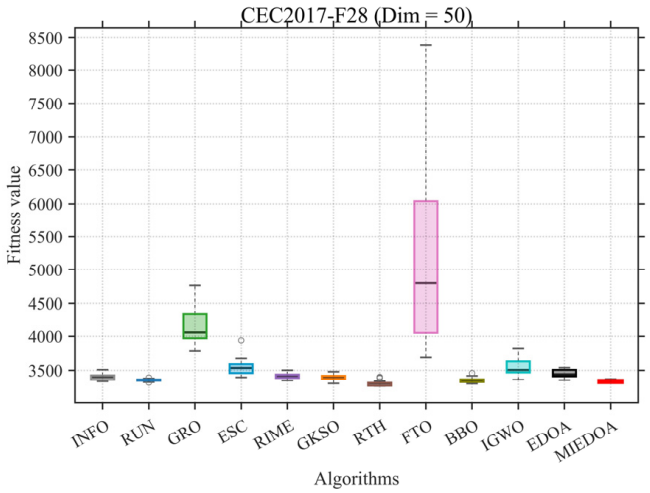
(**i**) CEC2017-F21 (Dim = 50)



(**j**) CEC2017-F24 (Dim = 50)

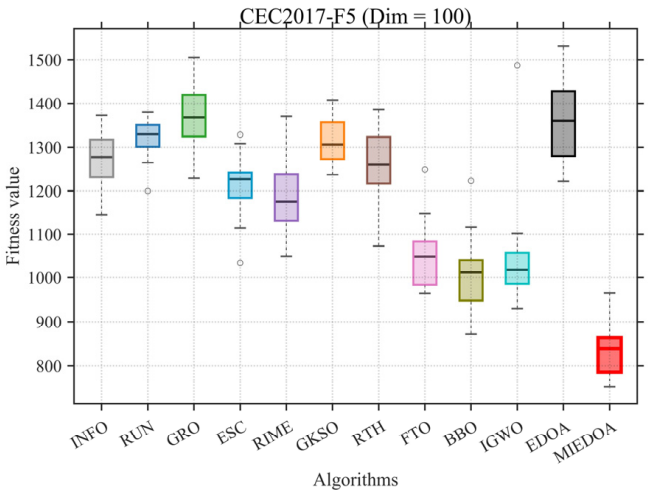


(**k**) CEC2017-F26 (Dim = 50)

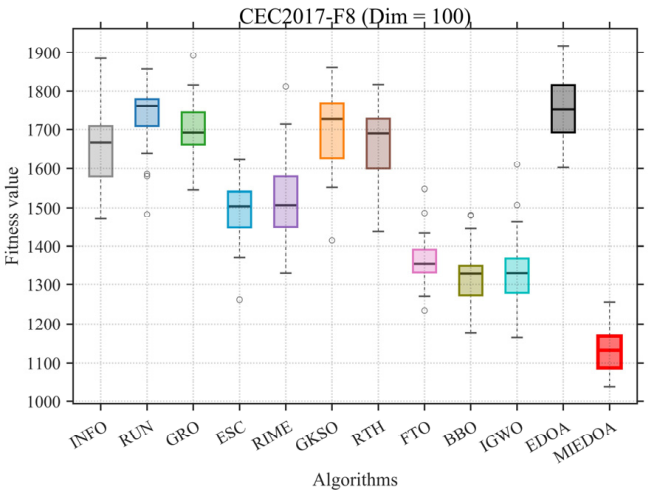


(**l**) CEC2017-F28 (Dim = 50)

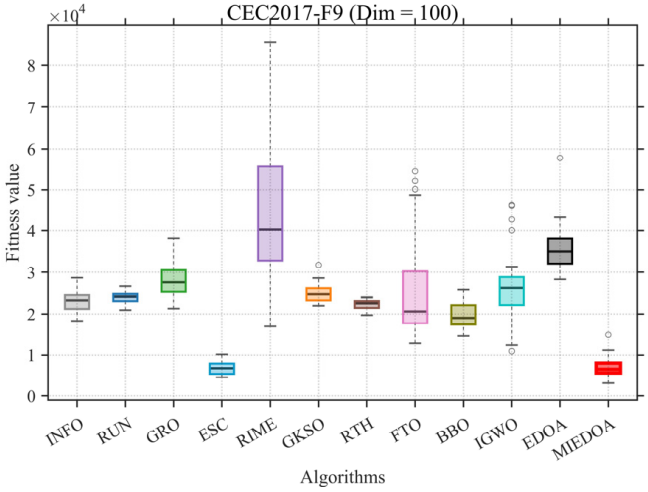
Figure 6. *Cont.*



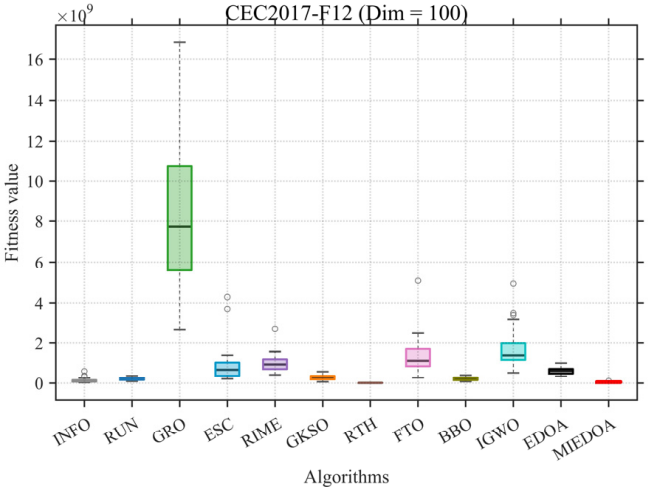
(**m**) CEC2017-F5 (Dim = 100)



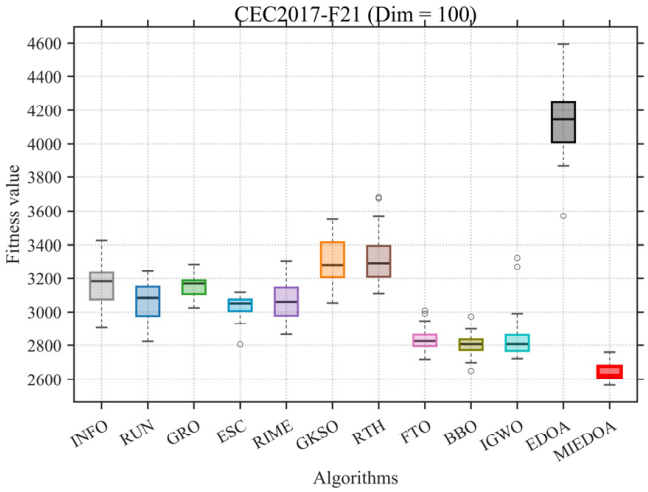
(**n**) CEC2017-F8 (Dim = 100)



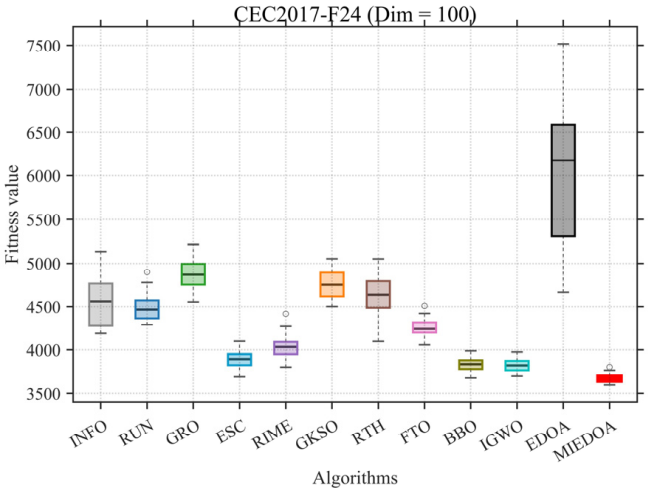
(**o**) CEC2017-F9 (Dim = 100)



(**p**) CEC2017-F12 (Dim = 100)



(**q**) CEC2017-F21 (Dim = 100)



(**r**) CEC2017-F24 (Dim = 100)

Figure 6. Boxplot-Based Performance Comparison on the CEC2017 Benchmark Functions.

Table 5. Performance Comparison of Algorithms on the CEC2017 Benchmark Functions (Dim = 30).

ID	Metric	INFO	RUN	GRO	ESC	RIME	GKSO	RTH	FTO	BBO	IGWO	EDOA	MIEDOA
F1	mean	3.1620×10^{3}	8.6848×10^{3}	1.1956×10^{8}	2.3462×10^{3}	2.3891×10^{6}	3.9303×10^{3}	5.4225×10^{3}	1.9760×10^{6}	1.7768×10^{4}	6.6871×10^{6}	2.8167×10^{4}	4.6883×10^{3}
	std	4.6086×10^{3}	7.4394×10^{3}	9.4428×10^{7}	2.6291×10^{3}	8.8821×10^{5}	4.8282×10^{3}	5.9830×10^{3}	2.9193×10^{6}	1.3160×10^{4}	5.7062×10^{6}	8.1599×10^{3}	4.7581×10^{3}
F2	mean	3.0598×10^{20}	9.0762×10^{19}	3.9804×10^{23}	1.5968×10^{25}	3.1977×10^{16}	2.2922×10^{14}	3.8325×10^{14}	1.8506×10^{23}	2.4128×10^{12}	5.2666×10^{17}	3.6423×10^{13}	1.0459×10^{13}
	std	1.6639×10^{21}	4.4443×10^{20}	1.0612×10^{24}	8.7453×10^{25}	7.1310×10^{16}	1.1016×10^{15}	2.0859×10^{15}	9.6238×10^{23}	5.9702×10^{12}	1.0727×10^{18}	7.4571×10^{13}	2.3417×10^{13}
F3	mean	6.4243×10^{3}	2.3642×10^{3}	4.7626×10^{4}	7.8135×10^{4}	2.4229×10^{4}	2.5282×10^{3}	3.0009×10^{2}	7.6799×10^{3}	5.6360×10^{3}	1.1179×10^{4}	1.8270×10^{4}	9.6543×10^{2}
	std	3.4897×10^{3}	1.0875×10^{3}	7.2700×10^{3}	1.4957×10^{4}	9.7957×10^{3}	1.2205×10^{3}	1.5441×10^{-1}	3.3457×10^{3}	2.8133×10^{3}	4.6494×10^{3}	8.9671×10^{3}	3.5338×10^{2}
F4	mean	4.9301×10^{2}	5.0438×10^{2}	5.4763×10^{2}	5.0753×10^{2}	5.3479×10^{2}	5.0071×10^{2}	4.3093×10^{2}	5.2598×10^{2}	4.9044×10^{2}	5.0937×10^{2}	5.0878×10^{2}	4.9394×10^{2}
	std	3.1532×10^{1}	1.7666×10^{1}	3.0673×10^{1}	1.3431×10^{1}	5.0377×10^{1}	3.1246×10^{1}	3.4528×10^{1}	1.6247×10^{1}	3.5232×10^{1}	1.2350×10^{1}	1.7721×10^{1}	1.2354×10^{1}
F5	mean	6.3121×10^{2}	6.8307×10^{2}	5.9375×10^{2}	6.0444×10^{2}	5.9914×10^{2}	6.8035×10^{2}	6.8723×10^{2}	5.7988×10^{2}	5.8018×10^{2}	5.9217×10^{2}	7.3261×10^{2}	5.5031×10^{2}
	std	3.6410×10^{1}	3.5298×10^{1}	1.8446×10^{1}	1.6080×10^{1}	2.5371×10^{1}	3.5576×10^{1}	3.9126×10^{1}	1.4440×10^{1}	2.5414×10^{1}	5.5634×10^{1}	4.9685×10^{1}	1.3193×10^{1}
F6	mean	6.1916×10^{2}	6.4606×10^{2}	6.1104×10^{2}	6.0001×10^{2}	6.0819×10^{2}	6.3526×10^{2}	6.4340×10^{2}	6.1448×10^{2}	6.1035×10^{2}	6.0103×10^{2}	6.5727×10^{2}	6.0007×10^{2}
	std	6.9914×10^{0}	7.9798×10^{0}	3.4916×10^{0}	1.0703×10^{-2}	3.5330×10^{0}	6.7898×10^{0}	9.3571×10^{0}	5.9354×10^{0}	6.8611×10^{0}	4.7820×10^{-1}	6.1285×10^{0}	1.6290×10^{-2}
F7	mean	9.6713×10^{2}	1.0462×10^{3}	8.4507×10^{2}	8.5113×10^{2}	8.4401×10^{2}	9.4489×10^{2}	1.0679×10^{3}	8.5326×10^{2}	8.5984×10^{2}	8.6434×10^{2}	9.5608×10^{2}	7.8566×10^{2}
	std	6.2831×10^{1}	7.4017×10^{1}	3.7486×10^{1}	1.1730×10^{1}	2.8369×10^{1}	5.0593×10^{1}	9.5281×10^{1}	2.6291×10^{1}	3.5651×10^{1}	5.6550×10^{1}	5.7253×10^{1}	1.7539×10^{1}
F8	mean	9.1848×10^{2}	9.3932×10^{2}	8.8792×10^{2}	9.0724×10^{2}	8.9203×10^{2}	9.3349×10^{2}	9.3632×10^{2}	8.6949×10^{2}	8.6820×10^{2}	8.8230×10^{2}	9.6077×10^{2}	8.5191×10^{2}
	std	3.1790×10^{1}	2.6159×10^{1}	1.8421×10^{1}	1.8246×10^{1}	3.2731×10^{1}	2.6896×10^{1}	2.9727×10^{1}	1.5607×10^{1}	1.6254×10^{1}	5.4599×10^{1}	3.5718×10^{1}	1.7315×10^{1}
F9	mean	2.8979×10^{3}	3.8055×10^{3}	1.5837×10^{3}	9.0053×10^{2}	1.8253×10^{3}	3.2456×10^{3}	3.8736×10^{3}	1.7381×10^{3}	1.6367×10^{3}	9.8312×10^{2}	4.4206×10^{3}	9.0087×10^{2}
	std	8.5804×10^{2}	6.4084×10^{2}	4.1456×10^{2}	7.6591×10^{-1}	8.0847×10^{2}	8.2092×10^{2}	7.1977×10^{2}	3.6729×10^{2}	4.9130×10^{2}	1.5705×10^{2}	8.9043×10^{2}	2.3148×10^{0}
F10	mean	4.9382×10^{3}	4.9150×10^{3}	4.6342×10^{3}	7.1159×10^{3}	4.4524×10^{3}	4.7857×10^{3}	5.2559×10^{3}	5.2283×10^{3}	4.1534×10^{3}	7.2107×10^{3}	5.3589×10^{3}	4.8456×10^{3}
	std	6.6713×10^{2}	1.0808×10^{3}	5.5053×10^{2}	3.5310×10^{2}	6.3837×10^{2}	5.9145×10^{2}	6.2341×10^{2}	8.4170×10^{2}	7.2607×10^{2}	1.8092×10^{3}	7.4333×10^{2}	5.6018×10^{2}
F11	mean	1.2547×10^{3}	1.2085×10^{3}	1.3164×10^{3}	1.1930×10^{3}	1.3268×10^{3}	1.2183×10^{3}	1.2552×10^{3}	1.2576×10^{3}	1.2384×10^{3}	1.2230×10^{3}	1.2758×10^{3}	1.1859×10^{3}
	std	5.3962×10^{1}	2.9283×10^{1}	7.0407×10^{1}	2.8268×10^{1}	6.7269×10^{1}	4.9145×10^{1}	5.1844×10^{1}	4.5398×10^{1}	3.9945×10^{1}	3.3829×10^{1}	4.4191×10^{1}	3.2611×10^{1}
F12	mean	2.8798×10^{5}	1.6535×10^{6}	1.7616×10^{6}	1.0620×10^{6}	1.3617×10^{7}	1.0401×10^{6}	3.1398×10^{4}	2.3093×10^{6}	1.5833×10^{6}	3.1959×10^{6}	1.2465×10^{7}	3.5492×10^{5}
	std	3.8730×10^{5}	8.1556×10^{5}	1.7800×10^{6}	9.1257×10^{5}	1.2978×10^{7}	1.4969×10^{6}	1.6226×10^{4}	1.7716×10^{6}	9.3613×10^{5}	2.6533×10^{6}	6.3667×10^{6}	2.1872×10^{5}
F13	mean	2.2104×10^{4}	2.2218×10^{4}	1.8626×10^{4}	1.2170×10^{4}	1.6129×10^{5}	2.0517×10^{4}	2.1591×10^{4}	3.1136×10^{4}	3.7566×10^{4}	1.3908×10^{5}	5.6561×10^{4}	3.0477×10^{4}
	std	1.9770×10^{4}	1.2034×10^{4}	1.3163×10^{4}	8.7024×10^{3}	2.2981×10^{5}	1.8819×10^{4}	2.0426×10^{4}	1.8932×10^{4}	3.1441×10^{4}	6.5417×10^{4}	3.0843×10^{4}	1.5087×10^{4}
F14	mean	3.9345×10^{3}	4.2027×10^{3}	3.4786×10^{4}	1.9053×10^{5}	5.9698×10^{4}	6.5330×10^{3}	2.2155×10^{3}	8.1418×10^{3}	2.0244×10^{4}	1.3385×10^{4}	3.2958×10^{4}	1.6092×10^{3}
	std	2.7420×10^{3}	2.6721×10^{3}	5.4600×10^{4}	2.4783×10^{5}	4.9669×10^{4}	5.1174×10^{3}	5.1651×10^{2}	5.6985×10^{3}	2.7772×10^{4}	1.3314×10^{4}	3.4031×10^{4}	3.4313×10^{1}
F15	mean	7.3086×10^{3}	1.1870×10^{4}	7.3584×10^{3}	7.7058×10^{3}	1.6000×10^{4}	1.0907×10^{4}	7.9519×10^{3}	1.3263×10^{4}	1.2187×10^{4}	3.4244×10^{4}	2.8612×10^{4}	2.7481×10^{3}
	std	8.0203×10^{3}	3.3235×10^{3}	5.4409×10^{3}	8.5879×10^{3}	1.1036×10^{4}	1.1185×10^{4}	6.5907×10^{3}	1.2679×10^{4}	7.6055×10^{3}	2.1180×10^{4}	1.5244×10^{4}	3.5273×10^{2}
F16	mean	2.6433×10^{3}	2.6841×10^{3}	2.3324×10^{3}	2.3844×10^{3}	2.6036×10^{3}	2.5816×10^{3}	2.8764×10^{3}	2.3210×10^{3}	2.4952×10^{3}	2.2255×10^{3}	3.2828×10^{3}	2.2128×10^{3}
	std	3.6037×10^{2}	3.5559×10^{2}	2.1636×10^{2}	2.1185×10^{2}	2.9565×10^{2}	3.0783×10^{2}	3.1257×10^{2}	2.3829×10^{2}	2.5173×10^{2}	4.8949×10^{2}	3.7534×10^{2}	2.8558×10^{2}
F17	mean	2.3554×10^{3}	2.2204×10^{3}	1.8956×10^{3}	1.8379×10^{3}	2.1007×10^{3}	2.2074×10^{3}	2.4225×10^{3}	1.9320×10^{3}	2.0225×10^{3}	1.8958×10^{3}	2.5360×10^{3}	1.9034×10^{3}
	std	2.6278×10^{2}	1.5768×10^{2}	1.2061×10^{2}	6.8474×10^{1}	1.6959×10^{2}	2.0549×10^{2}	2.6988×10^{2}	1.0646×10^{2}	1.7112×10^{2}	1.3951×10^{2}	2.4115×10^{2}	1.0171×10^{2}
F18	mean	8.0632×10^{4}	6.2664×10^{4}	3.2197×10^{5}	7.3218×10^{5}	9.5863×10^{5}	1.2981×10^{5}	2.4117×10^{4}	2.0043×10^{5}	4.8173×10^{5}	3.5057×10^{5}	4.7254×10^{5}	1.9995×10^{4}
	std	5.4610×10^{4}	2.4433×10^{4}	3.8662×10^{5}	6.1432×10^{5}	1.0030×10^{6}	1.4645×10^{5}	1.6530×10^{4}	1.4311×10^{5}	4.8426×10^{5}	3.1417×10^{5}	4.8750×10^{5}	1.1852×10^{4}
F19	mean	9.2808×10^{3}	8.1369×10^{3}	7.9671×10^{3}	8.7590×10^{3}	1.6038×10^{4}	1.0201×10^{4}	8.9234×10^{3}	1.6023×10^{4}	8.4577×10^{3}	1.4422×10^{4}	1.8466×10^{6}	2.3873×10^{3}
	std	8.0512×10^{3}	8.2333×10^{3}	7.7312×10^{3}	1.0420×10^{4}	1.3089×10^{4}	1.0121×10^{4}	9.5775×10^{3}	1.3241×10^{4}	3.9949×10^{3}	1.0531×10^{4}	1.2172×10^{6}	2.3758×10^{2}
F20	mean	2.5542×10^{3}	2.4393×10^{3}	2.2749×10^{3}	2.2302×10^{3}	2.4469×10^{3}	2.4855×10^{3}	2.6766×10^{3}	2.3928×10^{3}	2.3927×10^{3}	2.2732×10^{3}	2.6343×10^{3}	2.2184×10^{3}
	std	1.9864×10^{2}	1.2690×10^{2}	7.0637×10^{1}	9.9713×10^{1}	1.8390×10^{2}	1.1802×10^{2}	1.8899×10^{2}	1.8968×10^{2}	1.5367×10^{2}	1.6460×10^{2}	1.6686×10^{2}	9.9597×10^{1}
F21	mean	2.4149×10^{3}	2.4413×10^{3}	2.3756×10^{3}	2.4024×10^{3}	2.3986×10^{3}	2.4442×10^{3}	2.4477×10^{3}	2.3628×10^{3}	2.3718×10^{3}	2.3793×10^{3}	2.5449×10^{3}	2.3557×10^{3}
	std	3.0440×10^{1}	4.2041×10^{1}	1.7197×10^{1}	1.5551×10^{1}	2.3649×10^{1}	2.9942×10^{1}	3.3504×10^{1}	1.2583×10^{1}	1.7603×10^{1}	5.2366×10^{1}	6.2385×10^{1}	1.6693×10^{1}
F22	mean	5.1764×10^{3}	3.9644×10^{3}	2.3713×10^{3}	3.1210×10^{3}	4.7406×10^{3}	2.8424×10^{3}	4.7933×10^{3}	6.0571×10^{3}	2.7324×10^{3}	3.0027×10^{3}	5.5424×10^{3}	2.9837×10^{3}
	std	2.1764×10^{3}	2.5453×10^{3}	3.7605×10^{1}	2.1013×10^{3}	1.8595×10^{3}	1.4070×10^{3}	2.1220×10^{3}	1.7960×10^{3}	1.1295×10^{3}	1.8203×10^{3}	2.3946×10^{3}	1.5647×10^{3}
F23	mean	2.8013×10^{3}	2.8037×10^{3}	2.7528×10^{3}	2.7389×10^{3}	2.7594×10^{3}	2.8469×10^{3}	2.8684×10^{3}	2.7329×10^{3}	2.7450×10^{3}	2.7316×10^{3}	3.3870×10^{3}	2.7039×10^{3}
	std	4.8536×10^{1}	3.5314×10^{1}	2.1455×10^{1}	1.4413×10^{1}	2.2951×10^{1}	4.8682×10^{1}	6.4264×10^{1}	3.0490×10^{1}	3.5455×10^{1}	5.7039×10^{1}	1.3781×10^{2}	1.2510×10^{1}
F24	mean	2.9732×10^{3}	2.9373×10^{3}	2.9177×10^{3}	2.9341×10^{3}	2.9256×10^{3}	3.0187×10^{3}	3.0502×10^{3}	2.9008×10^{3}	2.8935×10^{3}	2.8985×10^{3}	3.3629×10^{3}	2.8757×10^{3}
	std	4.4132×10^{1}	2.9714×10^{1}	1.9918×10^{1}	1.9690×10^{1}	3.3554×10^{1}	5.0532×10^{1}	7.9059×10^{1}	2.2371×10^{1}	3.2369×10^{1}	6.0948×10^{1}	1.9731×10^{2}	1.8936×10^{1}
F25	mean	2.8962×10^{3}	2.9044×10^{3}	2.9538×10^{3}	2.8889×10^{3}	2.9079×10^{3}	2.9021×10^{3}	2.8913×10^{3}	2.9146×10^{3}	2.8995×10^{3}	2.8960×10^{3}	2.9421×10^{3}	2.8871×10^{3}
	std	2.1589×10^{1}	1.8562×10^{1}	3.1048×10^{1}	2.9360×10^{0}	1.8138×10^{1}	1.6751×10^{1}	9.9385×10^{0}	9.3269×10^{0}	2.2365×10^{1}	1.1994×10^{1}	1.3960×10^{1}	8.9469×10^{-1}

Table 5. *Cont.*

ID	Metric	INFO	RUN	GRO	ESC	RIME	GKSO	RTH	FTO	BBO	IGWO	EDOA	MIEDOA
F26	mean	4.9011×10^{3}	5.5384×10^{3}	4.3531×10^{3}	4.2963×10^{3}	5.1168×10^{3}	5.4855×10^{3}	5.7906×10^{3}	4.5959×10^{3}	4.1522×10^{3}	4.0516×10^{3}	7.3192×10^{3}	4.2627×10^{3}
	std	1.2785×10^{3}	1.4283×10^{3}	9.2446×10^{2}	2.5868×10^{2}	5.0151×10^{2}	1.0433×10^{3}	1.1700×10^{3}	3.0152×10^{2}	1.0904×10^{3}	7.2638×10^{2}	1.9857×10^{3}	1.6831×10^{2}
F27	mean	3.2607×10^{3}	3.2834×10^{3}	3.2630×10^{3}	3.2148×10^{3}	3.2298×10^{3}	3.2638×10^{3}	3.2566×10^{3}	3.2526×10^{3}	3.2329×10^{3}	3.2070×10^{3}	3.8406×10^{3}	3.2146×10^{3}
	std	2.7738×10^{1}	3.4776×10^{1}	2.1624×10^{1}	8.2894×10^{0}	1.3028×10^{1}	2.8809×10^{1}	3.7037×10^{1}	1.7332×10^{1}	1.6123×10^{1}	1.0385×10^{1}	3.9952×10^{2}	7.8615×10^{0}
F28	mean	3.2256×10^{3}	3.2177×10^{3}	3.3278×10^{3}	3.2494×10^{3}	3.2764×10^{3}	3.2341×10^{3}	3.1629×10^{3}	3.6273×10^{3}	3.2266×10^{3}	3.2449×10^{3}	3.2592×10^{3}	3.2265×10^{3}
	std	2.1995×10^{1}	2.0804×10^{1}	4.1203×10^{1}	2.0738×10^{1}	2.9430×10^{1}	2.0798×10^{1}	6.1906×10^{1}	1.0006×10^{3}	2.3651×10^{1}	2.2998×10^{1}	2.5235×10^{1}	2.4286×10^{1}
F29	mean	4.0157×10^{3}	4.1442×10^{3}	3.7573×10^{3}	3.5401×10^{3}	3.8815×10^{3}	4.0513×10^{3}	4.1010×10^{3}	3.8969×10^{3}	3.7204×10^{3}	3.5455×10^{3}	4.9492×10^{3}	3.6109×10^{3}
	std	2.2909×10^{2}	2.0931×10^{2}	1.8274×10^{2}	1.0574×10^{2}	2.0519×10^{2}	2.4092×10^{2}	2.3881×10^{2}	2.1339×10^{2}	1.9395×10^{2}	1.1944×10^{2}	3.7186×10^{2}	1.3504×10^{2}
F30	mean	1.1657×10^{4}	8.4709×10^{4}	5.1696×10^{4}	1.2342×10^{4}	5.3885×10^{5}	5.0844×10^{4}	9.6331×10^{3}	2.5526×10^{5}	8.9671×10^{4}	4.3975×10^{5}	4.9353×10^{6}	3.4215×10^{4}
	std	5.7271×10^{3}	1.1245×10^{5}	3.7336×10^{4}	4.1005×10^{3}	4.9576×10^{5}	8.0275×10^{4}	3.5187×10^{3}	2.5545×10^{5}	7.3391×10^{4}	2.8842×10^{5}	2.6318×10^{6}	1.3524×10^{4}

Table 6. Performance Comparison of Algorithms on the CEC2017 Benchmark Functions (Dim = 50).

ID	Metric	INFO	RUN	GRO	ESC	RIME	GKSO	RTH	FTO	BBO	IGWO	EDOA	MIEDOA
F1	mean	2.4676×10^{6}	5.0245×10^{4}	5.6424×10^{9}	2.0794×10^{6}	2.1923×10^{7}	3.3485×10^{5}	3.2177×10^{3}	9.1844×10^{8}	4.5864×10^{5}	8.1419×10^{8}	9.2991×10^{5}	6.5783×10^{3}
	std	5.9750×10^{6}	1.7994×10^{4}	2.4557×10^{9}	6.9547×10^{6}	5.1665×10^{6}	1.6707×10^{5}	4.9764×10^{3}	5.9548×10^{8}	2.3265×10^{5}	8.0395×10^{8}	2.9224×10^{5}	5.6077×10^{3}
F2	mean	1.2243×10^{43}	1.7433×10^{48}	3.0883×10^{51}	2.4557×10^{48}	1.5579×10^{39}	1.4250×10^{38}	1.4729×10^{36}	6.9769×10^{48}	1.7127×10^{28}	7.8586×10^{42}	1.3874×10^{38}	4.5364×10^{32}
	std	4.1156×10^{43}	8.7904×10^{48}	1.4283×10^{52}	1.3450×10^{49}	7.3502×10^{39}	7.5728×10^{38}	8.0673×10^{36}	2.5115×10^{49}	9.1959×10^{28}	4.2632×10^{43}	5.4242×10^{38}	1.7715×10^{33}
F3	mean	7.0418×10^{4}	3.8644×10^{4}	1.3690×10^{5}	2.1111×10^{5}	1.5144×10^{5}	4.4136×10^{4}	1.2474×10^{4}	7.1458×10^{4}	6.8479×10^{4}	6.8554×10^{4}	9.2891×10^{4}	5.9468×10^{4}
	std	1.5199×10^{4}	9.9770×10^{3}	2.0256×10^{4}	3.3194×10^{4}	3.0192×10^{4}	1.0674×10^{4}	5.3651×10^{3}	1.2539×10^{4}	1.8924×10^{4}	1.6422×10^{4}	2.6710×10^{4}	1.1125×10^{4}
F4	mean	5.8636×10^{2}	5.5132×10^{2}	1.1843×10^{3}	6.2956×10^{2}	6.4598×10^{2}	6.1586×10^{2}	5.2481×10^{2}	8.0558×10^{2}	5.7453×10^{2}	6.4281×10^{2}	6.4345×10^{2}	5.7020×10^{2}
	std	6.0207×10^{1}	5.9205×10^{1}	3.2625×10^{2}	4.9351×10^{1}	5.7946×10^{1}	3.9014×10^{1}	5.9806×10^{1}	9.6561×10^{1}	4.1741×10^{1}	5.5409×10^{1}	5.2811×10^{1}	5.5649×10^{1}
F5	mean	7.7255×10^{2}	8.4473×10^{2}	7.6171×10^{2}	7.4615×10^{2}	7.1180×10^{2}	8.1365×10^{2}	8.0834×10^{2}	6.6888×10^{2}	6.7738×10^{2}	6.8654×10^{2}	8.4921×10^{2}	6.2192×10^{2}
	std	3.4516×10^{1}	2.2234×10^{1}	3.3264×10^{1}	3.9133×10^{1}	4.9512×10^{1}	4.6542×10^{1}	3.5013×10^{1}	2.9222×10^{1}	3.1864×10^{1}	9.3992×10^{1}	4.9484×10^{1}	3.1059×10^{1}
F6	mean	6.4236×10^{2}	6.5669×10^{2}	6.2650×10^{2}	6.0013×10^{2}	6.2251×10^{2}	6.5183×10^{2}	6.4711×10^{2}	6.2880×10^{2}	6.2104×10^{2}	6.0445×10^{2}	6.6508×10^{2}	6.0030×10^{2}
	std	8.8088×10^{0}	7.0534×10^{0}	4.5624×10^{0}	1.8353×10^{-1}	6.3471×10^{0}	8.2752×10^{0}	6.9053×10^{0}	1.2190×10^{1}	7.9234×10^{0}	1.4874×10^{0}	6.0642×10^{0}	1.7832×10^{-1}
F7	mean	1.3027×10^{3}	1.4304×10^{3}	1.1620×10^{3}	1.0279×10^{3}	1.0581×10^{3}	1.2736×10^{3}	1.5017×10^{3}	1.0492×10^{3}	1.0267×10^{3}	1.0134×10^{3}	1.2863×10^{3}	8.8201×10^{2}
	std	8.9616×10^{1}	9.7557×10^{1}	9.2161×10^{1}	2.2506×10^{1}	6.1652×10^{1}	1.4747×10^{2}	1.0777×10^{2}	5.2298×10^{1}	6.1605×10^{1}	9.9806×10^{1}	1.1085×10^{2}	2.4143×10^{1}
F8	mean	1.0896×10^{3}	1.1345×10^{3}	1.0649×10^{3}	1.0397×10^{3}	1.0127×10^{3}	1.1146×10^{3}	1.1387×10^{3}	9.8681×10^{2}	9.6389×10^{2}	9.7133×10^{2}	1.1447×10^{3}	9.1589×10^{2}
	std	5.1776×10^{1}	3.6428×10^{1}	3.6147×10^{1}	3.0120×10^{1}	4.6569×10^{1}	5.1486×10^{1}	4.9223×10^{1}	3.3096×10^{1}	3.0510×10^{1}	6.3697×10^{1}	3.8726×10^{1}	2.8121×10^{1}
F9	mean	8.4923×10^{3}	1.0580×10^{4}	6.1627×10^{3}	9.6209×10^{2}	7.1198×10^{3}	1.1003×10^{4}	1.0979×10^{4}	6.4778×10^{3}	4.7637×10^{3}	3.0762×10^{3}	1.4563×10^{4}	9.9557×10^{2}
	std	2.0211×10^{3}	1.6080×10^{3}	1.6371×10^{3}	5.8650×10^{1}	3.8424×10^{3}	2.1289×10^{3}	1.3533×10^{3}	3.8396×10^{3}	1.2403×10^{3}	1.8964×10^{3}	2.8019×10^{3}	1.1399×10^{2}
F10	mean	8.1772×10^{3}	7.7064×10^{3}	8.5292×10^{3}	1.3200×10^{4}	8.0667×10^{3}	7.8416×10^{3}	7.7780×10^{3}	9.5725×10^{3}	6.4413×10^{3}	1.2241×10^{4}	8.9460×10^{3}	7.6868×10^{3}
	std	7.7547×10^{2}	1.1963×10^{3}	6.6910×10^{2}	4.5130×10^{2}	1.0238×10^{3}	8.1360×10^{2}	1.2402×10^{3}	1.1108×10^{3}	8.9591×10^{2}	3.6788×10^{3}	1.0843×10^{3}	9.9797×10^{2}
F11	mean	1.3706×10^{3}	1.2971×10^{3}	3.2016×10^{3}	1.7685×10^{3}	1.6514×10^{3}	1.3589×10^{3}	1.3294×10^{3}	1.4808×10^{3}	1.3549×10^{3}	1.6208×10^{3}	1.6167×10^{3}	1.3850×10^{3}
	std	8.0749×10^{1}	4.1417×10^{1}	9.0952×10^{2}	1.1724×10^{3}	8.8291×10^{1}	5.5140×10^{1}	6.9501×10^{1}	1.0885×10^{2}	5.0403×10^{1}	1.9764×10^{2}	1.4311×10^{2}	7.1952×10^{1}
F12	mean	4.5373×10^{6}	1.0082×10^{7}	1.4553×10^{8}	7.9433×10^{6}	1.3085×10^{8}	1.0365×10^{7}	7.2552×10^{5}	4.6966×10^{7}	1.3525×10^{7}	4.3417×10^{7}	7.7465×10^{7}	5.7271×10^{6}
	std	3.5687×10^{6}	5.2938×10^{6}	2.4235×10^{8}	4.8334×10^{6}	7.6595×10^{7}	5.9168×10^{6}	4.4739×10^{5}	3.8470×10^{7}	8.4524×10^{6}	2.4142×10^{7}	3.9670×10^{7}	2.2186×10^{6}
F13	mean	1.2751×10^{4}	2.5814×10^{4}	1.8918×10^{5}	1.1868×10^{4}	2.8370×10^{5}	2.6970×10^{4}	9.7380×10^{3}	9.9988×10^{4}	6.1412×10^{4}	1.2043×10^{6}	6.2828×10^{4}	1.4078×10^{4}
	std	7.1660×10^{3}	9.7975×10^{3}	2.8689×10^{5}	5.3545×10^{3}	1.5104×10^{5}	1.3628×10^{4}	8.3805×10^{3}	7.9215×10^{4}	2.9615×10^{4}	1.0510×10^{6}	2.7926×10^{4}	9.4802×10^{3}
F14	mean	5.8191×10^{4}	4.3885×10^{4}	2.4954×10^{5}	8.2212×10^{5}	3.7861×10^{5}	5.8073×10^{4}	8.5145×10^{3}	1.6377×10^{5}	1.7084×10^{5}	1.3961×10^{5}	1.7334×10^{5}	3.8521×10^{3}
	std	4.4948×10^{4}	2.8500×10^{4}	2.2991×10^{5}	8.2746×10^{5}	2.3789×10^{5}	4.5202×10^{4}	5.6275×10^{3}	1.0695×10^{5}	1.5435×10^{5}	9.2952×10^{4}	1.1627×10^{5}	1.3782×10^{3}
F15	mean	1.0505×10^{4}	2.1865×10^{4}	1.2014×10^{4}	7.4775×10^{3}	9.6154×10^{4}	9.2186×10^{3}	1.1876×10^{4}	2.1780×10^{4}	2.8255×10^{4}	1.0506×10^{5}	2.5170×10^{4}	1.5931×10^{4}
	std	8.3607×10^{3}	5.0263×10^{3}	6.3780×10^{3}	4.7407×10^{3}	9.2047×10^{4}	6.5229×10^{3}	8.1721×10^{3}	8.3806×10^{3}	1.5193×10^{4}	8.1751×10^{4}	9.7109×10^{3}	5.9578×10^{3}

Table 6. *Cont.*

ID	Metric	INFO	RUN	GRO	ESC	RIME	GKSO	RTH	FTO	BBO	IGWO	EDOA	MIEDOA
F16	mean	3.4053×10^{3}	3.2914×10^{3}	2.8921×10^{3}	3.3784×10^{3}	3.6939×10^{3}	3.5065×10^{3}	3.5478×10^{3}	3.0380×10^{3}	3.1559×10^{3}	2.7810×10^{3}	4.1414×10^{3}	3.0132×10^{3}
	std	5.8000×10^{2}	4.6818×10^{2}	4.2338×10^{2}	3.7785×10^{2}	3.8356×10^{2}	5.2674×10^{2}	4.0811×10^{2}	3.8084×10^{2}	3.7303×10^{2}	6.6237×10^{2}	7.2949×10^{2}	3.4633×10^{2}
F17	mean	3.3234×10^{3}	3.2682×10^{3}	2.6934×10^{3}	2.9639×10^{3}	3.2988×10^{3}	3.2396×10^{3}	3.5267×10^{3}	2.9223×10^{3}	3.0422×10^{3}	2.7841×10^{3}	3.7032×10^{3}	2.7893×10^{3}
	std	3.2433×10^{2}	3.4749×10^{2}	2.4221×10^{2}	2.7936×10^{2}	3.8933×10^{2}	3.2710×10^{2}	3.8280×10^{2}	3.6242×10^{2}	3.5831×10^{2}	4.9400×10^{2}	2.9446×10^{2}	2.2890×10^{2}
F18	mean	3.4243×10^{5}	1.1563×10^{5}	2.9832×10^{6}	3.7862×10^{6}	4.6213×10^{6}	3.6256×10^{5}	7.7529×10^{4}	5.3684×10^{5}	2.0587×10^{6}	1.2678×10^{6}	2.3463×10^{6}	1.4290×10^{5}
	std	3.0678×10^{5}	6.8458×10^{4}	2.6372×10^{6}	2.9217×10^{6}	3.3959×10^{6}	2.8213×10^{5}	4.2690×10^{4}	5.4608×10^{5}	1.1555×10^{6}	8.3775×10^{5}	1.4837×10^{6}	6.6740×10^{4}
F19	mean	1.5588×10^{4}	1.0183×10^{5}	2.4608×10^{4}	1.4589×10^{4}	2.6269×10^{5}	1.9742×10^{4}	1.7394×10^{4}	3.8093×10^{4}	3.0081×10^{4}	1.3251×10^{5}	1.5925×10^{6}	1.3663×10^{4}
	std	1.0766×10^{4}	7.1853×10^{4}	2.2754×10^{4}	6.5977×10^{3}	1.9202×10^{5}	1.1380×10^{4}	1.1524×10^{4}	1.2023×10^{4}	1.0172×10^{4}	8.6670×10^{4}	1.5092×10^{6}	7.9211×10^{3}
F20	mean	3.2317×10^{3}	3.0361×10^{3}	2.8337×10^{3}	3.1881×10^{3}	3.2084×10^{3}	3.1710×10^{3}	3.4873×10^{3}	3.2394×10^{3}	2.8724×10^{3}	3.1431×10^{3}	3.4939×10^{3}	2.9117×10^{3}
	std	3.7128×10^{2}	2.4064×10^{2}	2.5354×10^{2}	2.0820×10^{2}	3.0846×10^{2}	2.7459×10^{2}	2.9527×10^{2}	3.3267×10^{2}	2.2541×10^{2}	5.5429×10^{2}	4.1727×10^{2}	2.3610×10^{2}
F21	mean	2.5775×10^{3}	2.6026×10^{3}	2.5296×10^{3}	2.5413×10^{3}	2.5185×10^{3}	2.6405×10^{3}	2.6456×10^{3}	2.4664×10^{3}	2.4654×10^{3}	2.4602×10^{3}	2.8208×10^{3}	2.4082×10^{3}
	std	4.3895×10^{1}	4.7211×10^{1}	3.2704×10^{1}	3.5798×10^{1}	3.9023×10^{1}	4.9969×10^{1}	6.4352×10^{1}	2.7750×10^{1}	3.2329×10^{1}	6.7211×10^{1}	8.4432×10^{1}	3.2044×10^{1}
F22	mean	9.7244×10^{3}	1.0214×10^{4}	8.7059×10^{3}	1.4285×10^{4}	9.5927×10^{3}	9.5353×10^{3}	9.8765×10^{3}	1.1074×10^{4}	8.2961×10^{3}	1.2611×10^{4}	1.0169×10^{4}	9.2205×10^{3}
	std	1.2624×10^{3}	2.4027×10^{3}	2.9703×10^{3}	4.8388×10^{2}	1.6905×10^{3}	1.6376×10^{3}	9.8408×10^{2}	8.0812×10^{2}	1.4486×10^{3}	4.5172×10^{3}	1.7463×10^{3}	9.5297×10^{2}
F23	mean	3.1268×10^{3}	3.1331×10^{3}	3.0307×10^{3}	2.9508×10^{3}	3.0077×10^{3}	3.1555×10^{3}	3.1864×10^{3}	2.9759×10^{3}	2.9256×10^{3}	2.8862×10^{3}	4.2069×10^{3}	2.8608×10^{3}
	std	8.2643×10^{1}	1.0712×10^{2}	5.2331×10^{1}	4.4732×10^{1}	7.1139×10^{1}	9.5068×10^{1}	8.4963×10^{1}	5.0509×10^{1}	5.2843×10^{1}	6.7872×10^{1}	2.7069×10^{2}	3.3192×10^{1}
F24	mean	3.2574×10^{3}	3.1829×10^{3}	3.2082×10^{3}	3.1724×10^{3}	3.1374×10^{3}	3.3367×10^{3}	3.4149×10^{3}	3.1023×10^{3}	3.0786×10^{3}	3.0722×10^{3}	4.0507×10^{3}	3.0260×10^{3}
	std	8.4874×10^{1}	6.9935×10^{1}	5.2184×10^{1}	2.7026×10^{1}	5.2724×10^{1}	1.1597×10^{2}	1.2650×10^{2}	4.1351×10^{1}	4.3464×10^{1}	1.0251×10^{2}	3.6148×10^{2}	3.5501×10^{1}
F25	mean	3.1170×10^{3}	3.1132×10^{3}	3.6753×10^{3}	3.1264×10^{3}	3.1269×10^{3}	3.1013×10^{3}	3.0591×10^{3}	3.3070×10^{3}	3.0838×10^{3}	3.1905×10^{3}	3.1498×10^{3}	3.0461×10^{3}
	std	3.3569×10^{1}	2.3507×10^{1}	3.0727×10^{2}	3.9339×10^{1}	4.3309×10^{1}	2.3390×10^{1}	3.4095×10^{1}	8.5422×10^{1}	2.9387×10^{1}	8.8882×10^{1}	2.5970×10^{1}	2.9223×10^{1}
F26	mean	9.2278×10^{3}	1.1147×10^{4}	7.2731×10^{3}	5.5256×10^{3}	6.6356×10^{3}	7.8834×10^{3}	8.5935×10^{3}	6.5243×10^{3}	6.8930×10^{3}	5.6636×10^{3}	1.2456×10^{4}	5.1811×10^{3}
	std	1.4784×10^{3}	1.1412×10^{3}	1.6779×10^{3}	4.6269×10^{2}	4.9552×10^{2}	3.0890×10^{3}	2.5101×10^{3}	6.2446×10^{2}	1.5341×10^{3}	7.8846×10^{2}	9.9677×10^{2}	3.3846×10^{2}
F27	mean	3.6534×10^{3}	3.7856×10^{3}	3.6896×10^{3}	3.3953×10^{3}	3.5107×10^{3}	3.6794×10^{3}	3.5874×10^{3}	3.6241×10^{3}	3.3821×10^{3}	3.3431×10^{3}	5.5913×10^{3}	3.3977×10^{3}
	std	1.6523×10^{2}	1.1943×10^{2}	8.8764×10^{1}	5.0881×10^{1}	6.9922×10^{1}	1.4946×10^{2}	1.5344×10^{2}	7.0390×10^{1}	6.7757×10^{1}	6.2507×10^{1}	7.1049×10^{2}	9.7596×10^{1}
F28	mean	3.3979×10^{3}	3.3503×10^{3}	4.1441×10^{3}	3.5411×10^{3}	3.4144×10^{3}	3.3869×10^{3}	3.2982×10^{3}	5.2451×10^{3}	3.3426×10^{3}	3.5334×10^{3}	3.4472×10^{3}	3.3284×10^{3}
	std	5.1599×10^{1}	1.8124×10^{1}	2.3468×10^{2}	1.1500×10^{2}	4.7156×10^{1}	4.2015×10^{1}	3.7458×10^{1}	1.4420×10^{3}	3.4480×10^{1}	1.1677×10^{2}	5.2704×10^{1}	1.7427×10^{1}
F29	mean	4.9896×10^{3}	5.4053×10^{3}	4.5716×10^{3}	3.8221×10^{3}	4.8257×10^{3}	5.0627×10^{3}	4.9333×10^{3}	4.5796×10^{3}	4.3108×10^{3}	4.0305×10^{3}	6.6349×10^{3}	4.2762×10^{3}
	std	4.0424×10^{2}	5.0761×10^{2}	2.6498×10^{2}	2.0947×10^{2}	3.7224×10^{2}	2.9803×10^{2}	4.4623×10^{2}	3.2852×10^{2}	2.5601×10^{2}	4.4742×10^{2}	8.5533×10^{2}	3.6649×10^{2}
F30	mean	1.2382×10^{6}	1.2992×10^{7}	6.9687×10^{6}	1.3517×10^{6}	4.7708×10^{7}	1.3940×10^{7}	9.8070×10^{5}	1.4025×10^{7}	1.1303×10^{7}	1.6244×10^{7}	1.2504×10^{8}	3.3431×10^{6}
	std	4.7905×10^{5}	3.6045×10^{6}	3.7194×10^{6}	3.7963×10^{5}	1.6496×10^{7}	6.1312×10^{6}	1.6806×10^{5}	9.1297×10^{6}	1.8841×10^{6}	4.4477×10^{6}	1.7271×10^{7}	7.5164×10^{5}

Table 7. Performance Comparison of Algorithms on the CEC2017 Benchmark Functions (Dim = 100).

ID	Metric	INFO	RUN	GRO	ESC	RIME	GKSO	RTH	FTO	BBO	IGWO	EDOA	MIEDOA
F1	mean	4.0473×10^{9}	3.6245×10^{7}	6.5069×10^{10}	1.1636×10^{10}	5.3636×10^{8}	1.2550×10^{8}	1.7384×10^{4}	2.0676×10^{10}	1.5913×10^{7}	1.8615×10^{10}	1.0725×10^{8}	3.5172×10^{6}
	std	3.2737×10^{9}	1.7351×10^{7}	1.2507×10^{10}	4.7590×10^{9}	1.0137×10^{8}	4.3162×10^{7}	2.2804×10^{4}	7.0889×10^{9}	4.0312×10^{6}	6.9604×10^{9}	2.1151×10^{7}	1.2373×10^{6}
F2	mean	9.4834×10^{128}	1.8824×10^{139}	2.5676×10^{136}	1.2980×10^{123}	1.9171×10^{117}	2.4269×10^{121}	1.3038×10^{122}	5.6988×10^{130}	1.2514×10^{96}	7.5320×10^{110}	2.5637×10^{125}	6.5802×10^{99}
	std	5.1900×10^{129}	1.0310×10^{140}	1.4048×10^{137}	7.1010×10^{123}	7.8466×10^{117}	1.3293×10^{122}	7.1414×10^{122}	3.1158×10^{131}	6.7588×10^{96}	3.0219×10^{111}	1.2706×10^{126}	3.4538×10^{100}
F3	mean	3.0002×10^{5}	2.6081×10^{5}	3.6305×10^{5}	5.4495×10^{5}	6.1265×10^{5}	2.5471×10^{5}	1.4309×10^{5}	3.3273×10^{5}	3.5168×10^{5}	3.9068×10^{5}	4.0668×10^{5}	2.3306×10^{5}
	std	6.1815×10^{4}	2.7033×10^{4}	3.2788×10^{4}	6.2043×10^{4}	1.0285×10^{5}	1.8659×10^{4}	2.6710×10^{4}	5.7003×10^{4}	6.1410×10^{4}	6.2034×10^{4}	8.1927×10^{4}	1.9326×10^{4}
F4	mean	1.3191×10^{3}	1.0467×10^{3}	6.7256×10^{3}	1.6544×10^{3}	1.1234×10^{3}	1.0021×10^{3}	6.9522×10^{2}	3.1033×10^{3}	8.1390×10^{2}	2.1621×10^{3}	1.0364×10^{3}	8.2454×10^{2}
	std	2.9508×10^{2}	1.0124×10^{2}	1.4613×10^{3}	3.7549×10^{2}	1.0603×10^{2}	7.3761×10^{1}	5.6325×10^{1}	5.5169×10^{2}	4.5137×10^{1}	4.0830×10^{2}	1.0801×10^{2}	5.3654×10^{1}
F5	mean	1.2734×10^{3}	1.3241×10^{3}	1.3748×10^{3}	1.2108×10^{3}	1.1823×10^{3}	1.3135×10^{3}	1.2612×10^{3}	1.0461×10^{3}	1.0032×10^{3}	1.0317×10^{3}	1.3537×10^{3}	8.3384×10^{2}
	std	6.0198×10^{1}	3.8574×10^{1}	6.8173×10^{1}	6.1097×10^{1}	8.0642×10^{1}	4.9848×10^{1}	7.6532×10^{1}	6.6105×10^{1}	6.9467×10^{1}	9.7832×10^{1}	8.5924×10^{1}	5.4690×10^{1}
F6	mean	6.5668×10^{2}	6.6407×10^{2}	6.5143×10^{2}	6.0664×10^{2}	6.4676×10^{2}	6.6438×10^{2}	6.5525×10^{2}	6.5372×10^{2}	6.4231×10^{2}	6.1777×10^{2}	6.7087×10^{2}	6.1239×10^{2}
	std	4.9164×10^{0}	2.6404×10^{0}	5.6079×10^{0}	1.5273×10^{0}	7.6508×10^{0}	4.5631×10^{0}	3.3401×10^{0}	1.7066×10^{1}	5.8861×10^{0}	3.2731×10^{0}	4.3484×10^{0}	4.0077×10^{0}

Table 7. *Cont.*

ID	Metric	INFO	RUN	GRO	ESC	RIME	GKSO	RTH	FTO	BBO	IGWO	EDOA	MIEDOA
F7	mean	2.6445×10^{3}	2.8799×10^{3}	2.4122×10^{3}	1.7011×10^{3}	2.0049×10^{3}	2.5858×10^{3}	2.9168×10^{3}	1.9896×10^{3}	1.7808×10^{3}	1.6840×10^{3}	2.5352×10^{3}	1.2924×10^{3}
	std	1.8250×10^{2}	1.4117×10^{2}	1.8646×10^{2}	8.8307×10^{1}	1.7012×10^{2}	2.8806×10^{2}	2.1139×10^{2}	1.4023×10^{2}	1.9271×10^{2}	2.1337×10^{2}	2.8351×10^{2}	6.2755×10^{1}
F8	mean	1.6499×10^{3}	1.7322×10^{3}	1.6999×10^{3}	1.4913×10^{3}	1.5085×10^{3}	1.7015×10^{3}	1.6739×10^{3}	1.3615×10^{3}	1.3234×10^{3}	1.3309×10^{3}	1.7573×10^{3}	1.1296×10^{3}
	std	1.0021×10^{2}	7.9877×10^{1}	7.4028×10^{1}	7.3904×10^{1}	1.1921×10^{2}	9.8087×10^{1}	8.4656×10^{1}	6.1137×10^{1}	7.6778×10^{1}	9.1261×10^{1}	8.5143×10^{1}	5.5277×10^{1}
F9	mean	2.3139×10^{4}	2.3964×10^{4}	2.7978×10^{4}	6.7349×10^{3}	4.2612×10^{4}	2.5111×10^{4}	2.2248×10^{4}	2.6545×10^{4}	1.9483×10^{4}	2.6768×10^{4}	3.5545×10^{4}	6.9888×10^{3}
	std	2.6909×10^{3}	1.3307×10^{3}	3.7021×10^{3}	1.5706×10^{3}	1.5276×10^{4}	2.1574×10^{3}	1.0855×10^{3}	1.2956×10^{4}	3.0231×10^{3}	8.3813×10^{3}	5.6908×10^{3}	2.2744×10^{3}
F10	mean	1.6913×10^{4}	1.7019×10^{4}	2.1738×10^{4}	2.9329×10^{4}	1.8958×10^{4}	1.6597×10^{4}	1.6005×10^{4}	2.1029×10^{4}	1.4701×10^{4}	2.6098×10^{4}	1.8514×10^{4}	1.6258×10^{4}
	std	1.5617×10^{3}	4.1183×10^{3}	1.2554×10^{3}	8.4199×10^{2}	1.1231×10^{3}	1.1883×10^{3}	1.3861×10^{3}	2.2715×10^{3}	1.2692×10^{3}	7.3615×10^{3}	1.3959×10^{3}	1.3196×10^{3}
F11	mean	1.3956×10^{4}	4.5614×10^{3}	7.5385×10^{4}	7.7178×10^{4}	2.4050×10^{4}	6.1354×10^{3}	2.7695×10^{3}	1.8248×10^{4}	5.7932×10^{3}	2.2128×10^{4}	2.0507×10^{4}	2.4432×10^{4}
	std	5.1224×10^{3}	8.4400×10^{2}	1.4396×10^{4}	2.0378×10^{4}	6.7184×10^{3}	1.4249×10^{3}	4.2474×10^{2}	5.6376×10^{3}	1.0074×10^{3}	7.5095×10^{3}	8.1851×10^{3}	4.6885×10^{3}
F12	mean	1.4655×10^{8}	2.1337×10^{8}	8.1467×10^{9}	8.9447×10^{8}	9.9874×10^{8}	2.8404×10^{8}	7.0936×10^{6}	1.3520×10^{9}	2.0903×10^{8}	1.7512×10^{9}	6.1989×10^{8}	4.8332×10^{7}
	std	1.2077×10^{8}	6.7033×10^{7}	3.5587×10^{9}	9.1527×10^{8}	4.3062×10^{8}	1.3128×10^{8}	3.5589×10^{6}	8.8195×10^{8}	9.4549×10^{7}	9.9233×10^{8}	1.7323×10^{8}	2.0931×10^{7}
F13	mean	2.5077×10^{4}	8.1591×10^{4}	1.5858×10^{8}	7.4808×10^{6}	1.2530×10^{6}	5.5152×10^{4}	1.0019×10^{4}	1.7727×10^{6}	6.4090×10^{4}	1.2541×10^{7}	4.1524×10^{4}	9.5531×10^{3}
	std	8.5244×10^{3}	2.6302×10^{5}	3.9689×10^{8}	2.6988×10^{7}	6.3712×10^{5}	1.4593×10^{4}	8.5393×10^{3}	2.7071×10^{6}	3.2355×10^{4}	1.8383×10^{7}	9.9206×10^{3}	5.3356×10^{3}
F14	mean	8.1199×10^{5}	2.7274×10^{5}	5.0806×10^{6}	6.8339×10^{6}	5.9215×10^{6}	4.7038×10^{5}	1.0100×10^{5}	1.2248×10^{6}	2.2143×10^{6}	1.8783×10^{6}	2.8054×10^{6}	4.3667×10^{5}
	std	3.6658×10^{5}	7.8024×10^{4}	2.0086×10^{6}	3.6570×10^{6}	3.4713×10^{6}	1.7657×10^{5}	4.9504×10^{4}	5.7539×10^{5}	6.9362×10^{5}	1.2106×10^{6}	9.8098×10^{5}	1.9692×10^{5}
F15	mean	9.3038×10^{3}	1.9300×10^{4}	7.3673×10^{5}	4.0097×10^{4}	2.7338×10^{5}	2.7504×10^{4}	5.5414×10^{3}	7.1830×10^{4}	4.4295×10^{4}	8.5768×10^{5}	3.3689×10^{4}	4.3417×10^{3}
	std	6.4041×10^{3}	3.6252×10^{3}	1.1906×10^{6}	1.2703×10^{5}	1.1355×10^{5}	1.5962×10^{4}	5.8996×10^{3}	6.7576×10^{4}	1.9662×10^{4}	5.1667×10^{5}	1.0951×10^{4}	2.2350×10^{3}
F16	mean	6.4408×10^{3}	6.5561×10^{3}	6.8876×10^{3}	7.6020×10^{3}	7.0483×10^{3}	6.4092×10^{3}	6.2328×10^{3}	6.2484×10^{3}	5.6178×10^{3}	5.4131×10^{3}	9.4786×10^{3}	5.5814×10^{3}
	std	7.8621×10^{2}	6.2456×10^{2}	7.0670×10^{2}	6.1625×10^{2}	6.7982×10^{2}	7.0981×10^{2}	7.2262×10^{2}	7.8072×10^{2}	5.9760×10^{2}	9.7345×10^{2}	9.2050×10^{2}	6.7904×10^{2}
F17	mean	5.7561×10^{3}	5.8616×10^{3}	4.8826×10^{3}	5.5636×10^{3}	5.7376×10^{3}	5.5120×10^{3}	5.3953×10^{3}	5.1554×10^{3}	4.8613×10^{3}	4.4892×10^{3}	6.1645×10^{3}	4.7098×10^{3}
	std	7.1369×10^{2}	6.5793×10^{2}	4.8032×10^{2}	3.5764×10^{2}	5.4920×10^{2}	4.8477×10^{2}	6.3986×10^{2}	7.2231×10^{2}	4.8201×10^{2}	8.9666×10^{2}	5.1503×10^{2}	5.0517×10^{2}
F18	mean	1.3756×10^{6}	3.0654×10^{5}	5.2177×10^{6}	8.2502×10^{6}	8.9017×10^{6}	7.5523×10^{5}	4.4277×10^{5}	2.5562×10^{6}	3.5034×10^{6}	3.4469×10^{6}	3.5202×10^{6}	7.6539×10^{5}
	std	7.4958×10^{5}	1.1064×10^{5}	2.4971×10^{6}	4.4516×10^{6}	5.3012×10^{6}	3.2335×10^{5}	2.6795×10^{5}	1.2964×10^{6}	1.2315×10^{6}	1.8274×10^{6}	1.6122×10^{6}	3.4201×10^{5}
F19	mean	7.8615×10^{3}	3.6106×10^{5}	1.2996×10^{6}	1.9147×10^{4}	1.3993×10^{7}	1.1087×10^{5}	4.8729×10^{3}	4.9290×10^{5}	3.5672×10^{5}	3.3383×10^{6}	5.6091×10^{6}	6.7114×10^{3}
	std	6.4335×10^{3}	2.7948×10^{5}	1.2494×10^{6}	1.9513×10^{4}	1.0013×10^{7}	1.2489×10^{5}	3.8160×10^{3}	2.5281×10^{5}	2.7313×10^{5}	2.1568×10^{6}	5.2173×10^{6}	6.2663×10^{3}
F20	mean	5.4106×10^{3}	5.0978×10^{3}	4.9009×10^{3}	6.3474×10^{3}	5.6952×10^{3}	5.4310×10^{3}	5.5312×10^{3}	6.1031×10^{3}	4.7851×10^{3}	6.3562×10^{3}	6.0082×10^{3}	5.1589×10^{3}
	std	6.0898×10^{2}	4.2485×10^{2}	3.4990×10^{2}	2.8452×10^{2}	5.0201×10^{2}	5.7121×10^{2}	6.1262×10^{2}	6.8980×10^{2}	5.0556×10^{2}	1.3444×10^{3}	4.7634×10^{2}	4.4679×10^{2}
F21	mean	3.1590×10^{3}	3.0696×10^{3}	3.1545×10^{3}	3.0348×10^{3}	3.0567×10^{3}	3.3018×10^{3}	3.3239×10^{3}	2.8335×10^{3}	2.8057×10^{3}	2.8470×10^{3}	4.1405×10^{3}	2.6470×10^{3}
	std	1.1151×10^{2}	1.0365×10^{2}	5.8663×10^{1}	6.3401×10^{1}	1.0195×10^{2}	1.4341×10^{2}	1.5566×10^{2}	6.8146×10^{1}	6.6549×10^{1}	1.3623×10^{2}	2.0754×10^{2}	5.7748×10^{1}
F22	mean	2.0453×10^{4}	2.2138×10^{4}	2.3248×10^{4}	3.1587×10^{4}	2.1933×10^{4}	1.9866×10^{4}	1.9018×10^{4}	2.2825×10^{4}	1.7606×10^{4}	3.0723×10^{4}	2.1580×10^{4}	1.8661×10^{4}
	std	1.8158×10^{3}	6.1364×10^{3}	3.8244×10^{3}	6.9023×10^{2}	1.5959×10^{3}	1.5861×10^{3}	1.7717×10^{3}	1.4480×10^{3}	1.9533×10^{3}	5.7858×10^{3}	1.9286×10^{3}	1.6687×10^{3}
F23	mean	3.8198×10^{3}	3.5779×10^{3}	3.8951×10^{3}	3.1914×10^{3}	3.5459×10^{3}	3.8817×10^{3}	3.8500×10^{3}	3.5318×10^{3}	3.3814×10^{3}	3.3304×10^{3}	5.8749×10^{3}	3.1802×10^{3}
	std	1.4454×10^{2}	8.1217×10^{1}	8.8800×10^{1}	5.4428×10^{1}	7.2576×10^{1}	1.4617×10^{2}	1.4160×10^{2}	9.1201×10^{1}	7.7451×10^{1}	1.5025×10^{2}	3.8558×10^{2}	4.9765×10^{1}
F24	mean	4.5785×10^{3}	4.4966×10^{3}	4.8749×10^{3}	3.8955×10^{3}	4.0384×10^{3}	4.7593×10^{3}	4.6339×10^{3}	4.2487×10^{3}	3.8354×10^{3}	3.8292×10^{3}	6.0305×10^{3}	3.6816×10^{3}
	std	2.9046×10^{2}	1.6246×10^{2}	1.6348×10^{2}	1.1029×10^{2}	1.2767×10^{2}	1.6874×10^{2}	2.0852×10^{2}	1.1438×10^{2}	7.9878×10^{1}	7.6935×10^{1}	8.0512×10^{2}	5.5232×10^{1}
F25	mean	3.9196×10^{3}	3.6312×10^{3}	7.2758×10^{3}	4.5758×10^{3}	3.8142×10^{3}	3.6996×10^{3}	3.3547×10^{3}	5.2296×10^{3}	3.4850×10^{3}	4.6938×10^{3}	3.7220×10^{3}	3.5121×10^{3}
	std	1.6846×10^{2}	4.5088×10^{1}	1.0430×10^{3}	3.2442×10^{2}	8.3779×10^{1}	7.8716×10^{1}	6.3038×10^{1}	3.8450×10^{2}	5.4258×10^{1}	4.1724×10^{2}	7.3667×10^{1}	6.0002×10^{1}
F26	mean	2.1768×10^{4}	2.8351×10^{4}	2.4117×10^{4}	1.2147×10^{4}	1.4035×10^{4}	2.2134×10^{4}	2.1315×10^{4}	1.6012×10^{4}	1.4793×10^{4}	1.2711×10^{4}	3.0157×10^{4}	9.9803×10^{3}
	std	3.0207×10^{3}	2.0136×10^{3}	2.2256×10^{3}	1.1122×10^{3}	2.0854×10^{3}	3.9137×10^{3}	2.6970×10^{3}	1.2798×10^{3}	2.7727×10^{3}	9.7845×10^{2}	3.1327×10^{3}	6.9716×10^{2}
F27	mean	3.9896×10^{3}	4.5296×10^{3}	4.4266×10^{3}	3.7358×10^{3}	3.9207×10^{3}	4.2134×10^{3}	3.7108×10^{3}	4.0813×10^{3}	3.6488×10^{3}	3.6393×10^{3}	8.6979×10^{3}	3.5450×10^{3}
	std	2.1798×10^{2}	3.3493×10^{2}	1.3996×10^{2}	8.4433×10^{1}	1.2213×10^{2}	2.5514×10^{2}	1.2215×10^{2}	1.5982×10^{2}	7.5464×10^{1}	6.0142×10^{1}	2.8683×10^{3}	8.4423×10^{1}
F28	mean	4.1911×10^{3}	3.7500×10^{3}	1.0098×10^{4}	6.6143×10^{3}	4.0039×10^{3}	3.7810×10^{3}	3.4742×10^{3}	1.7249×10^{4}	3.5655×10^{3}	5.4755×10^{3}	3.8332×10^{3}	3.6137×10^{3}
	std	3.0260×10^{2}	5.3124×10^{1}	1.3793×10^{3}	9.1420×10^{2}	1.4879×10^{2}	8.2605×10^{1}	2.7025×10^{1}	4.3628×10^{2}	4.6151×10^{1}	7.2830×10^{2}	6.3911×10^{1}	3.8911×10^{1}
F29	mean	8.1867×10^{3}	1.0517×10^{4}	8.3659×10^{3}	7.0608×10^{3}	8.9659×10^{3}	9.0960×10^{3}	7.3285×10^{3}	8.6606×10^{3}	7.5926×10^{3}	6.8117×10^{3}	1.2067×10^{4}	7.1543×10^{3}
	std	5.4008×10^{2}	1.0360×10^{3}	6.7455×10^{2}	6.5889×10^{2}	8.9983×10^{2}	6.7765×10^{2}	5.8140×10^{2}	6.9868×10^{2}	6.0970×10^{2}	3.7559×10^{2}	9.0357×10^{2}	6.9395×10^{2}
F30	mean	8.3876×10^{5}	1.3711×10^{7}	5.4382×10^{7}	2.1942×10^{7}	1.2959×10^{8}	1.2008×10^{7}	1.5573×10^{4}	5.8127×10^{7}	8.2030×10^{6}	5.5572×10^{7}	1.2249×10^{8}	4.0154×10^{5}
	std	6.0372×10^{5}	4.3061×10^{6}	3.1998×10^{7}	4.0949×10^{7}	6.7285×10^{7}	9.2878×10^{6}	9.7761×10^{3}	3.3982×10^{7}	4.6382×10^{6}	2.5992×10^{7}	3.3387×10^{7}	2.1426×10^{5}

Tables 5–7 present the performance comparison results of all algorithms on the CEC2017 benchmark functions under 30-, 50-, and 100-dimensional settings. From the results, it can be observed that MIEDOA generally achieves competitive performance across different problem dimensions and maintains relatively stable optimization results on many benchmark functions. In the 30-dimensional case, MIEDOA obtains the best or near-best results on a considerable number of functions while exhibiting relatively small standard deviations. As the dimensionality increases to 50 and 100, the optimization difficulty becomes more challenging, and the performance differences among algorithms become more apparent. Under these higher-dimensional settings, MIEDOA continues to maintain competitive mean fitness values and satisfactory stability on many functions, whereas some comparative algorithms show larger performance degradation or fluctuations. Overall, the results in Tables 5–7 suggest that MIEDOA is capable of maintaining effective optimization performance across different dimensional scenarios and exhibits good adaptability when dealing with increasingly complex optimization problems.

Figure 6 presents the boxplot-based performance comparison of the competing algorithms on the CEC2017 benchmark functions. The boxplots provide a visual representation of the distribution characteristics, stability, and robustness of each algorithm over multiple independent runs. It can be observed that MIEDOA generally exhibits relatively lower median fitness values and narrower interquartile ranges on many benchmark functions, indicating that the algorithm is capable of producing competitive solutions with good consistency. In addition, the distribution of MIEDOA is relatively concentrated on several functions, suggesting reduced performance fluctuations across repeated runs. In contrast, some comparative algorithms show wider box distributions and a larger number of outliers on certain functions, reflecting greater sensitivity to random initialization and search stochasticity. Overall, the boxplot results suggest that MIEDOA maintains satisfactory stability and robustness while achieving competitive optimization performance on the CEC2017 benchmark suite.

3.4. Comparison of the CEC2020 Test Functions

To evaluate the effectiveness of the proposed MIEDOA, extensive numerical experiments were conducted on the CEC2020 benchmark suite. The performance of MIEDOA was compared with 11 state-of-the-art algorithms based on the mean and standard deviation obtained from 30 independent runs. To further assess the convergence behavior, Figure 7 illustrates the convergence curves of MIEDOA and the competing algorithms on selected functions under two different dimensional settings. In addition, Figure 8 presents the boxplot distributions of the results over 30 independent runs, providing a more comprehensive evaluation of the stability and robustness of each algorithm. Furthermore, Tables 8 and 9 summarize the detailed performance results of all 12 algorithms on the CEC2020 benchmark functions in two dimensions. In these tables, “Mean” represents the average fitness value obtained across 30 runs, while “Std” denotes the corresponding standard deviation, reflecting the stability of the algorithms.

Figure 7 illustrates the convergence behavior of different algorithms on the CEC2020 benchmark functions, which are generally more challenging due to stronger variable coupling and higher nonlinearity. From the figure, it can be observed that MIEDOA generally exhibits a relatively fast convergence speed during the early stages and maintains a stable optimization trend throughout the later iterations, suggesting a reasonable balance between global exploration and local exploitation. Compared with several competing algorithms, MIEDOA is often able to reach lower fitness values within fewer iterations and obtain competitive final solutions on many benchmark functions. In contrast, some comparative algorithms show slower convergence behavior or experience premature stagnation on certain functions, particularly hybrid and composition

functions, indicating difficulties in escaping local optima. Under increased problem complexity, MIEDOA still exhibits relatively stable convergence characteristics, suggesting good adaptability to challenging optimization landscapes. Overall, the results in Figure 7 indicate that MIEDOA possesses competitive convergence behavior and optimization capability on the CEC2020 benchmark suite.

Tables 8 and 9 present the performance comparison of all algorithms on the CEC2020 benchmark functions under 10-dimensional and 20-dimensional settings. From the results, it can be observed that MIEDOA achieves competitive performance on a considerable number of test functions, demonstrating satisfactory optimization capability and stability. In the 10-dimensional case, MIEDOA obtains the best or near-best mean values on several functions such as F1, F2, F5, and F7, while also exhibiting relatively small standard deviations, indicating good robustness over multiple independent runs. Although the performance differences among algorithms are relatively limited on some functions (e.g., F3, F4, F8, F9, and F10), MIEDOA generally maintains results comparable to those of the competing methods.

As the problem dimension increases to 20, the complexity of the optimization landscape becomes more pronounced, and the performance differences among algorithms become more evident. Under this scenario, MIEDOA remains competitive on several complex functions, particularly F5 and F7, where some comparative algorithms exhibit noticeable performance degradation or larger fluctuations. Moreover, MIEDOA frequently achieves relatively low mean values and moderate standard deviations on many functions, suggesting satisfactory robustness and adaptability to higher-dimensional optimization problems. In contrast, certain algorithms, such as GRO and RIME, produce larger mean errors and variances on some difficult functions, indicating relatively weaker stability under these conditions.

Overall, the results in Tables 8 and 9 suggest that MIEDOA is capable of achieving a favorable balance between solution quality and stability across different problem dimensions. Its performance under both low- and medium-dimensional settings indicates that the proposed algorithm has good applicability to complex optimization problems.

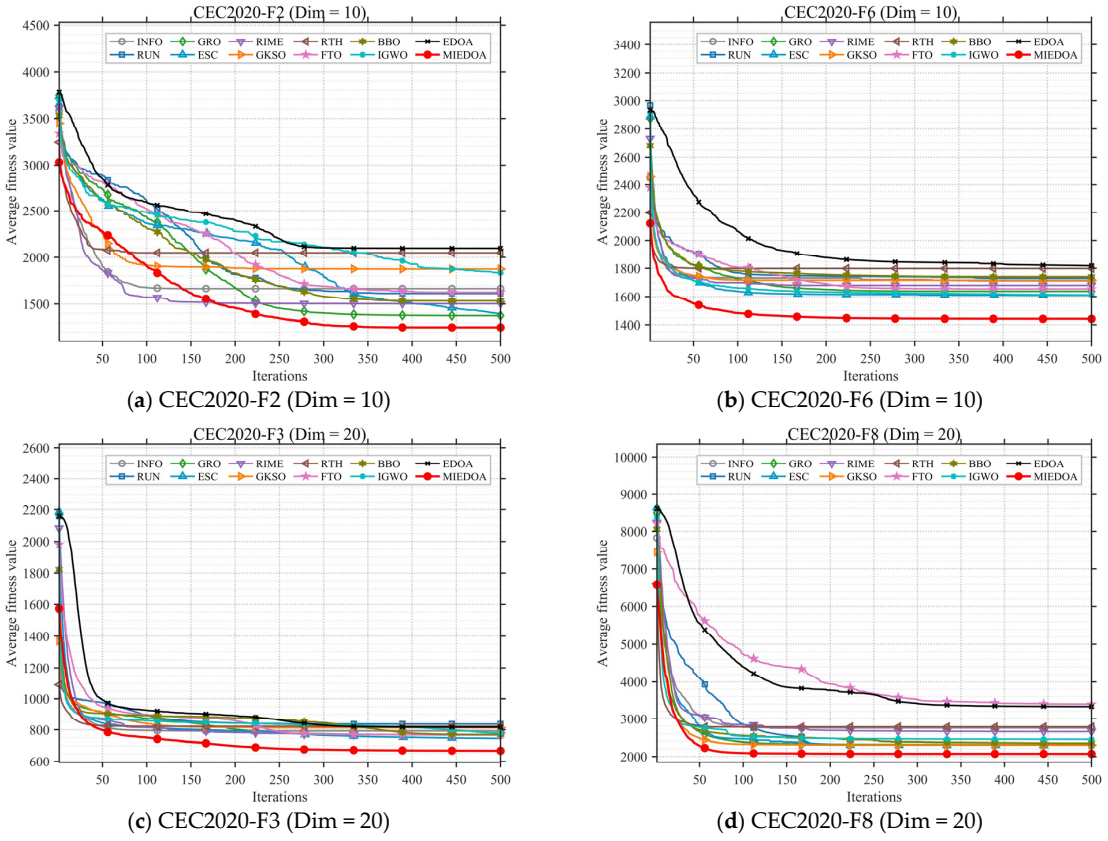
Figure 8 illustrates the boxplot-based performance comparison on the CEC2020 benchmark functions, providing a visualization of the distribution characteristics and stability of each algorithm over multiple independent runs. It can be observed that MIEDOA generally exhibits lower median fitness values and relatively narrower interquartile ranges on many functions, indicating competitive optimization accuracy and consistency. Moreover, its boxplots are often more compact, with relatively fewer outliers and shorter whiskers, suggesting reduced sensitivity to random initialization. In contrast, several comparative algorithms display wider distributions and a larger number of outliers on some hybrid and composition functions, reflecting greater performance variability. As the complexity of the benchmark functions increases, these differences become more noticeable in certain cases, while MIEDOA generally maintains a relatively concentrated performance distribution. Overall, the results suggest that MIEDOA is capable of producing high-quality solutions with satisfactory stability across multiple independent runs.

Table 8. Performance Comparison of Algorithms on the CEC2020 Benchmark Functions (Dim = 10).

ID	Metric	INFO	RUN	GRO	ESC	RIME	GKSO	RTH	FTO	BBO	IGWO	EDOA	MIEDOA
F1	mean	1.0001×10^{2}	3.2670×10^{3}	2.2806×10^{3}	1.7294×10^{3}	1.7306×10^{4}	2.5208×10^{3}	3.9736×10^{2}	7.1110×10^{3}	8.5732×10^{2}	4.9396×10^{4}	1.0001×10^{2}	3.2670×10^{3}
	std	2.3898×10^{-2}	2.1103×10^{3}	1.8517×10^{3}	1.7094×10^{3}	1.3595×10^{4}	3.0935×10^{3}	3.5499×10^{2}	4.9358×10^{3}	8.4568×10^{2}	2.3139×10^{4}	2.3898×10^{-2}	2.1103×10^{3}
F2	mean	1.6667×10^{3}	1.6148×10^{3}	1.3745×10^{3}	1.3882×10^{3}	1.5028×10^{3}	1.8735×10^{3}	2.0493×10^{3}	1.6275×10^{3}	1.5345×10^{3}	1.8305×10^{3}	1.6667×10^{3}	1.6148×10^{3}
	std	2.8218×10^{2}	3.1450×10^{2}	1.6293×10^{2}	1.6264×10^{2}	2.2479×10^{2}	3.3287×10^{2}	3.0920×10^{2}	2.2111×10^{2}	2.6205×10^{2}	3.9801×10^{2}	2.8218×10^{2}	3.1450×10^{2}
F3	mean	7.3448×10^{2}	7.5313×10^{2}	7.2052×10^{2}	7.1951×10^{2}	7.2511×10^{2}	7.3513×10^{2}	7.5309×10^{2}	7.2578×10^{2}	7.2709×10^{2}	7.2760×10^{2}	7.3448×10^{2}	7.5313×10^{2}
	std	9.3785×10^{0}	1.2450×10^{1}	6.0930×10^{0}	2.4885×10^{0}	6.4655×10^{0}	1.1295×10^{1}	1.5128×10^{1}	7.4381×10^{0}	5.7165×10^{0}	8.0932×10^{0}	9.3785×10^{0}	1.2450×10^{1}
F4	mean	1.9014×10^{3}	1.9024×10^{3}	1.9008×10^{3}	1.9014×10^{3}	1.9015×10^{3}	1.9013×10^{3}	1.9027×10^{3}	1.9011×10^{3}	1.9012×10^{3}	1.9024×10^{3}	1.9014×10^{3}	1.9024×10^{3}
	std	8.3238×10^{-1}	2.0559×10^{0}	2.8986×10^{-1}	2.8975×10^{-1}	7.9475×10^{-1}	5.5674×10^{-1}	1.5378×10^{0}	5.0577×10^{-1}	8.3388×10^{-1}	5.2331×10^{-1}	8.3238×10^{-1}	2.0559×10^{0}
F5	mean	2.1298×10^{3}	3.0822×10^{3}	3.9891×10^{3}	6.8684×10^{3}	6.7181×10^{3}	2.2667×10^{3}	2.1576×10^{3}	3.3552×10^{3}	3.6460×10^{3}	4.0328×10^{3}	2.1298×10^{3}	3.0822×10^{3}
	std	2.1941×10^{2}	7.6104×10^{2}	1.7327×10^{3}	5.1763×10^{3}	5.4710×10^{3}	2.4522×10^{2}	2.2487×10^{2}	1.1835×10^{3}	1.6386×10^{3}	2.0231×10^{3}	2.1941×10^{2}	7.6104×10^{2}
F6	mean	1.7135×10^{3}	1.7316×10^{3}	1.6382×10^{3}	1.6101×10^{3}	1.6808×10^{3}	1.7171×10^{3}	1.7988×10^{3}	1.6555×10^{3}	1.7405×10^{3}	1.6126×10^{3}	1.7135×10^{3}	1.7316×10^{3}
	std	9.0481×10^{1}	8.9155×10^{1}	5.5515×10^{1}	3.0132×10^{1}	7.5398×10^{1}	9.3586×10^{1}	1.2233×10^{2}	6.3233×10^{1}	7.0116×10^{1}	2.9313×10^{1}	9.0481×10^{1}	8.9155×10^{1}
F7	mean	2.3538×10^{3}	3.2052×10^{3}	2.6518×10^{3}	3.8805×10^{3}	6.3200×10^{3}	2.2404×10^{3}	2.4837×10^{3}	2.2672×10^{3}	5.6482×10^{3}	2.6520×10^{3}	2.3538×10^{3}	3.2052×10^{3}
	std	1.7416×10^{2}	2.2894×10^{3}	4.3036×10^{2}	3.5097×10^{3}	5.1400×10^{3}	1.1999×10^{2}	2.1347×10^{2}	8.4262×10^{1}	3.2026×10^{3}	2.2544×10^{2}	1.7416×10^{2}	2.2894×10^{3}
F8	mean	2.3004×10^{3}	2.3068×10^{3}	2.3009×10^{3}	2.3004×10^{3}	2.2964×10^{3}	2.2965×10^{3}	2.3021×10^{3}	2.2947×10^{3}	2.2999×10^{3}	2.3059×10^{3}	2.3004×10^{3}	2.3068×10^{3}
	std	1.2496×10^{1}	4.0337×10^{0}	4.6575×10^{-1}	3.2876×10^{-1}	2.2285×10^{1}	1.9126×10^{1}	1.2131×10^{1}	2.3795×10^{1}	1.6758×10^{1}	7.9759×10^{-1}	1.2496×10^{1}	4.0337×10^{0}
F9	mean	2.7400×10^{3}	2.7193×10^{3}	2.6821×10^{3}	2.7381×10^{3}	2.7403×10^{3}	2.6954×10^{3}	2.7623×10^{3}	2.7354×10^{3}	2.7392×10^{3}	2.7151×10^{3}	2.7400×10^{3}	2.7193×10^{3}
	std	6.6260×10^{1}	7.4553×10^{1}	9.5621×10^{1}	3.6167×10^{0}	4.5839×10^{1}	1.1029×10^{2}	1.2853×10^{1}	4.4884×10^{1}	7.1174×10^{0}	7.3785×10^{1}	6.6260×10^{1}	7.4553×10^{1}
F10	mean	2.9353×10^{3}	2.9244×10^{3}	2.9171×10^{3}	2.9342×10^{3}	2.9136×10^{3}	2.9272×10^{3}	2.9301×10^{3}	2.9324×10^{3}	2.9304×10^{3}	2.9023×10^{3}	2.9353×10^{3}	2.9244×10^{3}
	std	2.0485×10^{1}	2.3587×10^{1}	2.2397×10^{1}	2.1073×10^{1}	6.3801×10^{1}	3.4905×10^{1}	2.4285×10^{1}	2.2073×10^{1}	2.1163×10^{1}	1.3312×10^{1}	2.0485×10^{1}	2.3587×10^{1}

Table 9. Performance Comparison of Algorithms on the CEC2020 Benchmark Functions (Dim = 20).

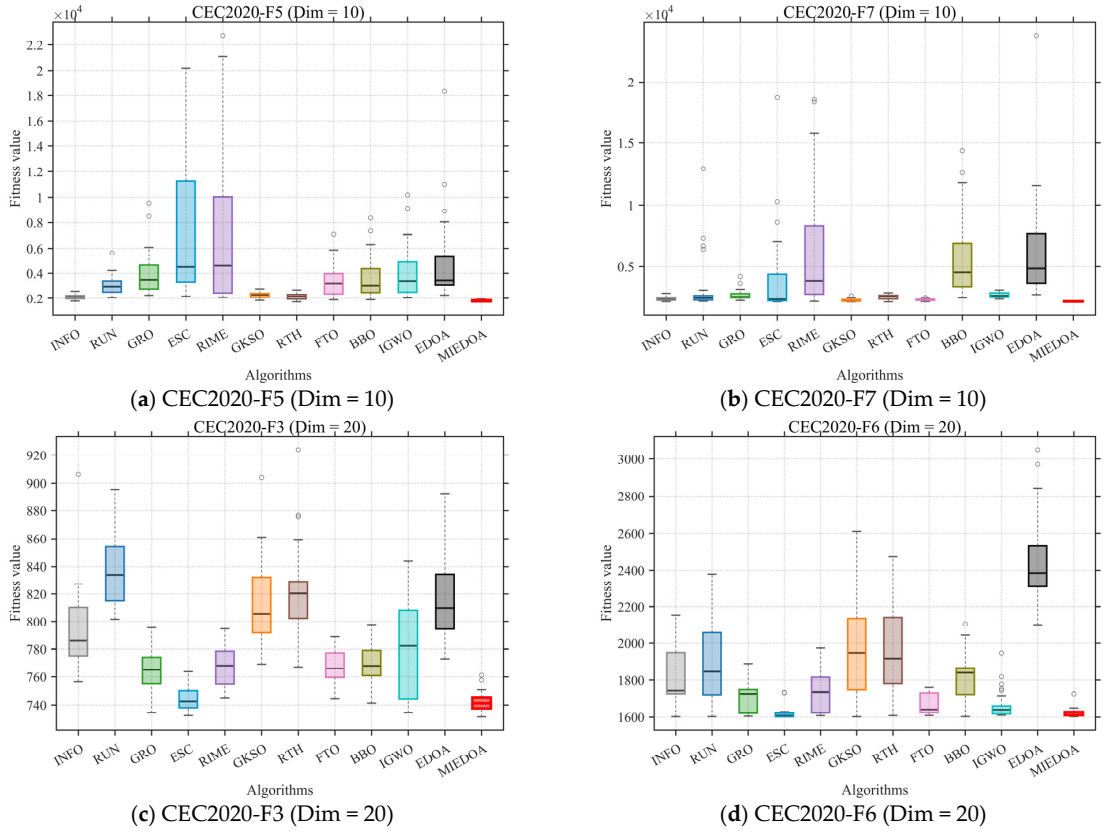
ID	Metric	INFO	RUN	GRO	ESC	RIME	GKSO	RTH	FTO	BBO	IGWO	EDOA	MIEDOA
F1	mean	1.1019×10^{2}	3.4804×10^{3}	3.8681×10^{6}	1.5770×10^{3}	2.5433×10^{5}	2.1690×10^{3}	1.5098×10^{3}	4.3496×10^{3}	2.9260×10^{3}	2.2674×10^{5}	1.1019×10^{2}	3.4804×10^{3}
	std	1.8082×10^{1}	4.9431×10^{3}	8.1395×10^{6}	1.4483×10^{3}	1.1564×10^{5}	2.5589×10^{3}	1.8332×10^{3}	3.8384×10^{3}	2.6295×10^{3}	9.3786×10^{4}	1.8082×10^{1}	4.9431×10^{3}
F2	mean	2.4730×10^{3}	2.3776×10^{3}	2.3453×10^{3}	2.1249×10^{3}	1.9683×10^{3}	2.6801×10^{3}	2.9110×10^{3}	2.1737×10^{3}	2.2596×10^{3}	3.4376×10^{3}	2.4730×10^{3}	2.3776×10^{3}
	std	4.1588×10^{2}	4.3482×10^{2}	4.3901×10^{2}	4.6993×10^{2}	2.6631×10^{2}	4.4631×10^{2}	4.8982×10^{2}	3.3749×10^{2}	3.1277×10^{2}	1.1596×10^{3}	4.1588×10^{2}	4.3482×10^{2}
F3	mean	7.9239×10^{2}	8.3636×10^{2}	7.6664×10^{2}	7.4449×10^{2}	7.6689×10^{2}	8.1299×10^{2}	8.2187×10^{2}	7.6784×10^{2}	7.6984×10^{2}	7.7888×10^{2}	7.9239×10^{2}	8.3636×10^{2}
	std	2.9780×10^{1}	2.5624×10^{1}	1.4351×10^{1}	8.5773×10^{0}	1.3325×10^{1}	2.8599×10^{1}	3.2000×10^{1}	1.1169×10^{1}	1.4643×10^{1}	3.5393×10^{1}	2.9780×10^{1}	2.5624×10^{1}
F4	mean	1.9080×10^{3}	1.9172×10^{3}	1.9060×10^{3}	1.9044×10^{3}	1.9054×10^{3}	1.9073×10^{3}	1.9104×10^{3}	1.9044×10^{3}	1.9031×10^{3}	1.9080×10^{3}	1.9080×10^{3}	1.9172×10^{3}
	std	5.0715×10^{0}	7.3807×10^{0}	2.4753×10^{0}	6.5121×10^{-1}	1.2142×10^{0}	2.8778×10^{0}	6.2683×10^{0}	1.0872×10^{0}	1.0104×10^{0}	2.0700×10^{0}	5.0715×10^{0}	7.3807×10^{0}
F5	mean	1.9542×10^{4}	1.3298×10^{4}	1.6911×10^{5}	4.4293×10^{5}	3.7354×10^{5}	1.3950×10^{4}	5.2738×10^{3}	1.4586×10^{4}	1.7977×10^{5}	9.6285×10^{4}	1.9542×10^{4}	1.3298×10^{4}
	std	1.7066×10^{4}	6.5220×10^{3}	1.0597×10^{5}	5.5383×10^{5}	2.3751×10^{5}	1.0804×10^{4}	3.1568×10^{3}	1.0186×10^{4}	1.0838×10^{5}	6.4643×10^{4}	1.7066×10^{4}	6.5220×10^{3}
F6	mean	1.8126×10^{3}	1.8867×10^{3}	1.7206×10^{3}	1.6189×10^{3}	1.7385×10^{3}	1.9571×10^{3}	1.9564×10^{3}	1.6664×10^{3}	1.8183×10^{3}	1.6667×10^{3}	1.8126×10^{3}	1.8867×10^{3}
	std	1.4439×10^{2}	2.0401×10^{2}	8.9260×10^{1}	3.2175×10^{1}	1.0743×10^{2}	2.4434×10^{2}	2.1955×10^{2}	5.4456×10^{1}	1.2336×10^{2}	7.4760×10^{1}	1.4439×10^{2}	2.0401×10^{2}
F7	mean	5.7481×10^{3}	7.5998×10^{3}	6.3220×10^{4}	1.2549×10^{5}	1.7572×10^{5}	5.5909×10^{3}	3.3386×10^{3}	9.3480×10^{3}	6.7757×10^{4}	2.0261×10^{4}	5.7481×10^{3}	7.5998×10^{3}
	std	3.3204×10^{3}	2.3420×10^{3}	5.5905×10^{4}	1.4552×10^{5}	1.7507×10^{5}	3.3851×10^{3}	4.6743×10^{2}	5.2700×10^{3}	5.1633×10^{4}	1.7759×10^{4}	3.3204×10^{3}	2.3420×10^{3}
F8	mean	2.7517×10^{3}	2.3017×10^{3}	2.3083×10^{3}	2.3003×10^{3}	2.6555×10^{3}	2.3001×10^{3}	2.7796×10^{3}	3.3979×10^{3}	2.3517×10^{3}	2.4463×10^{3}	2.7517×10^{3}	2.3017×10^{3}
	std	9.3443×10^{2}	2.4404×10^{0}	3.3939×10^{0}	1.2594×10^{0}	8.4777×10^{2}	4.4732×10^{0}	1.0953×10^{3}	1.4910×10^{3}	2.7687×10^{2}	7.7141×10^{2}	9.3443×10^{2}	2.4404×10^{0}
F9	mean	2.8876×10^{3}	2.8537×10^{3}	2.8290×10^{3}	2.8483×10^{3}	2.8524×10^{3}	2.8770×10^{3}	2.9147×10^{3}	2.8433×10^{3}	2.8343×10^{3}	2.8220×10^{3}	2.8876×10^{3}	2.8537×10^{3}
	std	2.9156×10^{1}	2.4058×10^{1}	1.4952×10^{1}	1.0859×10^{1}	2.0154×10^{1}	2.6134×10^{1}	4.2580×10^{1}	1.2301×10^{1}	1.1318×10^{1}	1.9658×10^{1}	2.9156×10^{1}	2.4058×10^{1}
F10	mean	2.9655×10^{3}	2.9798×10^{3}	2.9614×10^{3}	2.9309×10^{3}	2.9549×10^{3}	2.9506×10^{3}	2.9577×10^{3}	2.9712×10^{3}	2.9498×10^{3}	2.9159×10^{3}	2.9655×10^{3}	2.9798×10^{3}
	std	3.4912×10^{1}	3.5551×10^{1}	3.2510×10^{1}	2.6618×10^{1}	3.0081×10^{1}	3.2803×10^{1}	3.5011×10^{1}	3.2306×10^{1}	3.3655×10^{1}	9.9543×10^{0}	3.4912×10^{1}	3.5551×10^{1}



(**a**) CEC2020-F2 (Dim = 10) (**b**) CEC2020-F6 (Dim = 10)

(**c**) CEC2020-F3 (Dim = 20) (**d**) CEC2020-F8 (Dim = 20)

Figure 7. Convergence Behavior of Different Algorithms on the CEC2020 Benchmark Functions.



(**a**) CEC2020-F5 (Dim = 10) (**b**) CEC2020-F7 (Dim = 10)

(**c**) CEC2020-F3 (Dim = 20) (**d**) CEC2020-F6 (Dim = 20)

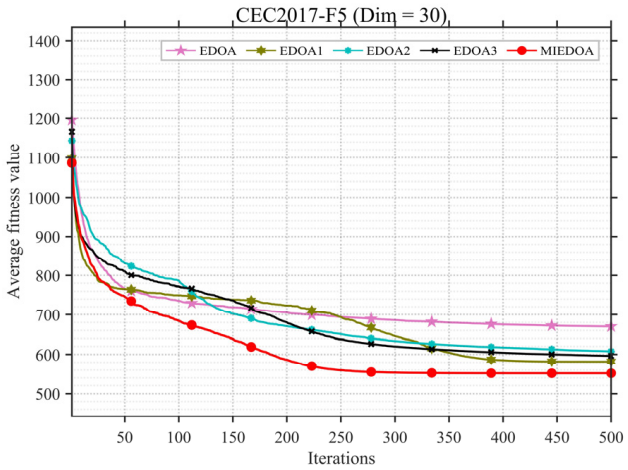
Figure 8. Boxplot-Based Performance Comparison on the CEC2020 Benchmark Functions.

3.5. Analysis of Strategy Effectiveness

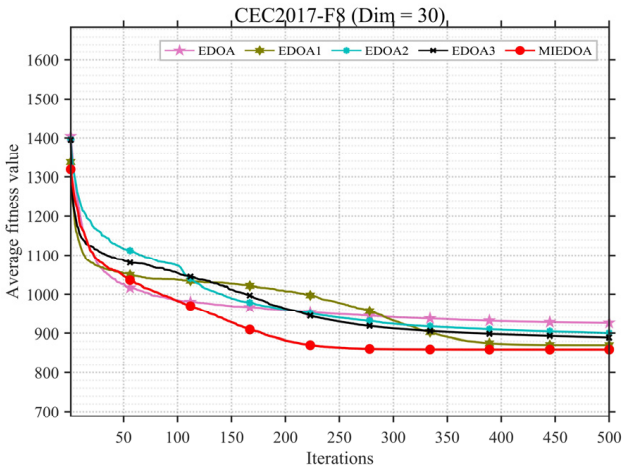
Analyzing strategy effectiveness is crucial for evaluating the performance of improved heuristic algorithms, as it provides deep insights into the specific contributions of each proposed strategy. Although overall experimental results can demonstrate an algorithm's superiority, they often fail to reveal precisely how individual strategies influence the optimization process. By systematically analyzing strategy effectiveness, we can quantify the specific impact of each component on convergence speed, solution accuracy, and robustness. This not only helps validate the rationality and necessity of the proposed improvements but also mitigates the risk of redundancy or inefficiency that may arise from the indiscriminate stacking of strategies. Furthermore, such analysis enhances the interpretability of the algorithm's design, providing a more compelling justification for its demonstrated performance advantages. Therefore, in this subsection, we conduct an analysis of strategy effectiveness for the proposed MIEDOA. Specifically, EDOA1 denotes the algorithm incorporating the Strategic Diversification Initialization (SDI) strategy into the original framework; EDOA2 denotes the algorithm incorporating the Organizational Synergy Learning (OSL) strategy; and EDOA3 denotes the algorithm incorporating the Adaptive Governance with Feedback Regulation strategy. The experimental results are presented below.

Figure 9 presents the results of the strategy effectiveness analysis, which aims to evaluate the contributions of the three proposed strategies to the overall performance of MIEDOA. It can be observed that the variants incorporating different improvement strategies exhibit varying optimization behaviors across the benchmark functions, indicating that each strategy influences the search process from a different perspective. Compared with the original EDOA and the partially improved variants, the complete MIEDOA generally achieves more competitive results on many test functions, suggesting that the combined use of SDI, OSL, and AGFR contributes to enhancing the overall search capability of the algorithm. Furthermore, the performance differences among the variants imply that population initialization, collaborative learning, and adaptive search regulation each play a role in improving optimization performance. Overall, the results indicate that the three strategies provide complementary effects, and their coordinated integration is beneficial for maintaining a balance between exploration and exploitation across different optimization scenarios.

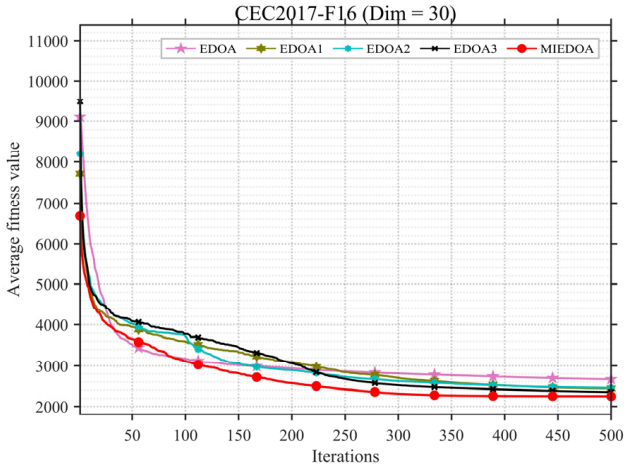
Tables 10–12 present the ablation experiment results of MIEDOA and its variants on the CEC2017 benchmark functions under 30-, 50-, and 100-dimensional settings. From the results, it can be observed that the optimization performance varies when different strategies are removed, indicating that each proposed component contributes to the overall search process to some extent. In many benchmark functions, the complete MIEDOA generally achieves more competitive mean results and maintains relatively stable performance across different dimensions. The variants incorporating only part of the proposed strategies are still able to improve upon the original EDOA on certain functions; however, their performance may become less consistent as the problem dimensionality increases. Moreover, the performance differences among the variants suggest that SDI, OSL, and AGFR contribute from different aspects, including population initialization, search guidance, and adaptive regulation. As the dimensionality increases from 30 to 100, the advantages of combining multiple strategies become more apparent on several complex functions, where the complete MIEDOA often maintains comparatively favorable optimization results. Overall, the ablation results indicate that the three strategies provide complementary contributions and that their coordinated integration is beneficial for enhancing the robustness and optimization capability of the proposed algorithm across different problem scales.



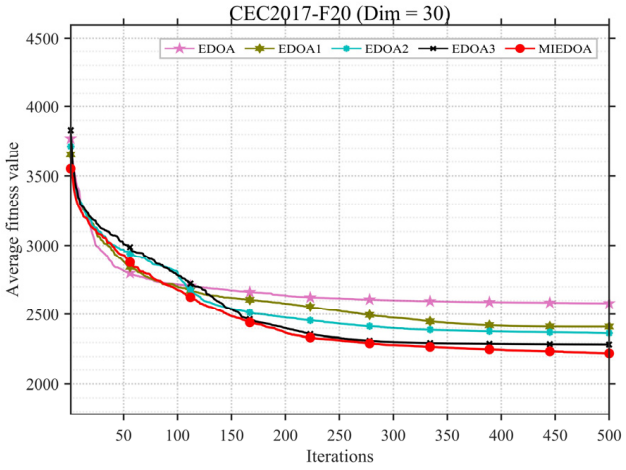
(**a**) CEC2017-F5 (Dim = 30)



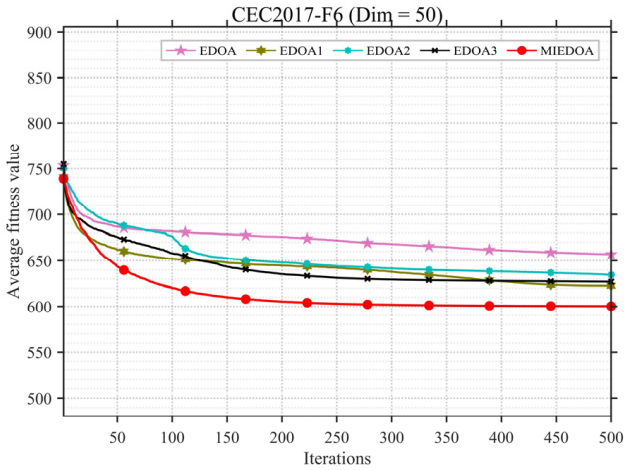
(**b**) CEC2017-F8 (Dim = 30)



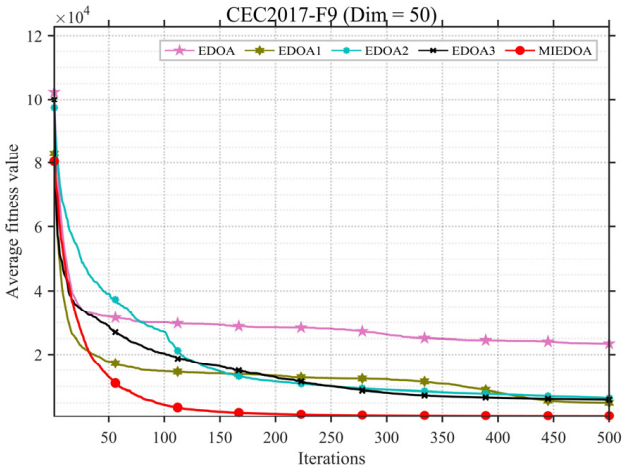
(**c**) CEC2017-F16 (Dim = 30)



(**d**) CEC2017-F20 (Dim = 30)

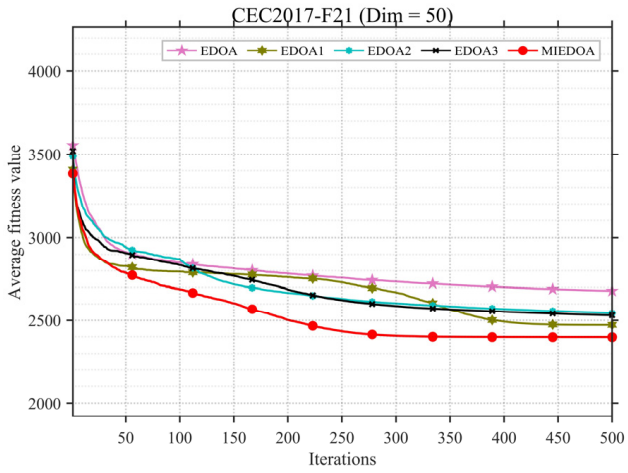


(**e**) CEC2017-F6 (Dim = 50)

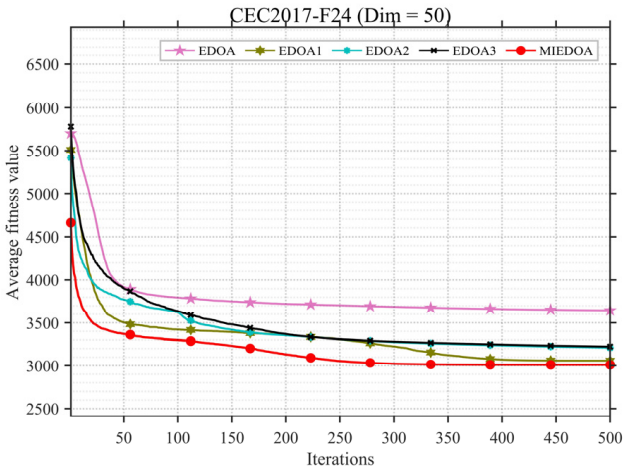


(**f**) CEC2017-F9 (Dim = 50)

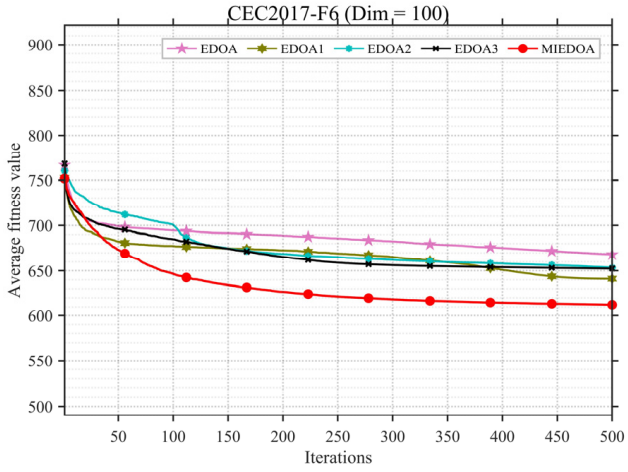
Figure 9. *Cont.*



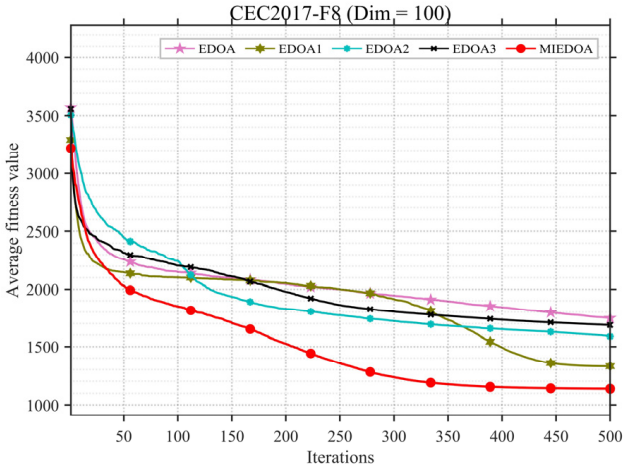
(**g**) CEC2017-F21 (Dim = 50)



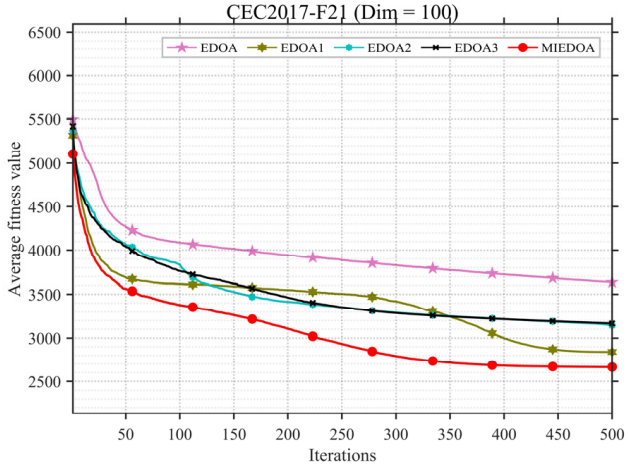
(**h**) CEC2017-F24 (Dim = 50)



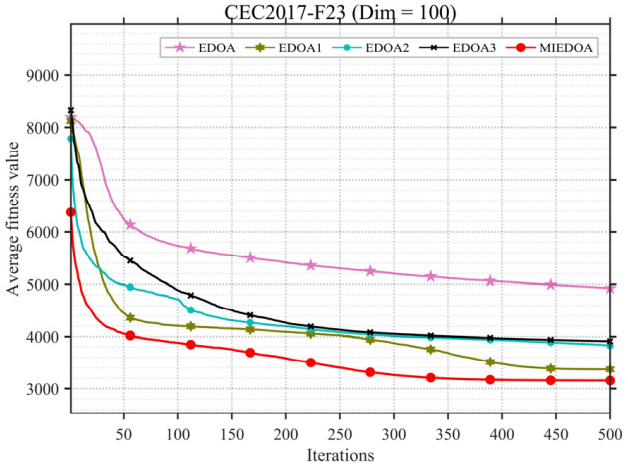
(**i**) CEC2017-F6 (Dim = 100)



(**j**) CEC2017-F8 (Dim = 100)



(**k**) CEC2017-F21 (Dim = 100)



(**l**) CEC2017-F23 (Dim = 100)

Figure 9. Experimental Results of Strategy Effectiveness Analysis.

Table 10. Results of Ablation Experiments on the CEC2017 Benchmark Functions (Dim = 30).

ID	Metric	EDOA	EDOA1	EDOA2	EDOA3	MIEDOA
F1	mean	2.4871×10^{6}	2.7492×10^{4}	4.7020×10^{7}	1.8345×10^{8}	4.1917×10^{3}
	std	1.2281×10^{6}	1.8614×10^{4}	3.6815×10^{7}	2.3338×10^{8}	4.4201×10^{3}
F2	mean	2.8300×10^{12}	3.7576×10^{12}	5.5795×10^{20}	5.2787×10^{25}	7.4797×10^{12}
	std	5.3389×10^{12}	1.3260×10^{13}	2.2740×10^{21}	2.7224×10^{26}	1.8020×10^{13}

Table 10. *Cont.*

ID	Metric	EDOA	EDOA1	EDOA2	EDOA3	MIEDOA
F3	mean	2.8896×10^{4}	4.9540×10^{3}	3.5541×10^{3}	4.8163×10^{4}	1.2251×10^{3}
	std	1.0251×10^{4}	3.1608×10^{3}	1.9738×10^{3}	6.2459×10^{3}	4.4238×10^{2}
F4	mean	4.7438×10^{2}	5.0251×10^{2}	5.2006×10^{2}	5.4592×10^{2}	4.9254×10^{2}
	std	2.3155×10^{1}	1.8951×10^{1}	1.3424×10^{1}	1.8656×10^{1}	1.1526×10^{1}
F5	mean	6.6463×10^{2}	5.8260×10^{2}	6.0624×10^{2}	5.9420×10^{2}	5.5346×10^{2}
	std	3.1408×10^{1}	1.9951×10^{1}	3.0612×10^{1}	2.0104×10^{1}	1.6967×10^{1}
F6	mean	6.4618×10^{2}	6.0882×10^{2}	6.1605×10^{2}	6.1004×10^{2}	6.0006×10^{2}
	std	7.0024×10^{0}	6.0473×10^{0}	4.1497×10^{0}	3.9793×10^{0}	1.3656×10^{-2}
F7	mean	9.0782×10^{2}	8.5043×10^{2}	8.5504×10^{2}	8.5108×10^{2}	7.8716×10^{2}
	std	5.8183×10^{1}	4.4541×10^{1}	2.7767×10^{1}	2.9253×10^{1}	1.2195×10^{1}
F8	mean	9.2201×10^{2}	8.6722×10^{2}	9.0862×10^{2}	8.8667×10^{2}	8.5833×10^{2}
	std	2.0979×10^{1}	1.5096×10^{1}	2.2863×10^{1}	2.0459×10^{1}	1.9686×10^{1}
F9	mean	5.1952×10^{3}	1.5311×10^{3}	1.7691×10^{3}	1.5579×10^{3}	9.0149×10^{2}
	std	1.5337×10^{3}	3.9141×10^{2}	4.7107×10^{2}	3.8061×10^{2}	3.6548×10^{0}
F10	mean	5.0717×10^{3}	4.3097×10^{3}	4.7973×10^{3}	4.6689×10^{3}	4.9583×10^{3}
	std	7.3684×10^{2}	5.4415×10^{2}	6.1786×10^{2}	5.3159×10^{2}	6.3095×10^{2}
F11	mean	1.2270×10^{3}	1.2530×10^{3}	1.2665×10^{3}	1.3177×10^{3}	1.1836×10^{3}
	std	3.9579×10^{1}	4.5135×10^{1}	3.8585×10^{1}	4.1458×10^{1}	3.6411×10^{1}
F12	mean	2.1055×10^{6}	1.7895×10^{6}	9.1346×10^{5}	1.5847×10^{6}	3.0611×10^{5}
	std	1.4090×10^{6}	8.4021×10^{5}	8.0579×10^{5}	8.9191×10^{5}	1.7822×10^{5}
F13	mean	3.1262×10^{4}	3.7897×10^{4}	1.3592×10^{4}	2.0688×10^{4}	2.9966×10^{4}
	std	2.2755×10^{4}	1.4269×10^{4}	7.5080×10^{3}	1.6295×10^{4}	1.3942×10^{4}
F14	mean	3.3959×10^{4}	1.5968×10^{4}	1.5245×10^{3}	2.9959×10^{4}	1.6195×10^{3}
	std	4.5154×10^{4}	1.3161×10^{4}	1.8824×10^{1}	3.6678×10^{4}	3.9119×10^{1}
F15	mean	1.3112×10^{4}	1.1038×10^{4}	2.1359×10^{3}	8.0525×10^{3}	2.7049×10^{3}
	std	1.4344×10^{4}	6.7827×10^{3}	4.3957×10^{2}	5.8883×10^{3}	4.9018×10^{2}
F16	mean	2.8009×10^{3}	2.3980×10^{3}	2.4241×10^{3}	2.2934×10^{3}	2.2195×10^{3}
	std	3.0610×10^{2}	3.0415×10^{2}	2.3649×10^{2}	2.2424×10^{2}	2.0373×10^{2}
F17	mean	2.3335×10^{3}	2.0610×10^{3}	2.0124×10^{3}	1.8628×10^{3}	1.8890×10^{3}
	std	1.9423×10^{2}	1.7128×10^{2}	1.2782×10^{2}	6.7943×10^{1}	1.1048×10^{2}
F18	mean	8.7324×10^{5}	5.7670×10^{5}	2.1967×10^{3}	2.8248×10^{5}	1.7099×10^{4}
	std	9.3184×10^{5}	4.7418×10^{5}	1.1363×10^{2}	2.4133×10^{5}	6.9473×10^{3}
F19	mean	9.5446×10^{3}	8.3345×10^{3}	2.0520×10^{3}	6.5384×10^{3}	2.4140×10^{3}
	std	8.6794×10^{3}	5.4430×10^{3}	4.7430×10^{1}	5.3726×10^{3}	2.1677×10^{2}
F20	mean	2.5875×10^{3}	2.4496×10^{3}	2.3791×10^{3}	2.3028×10^{3}	2.2528×10^{3}
	std	1.7992×10^{2}	1.3133×10^{2}	1.0171×10^{2}	8.8090×10^{1}	1.3075×10^{2}
F21	mean	2.4707×10^{3}	2.3746×10^{3}	2.4085×10^{3}	2.3788×10^{3}	2.3558×10^{3}
	std	2.7631×10^{1}	2.1028×10^{1}	2.6652×10^{1}	1.5688×10^{1}	1.7157×10^{1}
F22	mean	4.9684×10^{3}	2.5188×10^{3}	2.5915×10^{3}	2.3852×10^{3}	2.9413×10^{3}
	std	2.1081×10^{3}	8.2782×10^{2}	8.7272×10^{2}	9.2166×10^{1}	1.4802×10^{3}
F23	mean	3.1213×10^{3}	2.7486×10^{3}	2.7674×10^{3}	2.7426×10^{3}	2.7079×10^{3}
	std	1.0934×10^{2}	2.9347×10^{1}	2.5972×10^{1}	2.5728×10^{1}	1.4865×10^{1}
F24	mean	3.1851×10^{3}	2.8900×10^{3}	2.9327×10^{3}	2.9181×10^{3}	2.8790×10^{3}
	std	9.4239×10^{1}	2.6527×10^{1}	2.8156×10^{1}	2.7451×10^{1}	1.5106×10^{1}
F25	mean	2.9037×10^{3}	2.9023×10^{3}	2.9128×10^{3}	2.9510×10^{3}	2.8872×10^{3}
	std	2.4142×10^{1}	1.8950×10^{1}	1.6757×10^{1}	2.0067×10^{1}	7.0152×10^{-1}
F26	mean	5.9760×10^{3}	3.9947×10^{3}	4.6571×10^{3}	4.3344×10^{3}	4.2256×10^{3}
	std	1.9563×10^{3}	1.0778×10^{3}	5.6629×10^{2}	6.1560×10^{2}	1.9378×10^{2}
F27	mean	3.3897×10^{3}	3.2332×10^{3}	3.2359×10^{3}	3.2557×10^{3}	3.2141×10^{3}
	std	2.4033×10^{2}	1.8719×10^{1}	1.4927×10^{1}	1.5248×10^{1}	1.1685×10^{1}
F28	mean	3.2446×10^{3}	3.2213×10^{3}	3.2839×10^{3}	3.3170×10^{3}	3.2227×10^{3}
	std	2.0613×10^{1}	2.0819×10^{1}	2.8998×10^{1}	3.3060×10^{1}	2.3951×10^{1}
F29	mean	4.1955×10^{3}	3.6867×10^{3}	3.8627×10^{3}	3.7411×10^{3}	3.6196×10^{3}
	std	3.0505×10^{2}	1.7565×10^{2}	1.6824×10^{2}	1.1280×10^{2}	1.7307×10^{2}
F30	mean	8.7046×10^{4}	9.9673×10^{4}	2.5710×10^{4}	5.3162×10^{4}	3.6062×10^{4}
	std	6.7647×10^{4}	7.1344×10^{4}	1.1702×10^{4}	3.5398×10^{4}	2.0341×10^{4}

Table 11. Results of Ablation Experiments on the CEC2017 Benchmark Functions (Dim = 50).

ID	Metric	EDOA	EDOA1	EDOA2	EDOA3	MIEDOA
F1	mean	3.1403×10^{7}	5.4634×10^{5}	1.3784×10^{9}	6.0557×10^{9}	8.1930×10^{3}
	std	9.2911×10^{6}	3.7085×10^{5}	5.3097×10^{8}	2.7836×10^{9}	6.0760×10^{3}
F2	mean	3.3229×10^{26}	2.8702×10^{29}	8.2429×10^{48}	3.3909×10^{50}	2.7235×10^{32}
	std	1.4333×10^{27}	1.4971×10^{30}	4.4684×10^{49}	1.2788×10^{51}	1.2113×10^{33}

Table 11. *Cont.*

ID	Metric	EDOA	EDOA1	EDOA2	EDOA3	MIEDOA
F3	mean	1.3021×10^{5}	5.7335×10^{4}	4.8441×10^{4}	1.3169×10^{5}	5.8910×10^{4}
	std	2.5183×10^{4}	1.8049×10^{4}	1.4029×10^{4}	1.8128×10^{4}	1.3342×10^{4}
F4	mean	5.6014×10^{2}	5.8152×10^{2}	7.6492×10^{2}	1.2890×10^{3}	5.6876×10^{2}
	std	5.3735×10^{1}	4.1572×10^{1}	6.3753×10^{1}	4.9130×10^{2}	4.8805×10^{1}
F5	mean	8.0867×10^{2}	6.7225×10^{2}	7.4455×10^{2}	7.6181×10^{2}	6.1750×10^{2}
	std	4.4666×10^{1}	4.0291×10^{1}	4.3056×10^{1}	3.8651×10^{1}	2.4631×10^{1}
F6	mean	6.5649×10^{2}	6.2281×10^{2}	6.3321×10^{2}	6.2731×10^{2}	6.0032×10^{2}
	std	6.1621×10^{0}	8.0158×10^{0}	7.7194×10^{0}	5.2633×10^{0}	1.7147×10^{-1}
F7	mean	1.1855×10^{3}	1.0361×10^{3}	1.1029×10^{3}	1.1357×10^{3}	8.7743×10^{2}
	std	7.7296×10^{1}	6.8001×10^{1}	4.6837×10^{1}	7.2367×10^{1}	2.8792×10^{1}
F8	mean	1.0929×10^{3}	9.7735×10^{2}	1.0478×10^{3}	1.0681×10^{3}	9.1433×10^{2}
	std	2.7216×10^{1}	2.8185×10^{1}	4.0454×10^{1}	3.2063×10^{1}	3.3556×10^{1}
F9	mean	2.4772×10^{4}	5.2356×10^{3}	6.5030×10^{3}	5.6878×10^{3}	1.0443×10^{3}
	std	5.4561×10^{3}	1.6592×10^{3}	2.0129×10^{3}	1.5790×10^{3}	1.7845×10^{2}
F10	mean	7.6249×10^{3}	6.7452×10^{3}	8.7992×10^{3}	8.8598×10^{3}	7.9187×10^{3}
	std	1.1445×10^{3}	1.0392×10^{3}	6.8097×10^{2}	6.7145×10^{2}	1.0532×10^{3}
F11	mean	1.3907×10^{3}	1.3642×10^{3}	1.5880×10^{3}	2.9303×10^{3}	1.3584×10^{3}
	std	6.3525×10^{1}	5.9972×10^{1}	1.4798×10^{2}	6.6941×10^{2}	6.1113×10^{1}
F12	mean	2.6242×10^{7}	1.3696×10^{7}	5.2371×10^{7}	8.9215×10^{7}	4.9593×10^{6}
	std	1.9433×10^{7}	8.4708×10^{6}	5.3893×10^{7}	5.6766×10^{7}	2.4366×10^{6}
F13	mean	1.1226×10^{5}	5.7903×10^{4}	8.0841×10^{4}	2.1231×10^{5}	1.3652×10^{4}
	std	4.6136×10^{4}	2.3813×10^{4}	3.0960×10^{4}	3.6119×10^{5}	8.1772×10^{3}
F14	mean	1.9416×10^{5}	1.5404×10^{5}	1.7817×10^{3}	2.4793×10^{5}	4.4759×10^{3}
	std	1.4084×10^{5}	1.1606×10^{5}	5.1064×10^{1}	2.0729×10^{5}	2.2761×10^{3}
F15	mean	2.2907×10^{4}	2.3757×10^{4}	1.1228×10^{4}	1.2100×10^{4}	1.6673×10^{4}
	std	1.4651×10^{4}	9.8516×10^{3}	4.8209×10^{3}	6.3449×10^{3}	7.9940×10^{3}
F16	mean	3.4708×10^{3}	3.0662×10^{3}	3.4286×10^{3}	2.9678×10^{3}	3.1719×10^{3}
	std	4.7843×10^{2}	3.7037×10^{2}	3.8421×10^{2}	3.3713×10^{2}	3.5249×10^{2}
F17	mean	3.0895×10^{3}	3.0635×10^{3}	3.1803×10^{3}	2.7921×10^{3}	2.7872×10^{3}
	std	3.9666×10^{2}	2.4607×10^{2}	3.3528×10^{2}	2.5401×10^{2}	2.0658×10^{2}
F18	mean	2.2571×10^{6}	1.7858×10^{6}	5.2764×10^{4}	2.4488×10^{6}	1.4732×10^{5}
	std	1.3462×10^{6}	1.1713×10^{6}	8.8823×10^{4}	1.2289×10^{6}	5.7095×10^{4}
F19	mean	2.0683×10^{4}	3.4647×10^{4}	1.2056×10^{4}	1.9864×10^{4}	1.3900×10^{4}
	std	1.1486×10^{4}	1.7833×10^{4}	8.8373×10^{3}	1.0884×10^{4}	7.7647×10^{3}
F20	mean	3.2445×10^{3}	2.9808×10^{3}	3.1291×10^{3}	2.8688×10^{3}	2.9168×10^{3}
	std	3.4770×10^{2}	2.8840×10^{2}	2.7652×10^{2}	1.8775×10^{2}	2.4133×10^{2}
F21	mean	2.6907×10^{3}	2.4528×10^{3}	2.5530×10^{3}	2.5282×10^{3}	2.4063×10^{3}
	std	4.6988×10^{1}	2.8723×10^{1}	5.0106×10^{1}	3.5297×10^{1}	2.2122×10^{1}
F22	mean	9.5211×10^{3}	8.6329×10^{3}	1.0554×10^{4}	8.9007×10^{3}	9.2859×10^{3}
	std	9.3610×10^{2}	1.6863×10^{3}	7.1945×10^{2}	3.0609×10^{3}	1.0223×10^{3}
F23	mean	3.6855×10^{3}	2.9282×10^{3}	3.0478×10^{3}	3.0243×10^{3}	2.8509×10^{3}
	std	1.9884×10^{2}	5.1666×10^{1}	6.4592×10^{1}	5.1632×10^{1}	2.7726×10^{1}
F24	mean	3.5875×10^{3}	3.0673×10^{3}	3.2166×10^{3}	3.2311×10^{3}	3.0167×10^{3}
	std	1.2244×10^{2}	3.3733×10^{1}	5.9724×10^{1}	4.0681×10^{1}	2.5003×10^{1}
F25	mean	3.0307×10^{3}	3.0812×10^{3}	3.2503×10^{3}	3.6583×10^{3}	3.0505×10^{3}
	std	4.3905×10^{1}	3.1511×10^{1}	6.3987×10^{1}	2.8376×10^{2}	3.0662×10^{1}
F26	mean	8.1937×10^{3}	6.9493×10^{3}	6.9725×10^{3}	7.3961×10^{3}	5.0671×10^{3}
	std	3.8375×10^{3}	1.5863×10^{3}	5.5075×10^{2}	1.2264×10^{3}	3.3420×10^{2}
F27	mean	4.0491×10^{3}	3.3935×10^{3}	3.5756×10^{3}	3.7271×10^{3}	3.3893×10^{3}
	std	7.5643×10^{2}	7.3327×10^{1}	1.1471×10^{2}	1.1343×10^{2}	8.9294×10^{1}
F28	mean	3.3118×10^{3}	3.3435×10^{3}	3.6037×10^{3}	4.1978×10^{3}	3.3252×10^{3}
	std	3.8380×10^{1}	3.4763×10^{1}	1.2177×10^{2}	2.1076×10^{2}	2.3376×10^{1}
F29	mean	5.1294×10^{3}	4.3476×10^{3}	4.8344×10^{3}	4.4789×10^{3}	4.2688×10^{3}
	std	2.7660×10^{2}	2.5841×10^{2}	4.1234×10^{2}	2.3477×10^{2}	2.7463×10^{2}
F30	mean	2.1586×10^{7}	1.1545×10^{7}	8.9163×10^{6}	5.9602×10^{6}	3.6382×10^{6}
	std	6.7401×10^{6}	2.6686×10^{6}	2.9369×10^{6}	2.5011×10^{6}	8.8543×10^{5}

Table 12. Results of Ablation Experiments on the CEC2017 Benchmark Functions (Dim = 100).

ID	Metric	EDOA	EDOA1	EDOA2	EDOA3	MIEDOA
F1	mean	2.8499×10^{8}	1.5963×10^{7}	1.8788×10^{10}	6.2967×10^{10}	3.5787×10^{6}
	std	3.9114×10^{7}	5.8744×10^{6}	3.7920×10^{9}	1.1800×10^{10}	1.3492×10^{6}
F2	mean	8.4311×10^{83}	1.9413×10^{96}	1.5905×10^{127}	1.3630×10^{135}	1.6090×10^{100}
	std	2.9762×10^{84}	8.6613×10^{96}	8.5522×10^{127}	7.4381×10^{135}	8.7634×10^{100}

Table 12. *Cont.*

ID	Metric	EDOA	EDOA1	EDOA2	EDOA3	MIEDOA
F3	mean	4.1363×10^{5}	3.5074×10^{5}	1.9572×10^{5}	3.6005×10^{5}	2.3621×10^{5}
	std	4.7328×10^{4}	5.2867×10^{4}	2.4293×10^{4}	3.6020×10^{4}	2.4084×10^{4}
F4	mean	8.1736×10^{2}	8.1428×10^{2}	2.4723×10^{3}	7.4092×10^{3}	8.1649×10^{2}
	std	7.9097×10^{1}	5.2306×10^{1}	5.5612×10^{2}	1.0156×10^{3}	6.6862×10^{1}
F5	mean	1.3247×10^{3}	9.8757×10^{2}	1.2857×10^{3}	1.3540×10^{3}	8.4213×10^{2}
	std	5.0195×10^{1}	6.1406×10^{1}	8.0920×10^{1}	4.9036×10^{1}	5.8352×10^{1}
F6	mean	6.6773×10^{2}	6.4082×10^{2}	6.5417×10^{2}	6.5388×10^{2}	6.1376×10^{2}
	std	3.0250×10^{0}	4.9055×10^{0}	5.9814×10^{0}	5.6973×10^{0}	5.7509×10^{0}
F7	mean	2.1232×10^{3}	1.8176×10^{3}	2.1635×10^{3}	2.4097×10^{3}	1.3303×10^{3}
	std	1.2335×10^{2}	1.7635×10^{2}	1.2083×10^{2}	1.3187×10^{2}	8.8795×10^{1}
F8	mean	1.7347×10^{3}	1.3173×10^{3}	1.5889×10^{3}	1.6792×10^{3}	1.1187×10^{3}
	std	6.5869×10^{1}	8.1576×10^{1}	6.5337×10^{1}	8.9992×10^{1}	5.5885×10^{1}
F9	mean	6.3663×10^{4}	1.9023×10^{4}	2.8800×10^{4}	2.9622×10^{4}	7.7020×10^{3}
	std	8.1704×10^{3}	2.6513×10^{3}	4.4965×10^{3}	4.1793×10^{3}	2.2103×10^{3}
F10	mean	1.7997×10^{4}	1.4079×10^{4}	2.1782×10^{4}	2.1556×10^{4}	1.6254×10^{4}
	std	1.3328×10^{3}	1.3010×10^{3}	1.1647×10^{3}	1.5155×10^{3}	1.4753×10^{3}
F11	mean	2.1180×10^{4}	6.1656×10^{3}	2.2573×10^{4}	8.1269×10^{4}	2.5122×10^{4}
	std	5.7470×10^{3}	1.2973×10^{3}	8.0864×10^{3}	1.4443×10^{4}	5.3177×10^{3}
F12	mean	4.1095×10^{8}	1.5248×10^{8}	1.9003×10^{9}	6.8874×10^{9}	4.2885×10^{7}
	std	1.7374×10^{8}	6.4967×10^{7}	6.1800×10^{8}	2.4035×10^{9}	2.1169×10^{7}
F13	mean	1.7959×10^{6}	6.4741×10^{4}	3.1518×10^{7}	9.1834×10^{7}	7.2660×10^{3}
	std	8.1281×10^{5}	1.9380×10^{4}	2.5306×10^{7}	1.1370×10^{8}	4.8199×10^{3}
F14	mean	2.5012×10^{6}	2.2174×10^{6}	1.3757×10^{5}	4.4601×10^{6}	4.8636×10^{5}
	std	1.0456×10^{6}	1.0513×10^{6}	1.4811×10^{5}	2.2297×10^{6}	2.7241×10^{5}
F15	mean	1.3010×10^{5}	4.1452×10^{4}	4.3370×10^{5}	9.1434×10^{5}	6.0084×10^{3}
	std	6.3821×10^{4}	1.2190×10^{4}	6.2141×10^{5}	2.2384×10^{6}	5.5555×10^{3}
F16	mean	6.4878×10^{3}	5.5150×10^{3}	7.0538×10^{3}	6.7791×10^{3}	5.3656×10^{3}
	std	7.5130×10^{2}	6.4103×10^{2}	7.2935×10^{2}	6.0570×10^{2}	7.2909×10^{2}
F17	mean	5.3635×10^{3}	4.6597×10^{3}	5.4935×10^{3}	4.9217×10^{3}	4.7617×10^{3}
	std	5.6436×10^{2}	6.4542×10^{2}	4.2431×10^{2}	4.1351×10^{2}	4.4473×10^{2}
F18	mean	3.6758×10^{6}	2.8727×10^{6}	3.6464×10^{5}	6.0329×10^{6}	8.0234×10^{5}
	std	1.8577×10^{6}	1.2540×10^{6}	2.1499×10^{5}	2.6749×10^{6}	4.0326×10^{5}
F19	mean	1.5077×10^{6}	3.5939×10^{5}	2.2431×10^{6}	1.0540×10^{6}	5.5373×10^{3}
	std	1.1724×10^{6}	2.0813×10^{5}	1.4291×10^{6}	7.4866×10^{5}	4.9543×10^{3}
F20	mean	5.1865×10^{3}	4.8405×10^{3}	5.5791×10^{3}	4.9615×10^{3}	5.2847×10^{3}
	std	5.7103×10^{2}	4.7449×10^{2}	5.3258×10^{2}	3.4510×10^{2}	4.1767×10^{2}
F21	mean	3.5715×10^{3}	2.8405×10^{3}	3.1536×10^{3}	3.1730×10^{3}	2.6344×10^{3}
	std	1.3731×10^{2}	6.8650×10^{1}	9.8549×10^{1}	7.3327×10^{1}	4.7902×10^{1}
F22	mean	2.1156×10^{4}	1.7926×10^{4}	2.4364×10^{4}	2.4254×10^{4}	1.8710×10^{4}
	std	1.6802×10^{3}	1.2281×10^{3}	1.3719×10^{3}	1.2571×10^{3}	1.3373×10^{3}
F23	mean	4.9524×10^{3}	3.3586×10^{3}	3.8231×10^{3}	3.8842×10^{3}	3.1879×10^{3}
	std	3.5927×10^{2}	9.7625×10^{1}	1.0524×10^{2}	9.4243×10^{1}	6.5119×10^{1}
F24	mean	5.5273×10^{3}	3.8351×10^{3}	4.4830×10^{3}	4.8515×10^{3}	3.6794×10^{3}
	std	3.8619×10^{2}	8.6271×10^{1}	1.6050×10^{2}	1.6417×10^{2}	4.9414×10^{1}
F25	mean	3.4363×10^{3}	3.4802×10^{3}	5.1654×10^{3}	7.6249×10^{3}	3.5043×10^{3}
	std	5.6768×10^{1}	5.5557×10^{1}	3.5381×10^{2}	1.0687×10^{3}	6.0569×10^{1}
F26	mean	1.6537×10^{4}	1.4675×10^{4}	1.7162×10^{4}	2.4939×10^{4}	9.9492×10^{3}
	std	9.3733×10^{3}	2.2280×10^{3}	1.2851×10^{3}	2.2394×10^{3}	5.9815×10^{2}
F27	mean	3.6287×10^{3}	3.6221×10^{3}	3.9475×10^{3}	4.4716×10^{3}	3.5350×10^{3}
	std	3.1747×10^{2}	7.7941×10^{1}	1.4357×10^{2}	1.9262×10^{2}	8.5543×10^{1}
F28	mean	3.5100×10^{3}	3.5574×10^{3}	6.8608×10^{3}	9.5644×10^{3}	3.6306×10^{3}
	std	6.2729×10^{1}	4.5728×10^{1}	9.3473×10^{2}	1.2911×10^{3}	6.4911×10^{1}
F29	mean	9.1075×10^{3}	7.6788×10^{3}	8.9788×10^{3}	8.6236×10^{3}	7.0079×10^{3}
	std	7.9587×10^{2}	4.7247×10^{2}	7.2441×10^{2}	5.4592×10^{2}	4.3350×10^{2}
F30	mean	2.4829×10^{7}	8.3553×10^{6}	5.9009×10^{7}	1.1649×10^{8}	3.7210×10^{5}
	std	1.0761×10^{7}	3.5241×10^{6}	2.7536×10^{7}	2.3926×10^{8}	1.7713×10^{5}

3.6. Statistical Analysis Based on the Wilcoxon Signed-Rank Test

Statistical analysis plays a crucial role in evaluating the performance of heuristic algorithms, as their stochastic nature often leads to variability in optimization results across independent runs. Relying solely on mean and standard deviation may not provide sufficient evidence to determine whether the observed performance differences are statistically significant. Therefore, the Wilcoxon signed-rank test, a non-parametric statistical method,

is widely adopted to perform pairwise comparisons between algorithms without assuming any specific data distribution. By considering both the magnitude and direction of differences between paired samples, this test can effectively assess whether one algorithm significantly outperforms another. Consequently, incorporating statistical analysis based on the Wilcoxon signed-rank test enhances the reliability and credibility of experimental results, providing a more rigorous and objective basis for performance evaluation of heuristic optimization algorithms [44]. The experimental results for this subsection are shown below.

Figure 10 presents the statistical analysis results based on the Wilcoxon signed-rank test at a significance level of $\alpha = 0.05$, which was used to assess the significance of the performance differences between MIEDOA and the comparative algorithms. From the results, it can be observed that MIEDOA achieves a dominant number of wins W against most competing algorithms, while the number of ties T and losses L remains relatively low. This indicates that the performance improvements of MIEDOA are not only evident in terms of mean values but are also statistically significant across multiple benchmark functions.

Specifically, on the majority of test functions, MIEDOA significantly outperforms traditional and recently developed algorithms, reflecting its strong optimization capability and robustness. Although a small number of ties or losses may occur on relatively simple functions—where most algorithms can achieve near-optimal solutions—the overall superiority of MIEDOA remains clear. The Wilcoxon test results further demonstrate that the proposed algorithm maintains consistent advantages rather than occasional improvements caused by randomness.

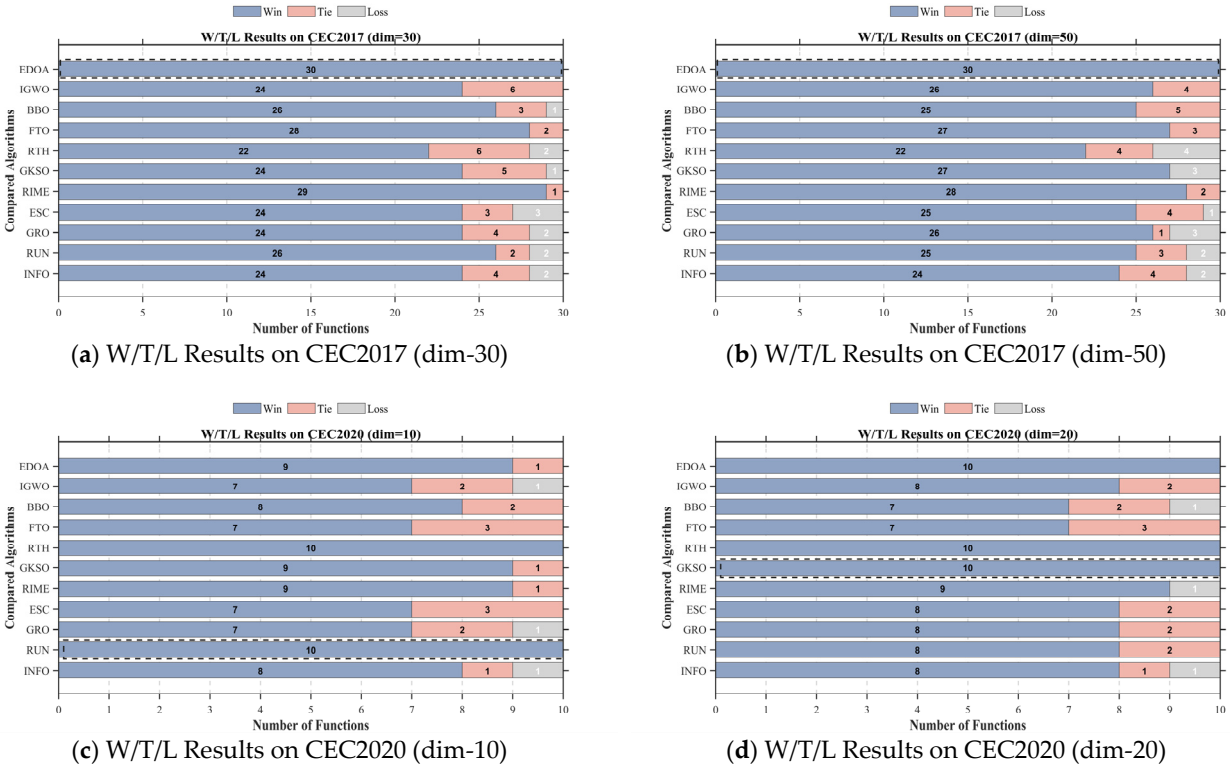
Overall, Figure 10 confirms that the performance gains achieved by MIEDOA are statistically reliable and significant, providing strong evidence for its effectiveness and competitiveness in solving complex optimization problems.

To further strengthen the statistical analysis, Holm post hoc tests and effect size analyses were additionally conducted. The detailed Holm-adjusted p-values are summarized in Appendix A Tables A1–A5, whereas the corresponding effect size results are reported in Appendix A Tables A6–A10. These results complement the Wilcoxon and Friedman analyses by evaluating not only whether the observed differences are statistically significant but also the extent of their practical impact.

Appendix A Tables A1–A5 report the Holm-adjusted p-values obtained from the post hoc statistical analysis. It can be observed that, for most pairwise comparisons, the adjusted p-values remain below the significance threshold, indicating that the performance differences identified in the main experiments are generally preserved after controlling the family-wise error rate. These results provide additional statistical support for the comparative performance of MIEDOA and suggest that the observed differences are not solely caused by random variations across independent runs.

Appendix A Tables A6–A10 present the corresponding effect size results, which complement the significance tests by quantifying the magnitude of the performance differences. The effect size values indicate that the advantages of MIEDOA over several comparative algorithms are associated with non-negligible practical effects on many benchmark functions. At the same time, relatively smaller effect sizes are observed in some pairwise comparisons, suggesting that the performance differences between highly competitive algorithms may be less pronounced despite being statistically significant. Therefore, the combined analysis of Holm-adjusted p-values and effect sizes provides a more comprehensive assessment of algorithm performance by considering both statistical significance and practical impact.

Overall, the results reported in Appendix A Tables A1–A10 are generally consistent with the conclusions drawn from the Wilcoxon signed-rank test and the Friedman mean rank analysis, further supporting the effectiveness and robustness of the proposed MIEDOA across different benchmark suites and dimensional settings.



(**a**) W/T/L Results on CEC2017 (dim-30)

(**b**) W/T/L Results on CEC2017 (dim-50)

(**c**) W/T/L Results on CEC2020 (dim-10)

(**d**) W/T/L Results on CEC2020 (dim-20)

Figure 10. Statistical Analysis of Experimental Results.

3.7. Statistical Analysis Based on the Friedman Mean Rank Test

The Friedman mean rank test is a widely adopted non-parametric statistical method used to evaluate the overall performance of multiple optimization algorithms across a set of benchmark problems. Unlike pairwise statistical tests, the Friedman test provides a comprehensive ranking of algorithms by considering their relative performance on each test function; this approach helps mitigate the influence of the specific characteristics of individual benchmark problems, thereby offering a more objective assessment of the algorithms' merits. Consequently, this method has become one of the most commonly used statistical tools for validating the robustness and overall competitiveness of meta-heuristic algorithms. Furthermore, while the Friedman mean rank can reveal the relative ordering of algorithms, it does not indicate whether the observed ranking differences are statistically significant. In light of this, we further conduct a Critical Difference (CD) analysis to determine whether the performance gaps between algorithms exceed the threshold for statistical significance. By combining the Friedman mean rank test with CD analysis, we are able to achieve a more rigorous and reliable statistical evaluation, thereby more clearly identifying those algorithms that demonstrate a statistically significant advantage over their competitors. The experimental results are presented below.

Table 13 presents the Friedman Mean Rank Test results of all compared algorithms on the CEC2017 and CEC2020 benchmark suites under different dimensional settings. According to the Friedman test, a smaller mean rank indicates better overall performance across the benchmark functions. As shown in the table, MIEDOA consistently achieves the lowest mean rank and obtains the first overall ranking in all five experimental scenarios, including CEC2017 with 30, 50, and 100 dimensions, as well as CEC2020 with 10 and 20 dimensions. The corresponding mean rank values of MIEDOA are 2.00, 2.43, 2.37, 1.90, and 1.80, respectively, which are noticeably lower than those of the comparative algorithms.

Furthermore, the ranking results remain relatively stable as the problem dimension increases, suggesting that the performance of MIEDOA is less affected by changes in problem

scale. Among the compared algorithms, BBO, ESC, and RTH generally obtain relatively favorable rankings in some scenarios, whereas EDOA frequently ranks near the bottom of the table. This observation indicates that the proposed improvement strategies contribute positively to the overall optimization performance of the original EDOA framework. Overall, the Friedman ranking results suggest that MIEDOA maintains competitive performance across different benchmark suites and dimensional settings, and the conclusions are generally consistent with the numerical results, convergence analysis, and boxplot comparisons presented in the previous sections.

Table 13. Friedman Mean Rank Test Results.

Suites	**CEC2017**						**CEC2020**			
Dimensions	**30**		**50**		**100**		**10**		**20**	
Algorithms	***M.R***	***T.R***	***M.R***	***T.R***	***M.R***	***T.R***	***M.R***	***T.R***	***M.R***	***T.R***
INFO	6.40	5	6.67	6	6.43	4	6.50	6	6.40	5
RUN	7.37	10	6.93	8	6.73	7	8.30	10	8.00	11
GRO	6.73	7	7.57	10	9.63	12	4.00	2	7.30	8
ESC	5.07	2	6.07	4	6.87	8	5.40	3	4.60	2
RIME	8.10	11	7.90	11	8.10	10	7.60	9	7.60	10
GKSO	6.77	8	6.73	7	6.67	6	6.40	5	6.60	7
RTH	6.50	6	5.87	3	4.03	3	8.60	11	7.30	8
FTO	6.83	9	7.10	9	7.43	9	5.90	4	5.70	3
BBO	5.23	3	4.47	2	3.77	2	6.50	6	6.10	4
IGWO	6.37	4	6.17	5	6.57	5	7.40	8	6.50	6
EDOA	10.63	12	10.10	12	9.40	11	9.50	12	10.10	12
MIEDOA	2.00	1	2.43	1	2.37	1	1.90	1	1.80	1

To further determine whether the differences observed in the Friedman Mean Rank Test are statistically significant, the Nemenyi post hoc test is employed to calculate the Critical Difference (CD). The CD value is computed as

$$CD = q_\alpha \sqrt{\frac{k(k+1)}{6N}} \tag{15}$$

where q_α denotes the critical value of the Nemenyi test at the significance level $\alpha = 0.05$, k is the number of compared algorithms, and N represents the number of benchmark functions. In this study, $k = 12$ algorithms are involved in all comparisons.

For the CEC2017 benchmark suite containing 30 test functions, the calculated CD value is 2.997. For the CEC2020 benchmark suite containing 10 test functions, the corresponding CD value is 5.191. According to the Nemenyi test, when the difference between the mean ranks of two algorithms exceeds the corresponding CD value, their performance difference can be considered statistically significant at the 0.05 significance level. Therefore, the experimental results indicate that within the CEC2017 test suite: in the 30-dimensional case, all algorithms exhibit a statistically significant difference compared to MIEDOA; in the 50-dimensional case, only BBO shows no statistically significant difference from MIEDOA, while the remaining algorithms all differ significantly; and in the 100-dimensional case, only BBO and RTH show no statistically significant difference from MIEDOA, whereas the remaining algorithms all differ significantly. Similarly, within the CEC2020 test suite, MIEDOA also demonstrates statistically significant differences relative to the majority of the comparative algorithms.

3.8. Parameter Sensitivity Analysis

Parameter sensitivity analysis constitutes an essential step in assessing the reliability and stability of meta-heuristic algorithms. Given that varying parameter settings can significantly influence the balance between exploration and exploitation, convergence behavior, and solution quality, evaluating the sensitivity of key parameters is crucial for understanding the performance characteristics of the proposed algorithm. Accordingly, this subsection investigates the impact of individual parameters on the optimization performance of MIEDOA, aiming to assess the robustness and adaptability of the proposed algorithm under different parameter configurations. The experimental results are presented below.

Figure 11 presents the parameter sensitivity analysis results of MIEDOA with respect to the parameters α, β, ω_{min}, ω_{max}, and η on representative CEC2017 benchmark functions under different dimensional settings. As shown in Figure 11a–f, different combinations of α and β lead to noticeable variations in convergence behavior, indicating that the initialization strategy influences both the search efficiency and solution quality of the algorithm. Among the tested configurations, the setting $\alpha = 0.6$ and $\beta = 0.03$ generally achieves relatively favorable convergence performance on most selected functions. Figure 11g–l illustrate the influence of ω_{min} and ω_{max}. It can be observed that excessively small or excessively large parameter values may lead to slower convergence or less competitive final solutions on some functions, whereas the setting $\omega_{min} = 0.3$ and $\omega_{max} = 0.8$ generally provides a balanced search behavior across different optimization scenarios. In addition, Figure 11m–r present the sensitivity analysis of the parameter η. The results suggest that different values of η affect the adaptive regulation intensity of AGFR, thereby influencing the convergence characteristics of the algorithm. Overall, $\eta = 3$ tends to provide relatively stable and competitive performance across the selected benchmark functions. These results indicate that the proposed parameter settings achieve a reasonable balance between convergence efficiency and solution quality, and the algorithm exhibits satisfactory robustness within a certain range of parameter variations.

3.9. Comparison with EDOA Variants and the CEC Winner Algorithm

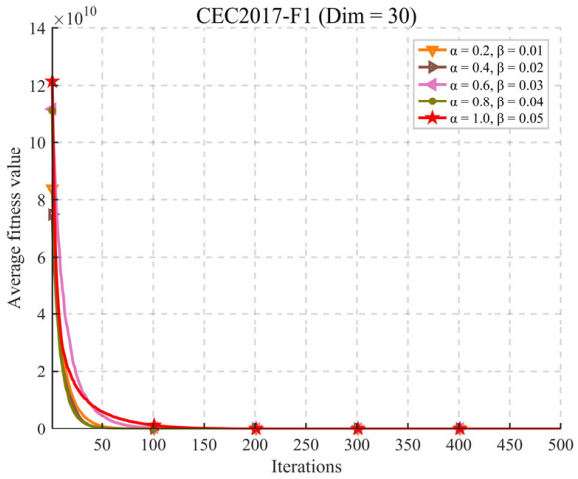
Comparisons with both state-of-the-art EDOA variants and CEC competition winner algorithms are of great importance for comprehensively evaluating the effectiveness and competitiveness of the proposed MIEDOA. On the one hand, comparisons with representative EDOA variants can clearly demonstrate whether the proposed improvement strategies provide additional benefits beyond existing modifications of the original EDOA framework. On the other hand, CEC winner algorithms are widely recognized as high-performance optimization methods and are commonly used as strong baselines for validating newly developed metaheuristic algorithms. Therefore, comparing MIEDOA with these advanced algorithms can provide a more rigorous assessment of its optimization capability, convergence behavior, and robustness. Based on this motivation, this subsection presents a comprehensive comparison between MIEDOA, several representative EDOA variants, and CEC winner algorithms, and the corresponding experimental results are reported as follows.

Figure 12 presents the convergence curves of MIEDOA, several representative EDOA variants LMEDO, MSEDO, and MEED, and CEC winner algorithms on selected CEC2017 benchmark functions under 50- and 100-dimensional settings. It can be observed that the convergence behaviors of the compared algorithms differ noticeably across the test functions. In many cases, MIEDOA exhibits a relatively rapid decrease in fitness values during the early and middle stages of the search and is often able to achieve lower final fitness values than the comparative methods. This trend can be observed on functions such as F5, F8, F20, F24, and F26, where MIEDOA maintains a competitive

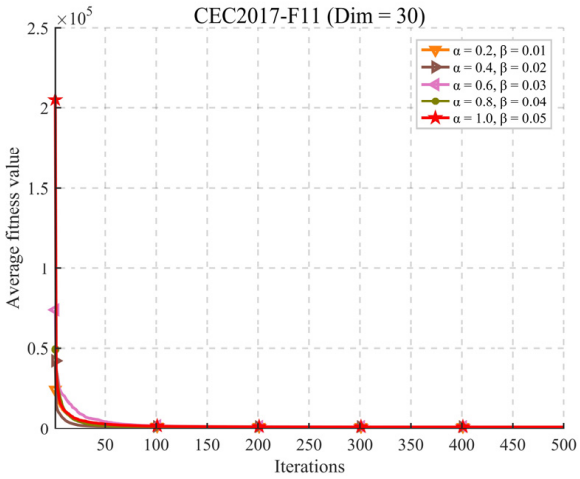
convergence trajectory throughout the optimization process. As the problem dimension increases from 50 to 100, the optimization difficulty becomes more challenging, yet MIEDOA generally preserves a stable convergence pattern and remains competitive on most selected functions. In contrast, some EDOA variants and comparative algorithms tend to exhibit slower convergence rates or earlier stagnation on certain functions, resulting in comparatively higher final fitness values. Overall, the convergence results suggest that the proposed MIEDOA is capable of maintaining effective search performance across different problem dimensions and demonstrates competitive optimization capability when compared with both existing EDOA variants and CEC winner algorithms.

Figure 13 presents the boxplot comparison between MIEDOA, several representative EDOA variants, and CEC winner algorithms on selected CEC2017 benchmark functions. The boxplots provide a visual assessment of the distribution characteristics and stability of the algorithms over multiple independent runs. As shown in the figure, MIEDOA generally exhibits lower median fitness values on most selected functions, indicating competitive optimization performance. In addition, the interquartile ranges of MIEDOA are relatively narrow in many cases, suggesting that the algorithm maintains a comparatively stable search behavior across repeated runs. For several benchmark functions, the number of outliers associated with MIEDOA is also relatively limited, indicating reduced sensitivity to random initialization and stochastic search factors. In contrast, some comparative algorithms display wider box distributions or larger performance fluctuations on certain functions, particularly under the 100-dimensional setting. Overall, the boxplot results suggest that MIEDOA is capable of producing competitive solutions while maintaining satisfactory robustness and consistency when compared with both existing EDOA variants and CEC winner algorithms.

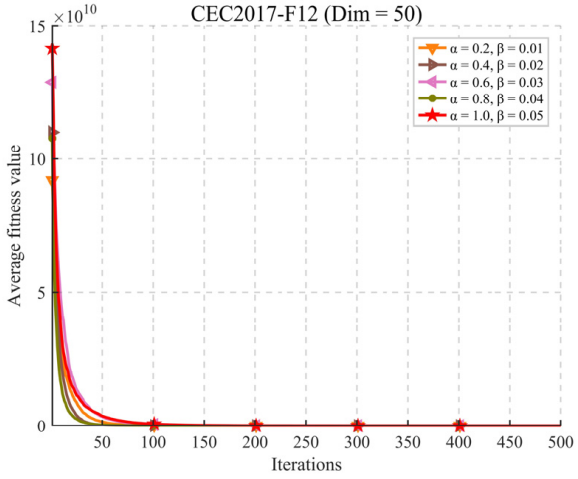
Tables 14 and 15 present the comparative results of MIEDOA, representative EDOA variants, and several CEC winner algorithms on the CEC2017 benchmark functions under 50- and 100-dimensional settings. From the results, it can be observed that MIEDOA achieves the best or near-best mean fitness values on a considerable number of benchmark functions in both dimensional scenarios. In addition, the corresponding standard deviations are generally maintained at relatively low levels on many functions, indicating satisfactory stability over multiple independent runs. As the problem dimension increases from 50 to 100, the optimization landscape becomes more challenging, leading to noticeable performance degradation for some comparative algorithms. Nevertheless, MIEDOA continues to maintain competitive optimization results on many benchmark functions and often exhibits smaller performance fluctuations than several EDOA variants. Compared with the original EDOA variants, including MEED, LMEDO, and MSEDO, the proposed MIEDOA generally achieves lower mean fitness values on most selected functions, suggesting that the introduced strategies contribute positively to the overall search process. Furthermore, when compared with the CEC winner algorithms, including L-SHADE, LSHADE-cnEpSin, and LSHADE-SPACMA, MIEDOA remains competitive on many benchmark functions and attains favorable results in several high-dimensional cases. Overall, the results reported in Tables 14 and 15 indicate that MIEDOA is capable of maintaining effective optimization performance across different problem dimensions and exhibits good robustness when compared with both closely related EDOA variants and state-of-the-art optimization algorithms.



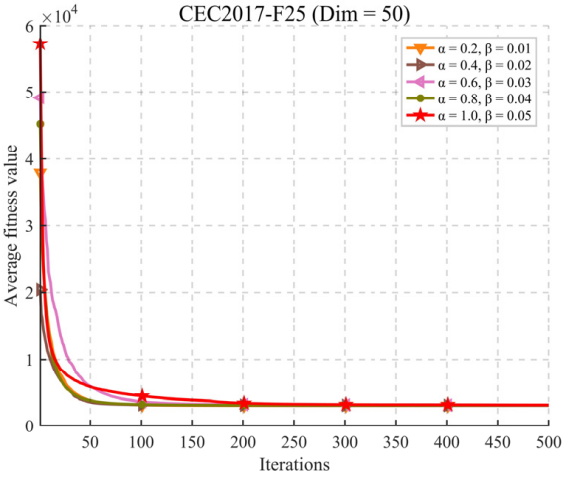
(**a**) CEC2017-F1 (Dim = 30)



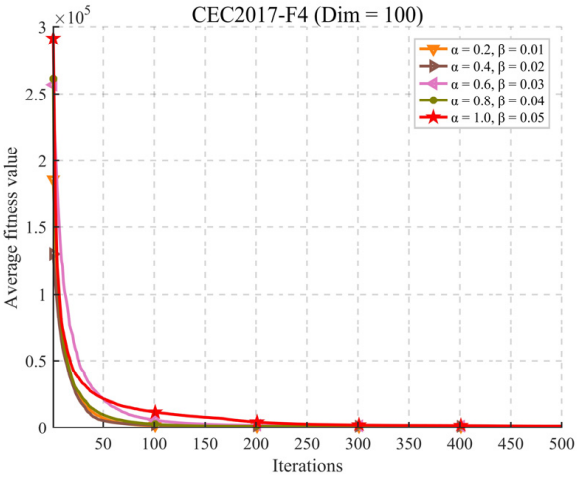
(**b**) CEC2017-F11 (Dim = 30)



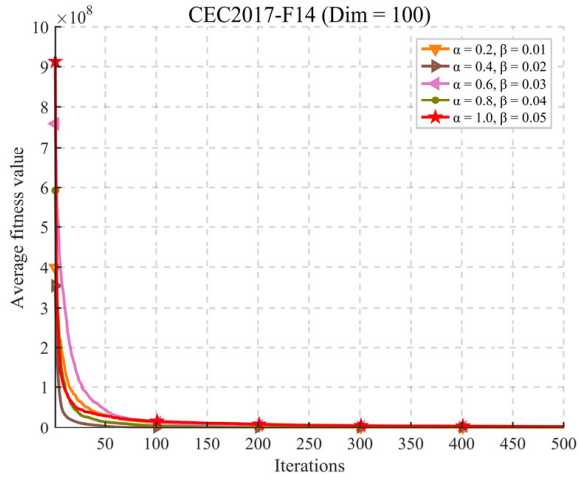
(**c**) CEC2017-F12 (Dim = 50)



(**d**) CEC2017-F25 (Dim = 50)

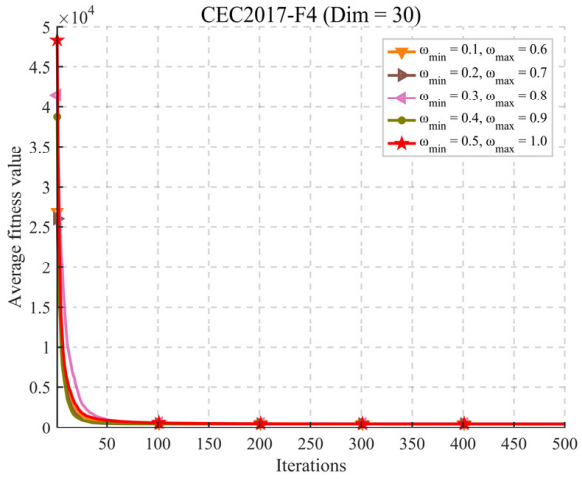


(**e**) CEC2017-F4 (Dim = 100)

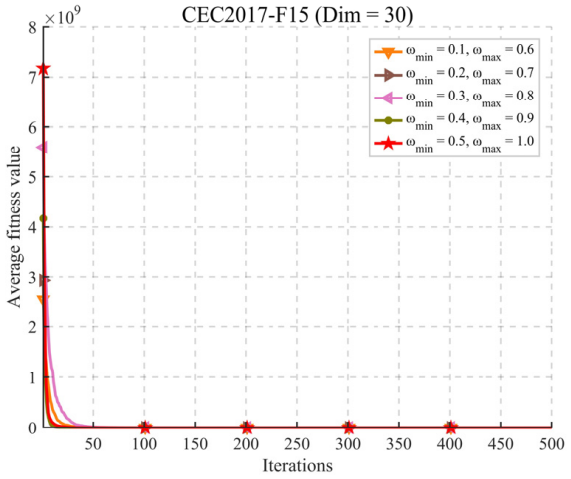


(**f**) CEC2017-F14 (Dim = 100)

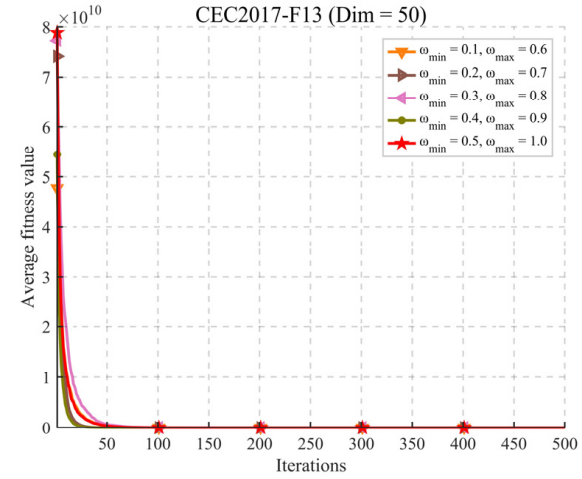
Figure 11. *Cont.*



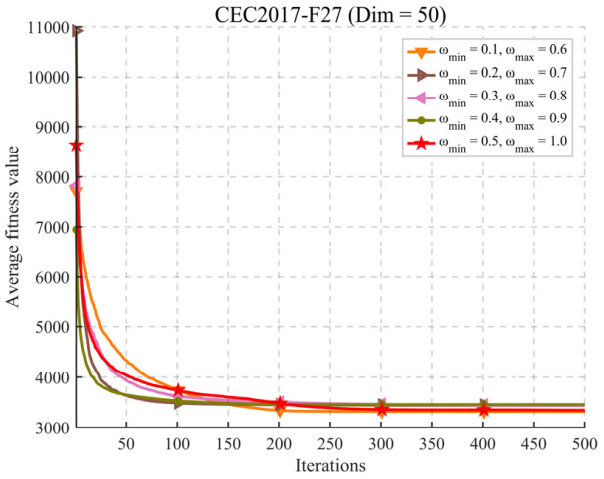
(**g**) CEC2017-F4 (Dim = 30)



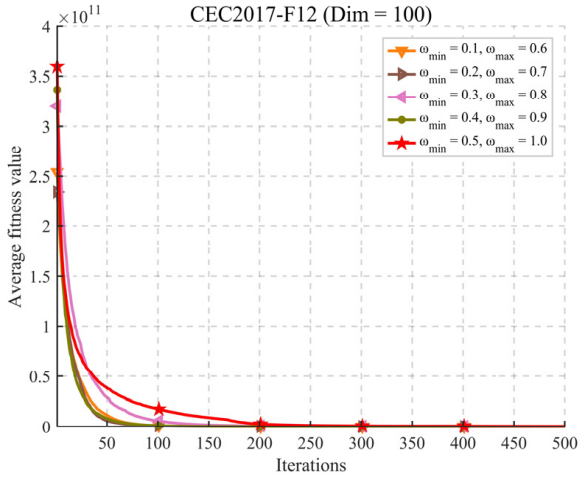
(**h**) CEC2017-F15 (Dim = 30)



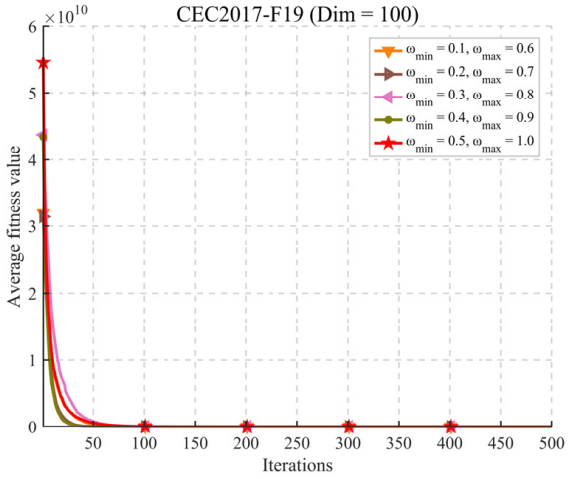
(**i**) CEC2017-F13 (Dim = 50)



(**j**) CEC2017-F27 (Dim = 50)

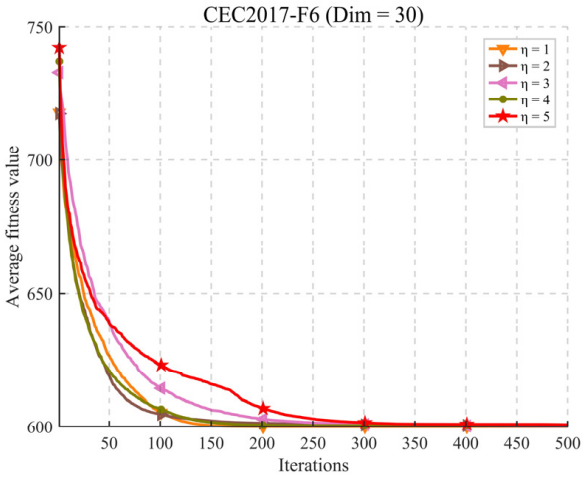


(**k**) CEC2017-F12 (Dim = 100)

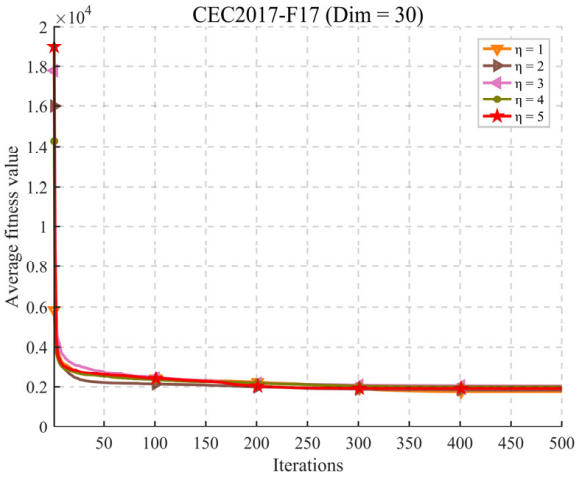


(**l**) CEC2017-F19 (Dim = 100)

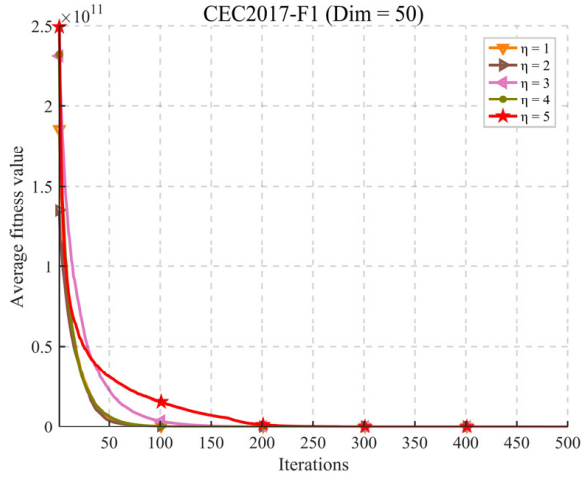
Figure 11. *Cont.*



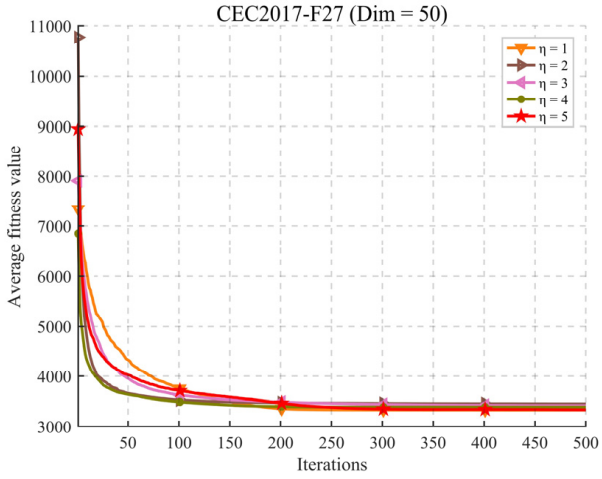
(**m**) CEC2017-F6 (Dim = 30)



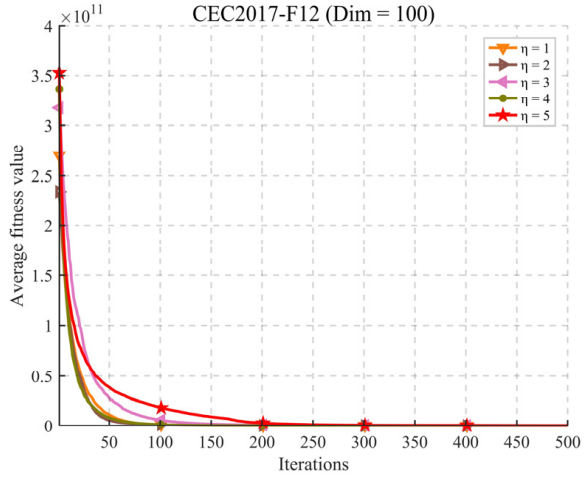
(**n**) CEC2017-F17 (Dim = 30)



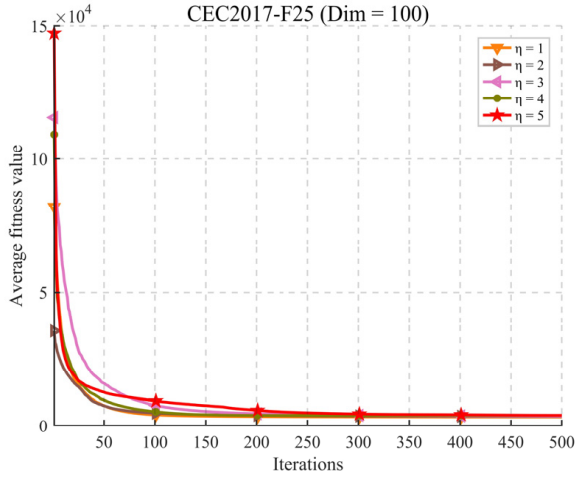
(**o**) CEC2017-F1 (Dim = 50)



(**p**) CEC2017-F27 (Dim = 50)

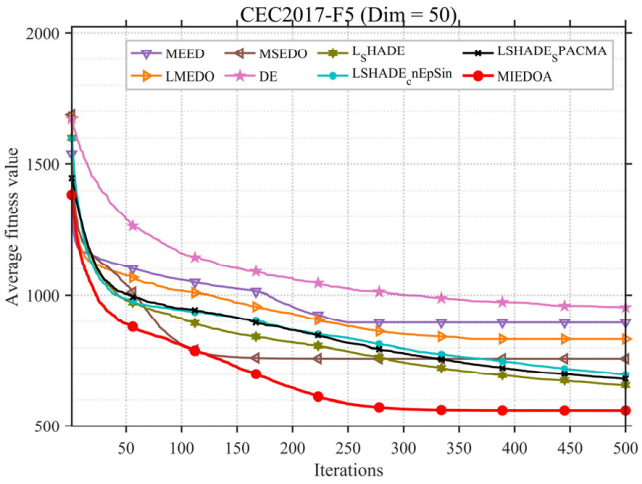


(**q**) CEC2017-F12 (Dim = 100)

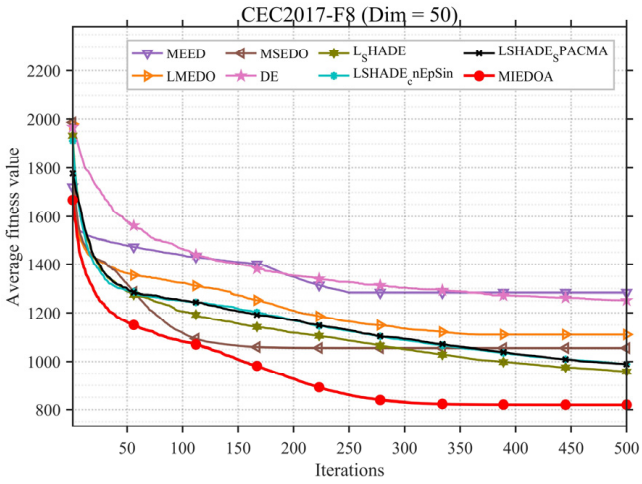


(**r**) CEC2017-F24 (Dim = 100)

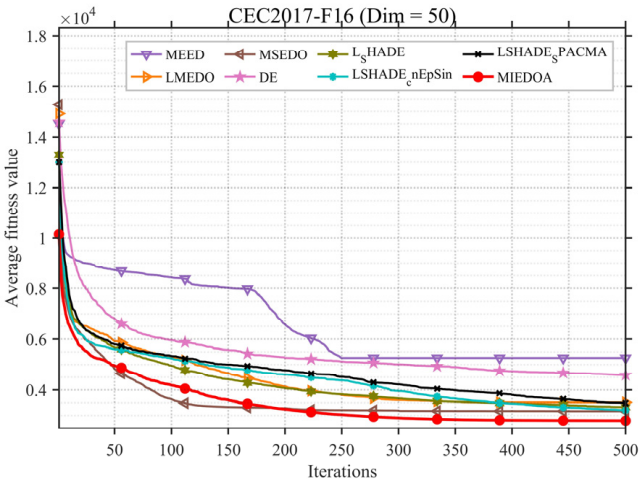
Figure 11. Experimental Results of Parameter Sensitivity Analysis.



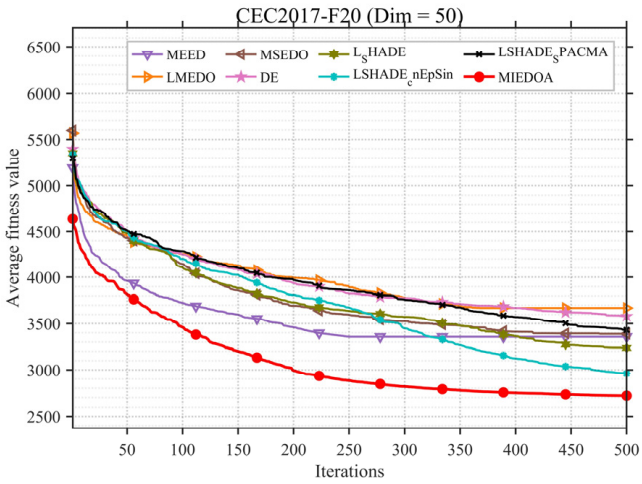
(**a**) CEC2017-F5 (Dim = 50)



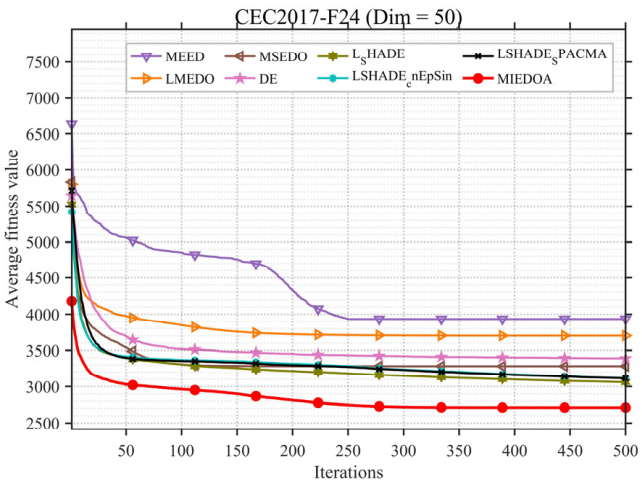
(**b**) CEC2017-F8 (Dim = 50)



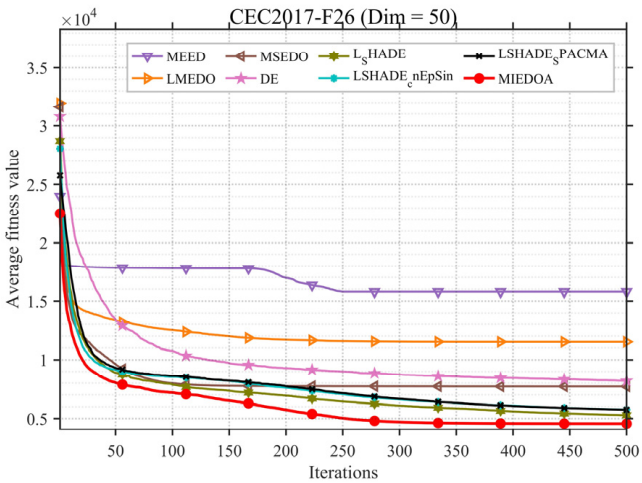
(**c**) CEC2017-F16 (Dim = 50)



(**d**) CEC2017-F20 (Dim = 50)

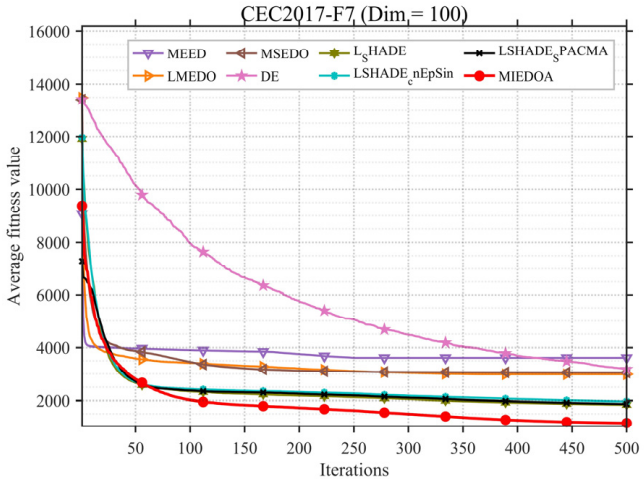


(**e**) CEC2017-F24 (Dim = 50)

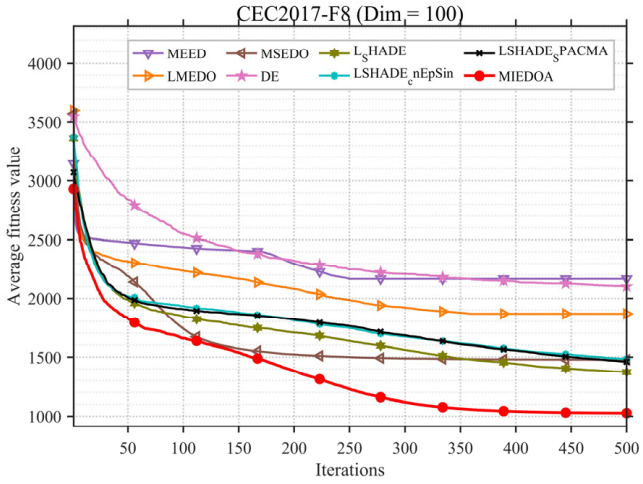


(**f**) CEC2017-F26 (Dim = 50)

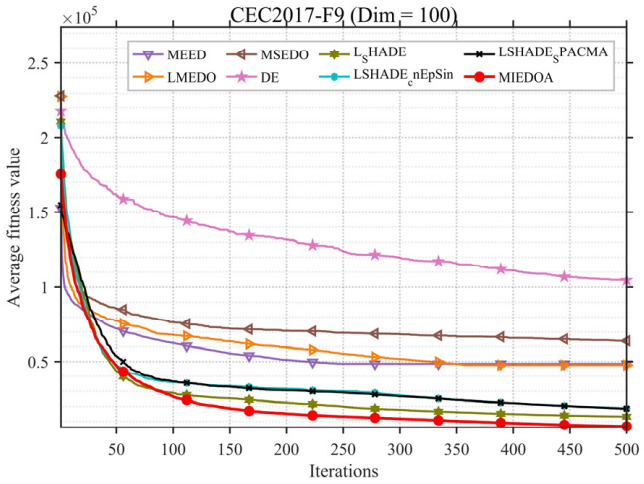
Figure 12. *Cont.*



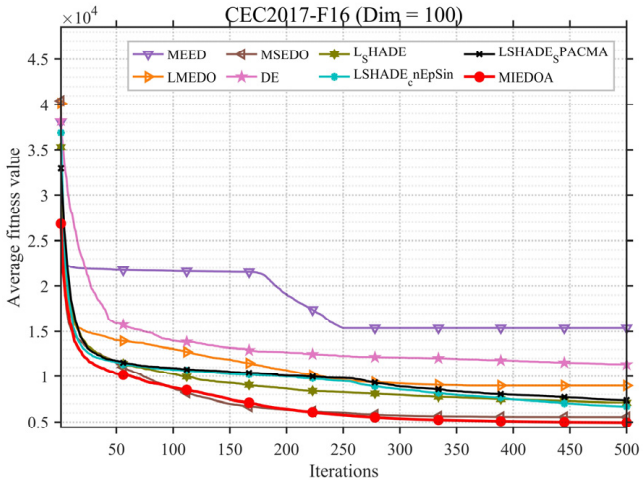
(**g**) CEC2017-F7 (Dim = 100)



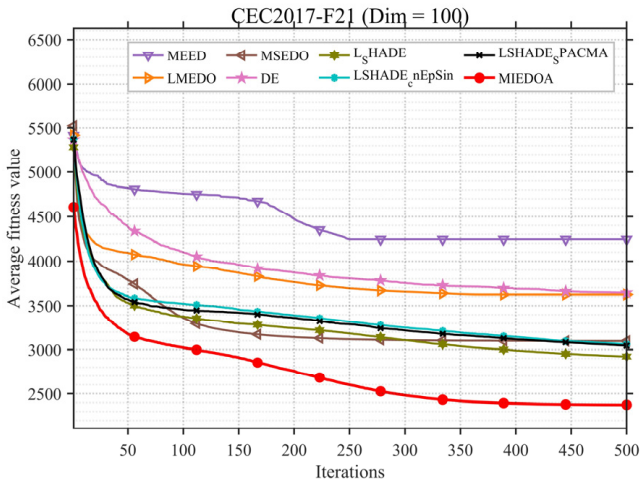
(**h**) CEC2017-F8 (Dim = 100)



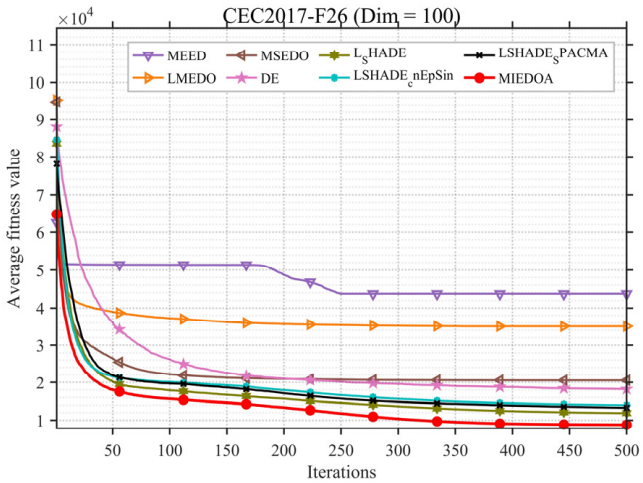
(**i**) CEC2017-F9 (Dim = 100)



(**j**) CEC2017-F16 (Dim = 100)



(**k**) CEC2017-F21 (Dim = 100)



(**l**) CEC2017-F26 (Dim = 100)

Figure 12. Convergence Curves Compared with EDOA Variants and the CEC Winner Algorithm.

Table 14. Experimental Results Compared with EDOA Variants and the CEC Winner Algorithm on the CEC2017 Benchmark Functions (Dim = 50).

ID	Metric	MEED	LMEDO	MSEDO	DE	L_SHADE	LSHADE_cnEpSin	LSHADE_SPACMA	MIEDOA
F1	mean	6.5519×10^{10}	3.6020×10^{10}	1.0528×10^{4}	3.2638×10^{9}	2.0666×10^{5}	1.7685×10^{6}	1.4056×10^{6}	7.5710×10^{3}
	std	1.0007×10^{10}	9.7602×10^{9}	1.1957×10^{4}	5.1866×10^{8}	1.3917×10^{5}	1.2666×10^{6}	1.6669×10^{6}	4.9496×10^{3}
F2	mean	6.4069×10^{80}	7.6980×10^{62}	9.2764×10^{44}	2.9497×10^{63}	6.5285×10^{29}	9.0291×10^{29}	3.0701×10^{40}	4.5228×10^{34}
	std	2.7138×10^{81}	4.0825×10^{63}	5.0733×10^{45}	9.7835×10^{63}	4.6646×10^{29}	2.7665×10^{29}	1.6814×10^{41}	1.8009×10^{35}
F3	mean	1.5436×10^{5}	5.2323×10^{4}	6.5824×10^{4}	3.1990×10^{5}	1.0094×10^{5}	5.8380×10^{4}	1.2262×10^{5}	6.2736×10^{4}
	std	1.8662×10^{4}	1.1955×10^{4}	1.9027×10^{4}	3.4325×10^{4}	8.5193×10^{4}	3.4820×10^{4}	9.2449×10^{4}	1.1831×10^{4}
F4	mean	1.4722×10^{4}	7.0242×10^{3}	5.6391×10^{2}	1.1084×10^{3}	5.7181×10^{2}	5.9935×10^{2}	5.9029×10^{2}	5.6837×10^{2}
	std	3.4190×10^{3}	2.5113×10^{3}	5.0668×10^{1}	9.7296×10^{1}	4.1879×10^{1}	3.8793×10^{1}	3.8625×10^{1}	3.6400×10^{1}
F5	mean	8.9600×10^{2}	8.3292×10^{2}	7.5929×10^{2}	9.5367×10^{2}	6.5706×10^{2}	6.9803×10^{2}	6.8146×10^{2}	6.2280×10^{2}
	std	4.7885×10^{1}	6.9653×10^{1}	5.8108×10^{1}	2.3561×10^{1}	1.9131×10^{1}	3.8141×10^{1}	3.6845×10^{1}	3.4669×10^{1}
F6	mean	6.7011×10^{2}	6.4187×10^{2}	6.3270×10^{2}	6.1791×10^{2}	6.0286×10^{2}	6.0658×10^{2}	6.0342×10^{2}	6.0033×10^{2}
	std	5.7944×10^{0}	8.7535×10^{0}	7.1703×10^{0}	1.2206×10^{0}	1.4529×10^{0}	2.1702×10^{0}	1.5769×10^{0}	2.1428×10^{-1}
F7	mean	1.7016×10^{3}	1.4208×10^{3}	1.3403×10^{3}	1.2971×10^{3}	9.6622×10^{2}	1.0026×10^{3}	9.8767×10^{2}	8.7221×10^{2}
	std	1.3087×10^{2}	1.1406×10^{2}	1.4211×10^{2}	3.0530×10^{1}	3.4930×10^{1}	4.6120×10^{1}	6.0107×10^{1}	2.4415×10^{1}
F8	mean	1.2830×10^{3}	1.1102×10^{3}	1.0549×10^{3}	1.2517×10^{3}	9.5861×10^{2}	9.8948×10^{2}	9.8906×10^{2}	9.1099×10^{2}
	std	5.0531×10^{1}	7.2003×10^{1}	5.5395×10^{1}	1.9443×10^{1}	2.4443×10^{1}	2.4123×10^{1}	2.8955×10^{1}	2.7583×10^{1}
F9	mean	1.7633×10^{4}	1.2927×10^{4}	1.7356×10^{4}	2.0658×10^{4}	1.7538×10^{3}	2.4812×10^{3}	2.3687×10^{3}	1.0178×10^{3}
	std	2.4243×10^{3}	2.4494×10^{3}	5.8379×10^{3}	2.4095×10^{3}	6.5384×10^{2}	7.1286×10^{2}	1.0906×10^{3}	1.6561×10^{2}
F10	mean	9.6585×10^{3}	1.2569×10^{4}	1.3831×10^{4}	1.2906×10^{4}	8.3165×10^{3}	9.1341×10^{3}	8.9930×10^{3}	7.9159×10^{3}
	std	5.9312×10^{2}	4.0599×10^{2}	2.6390×10^{3}	3.4004×10^{2}	6.7006×10^{2}	9.3921×10^{2}	1.3395×10^{3}	9.1959×10^{2}
F11	mean	1.3280×10^{4}	2.6364×10^{3}	1.2877×10^{3}	1.1737×10^{4}	1.3566×10^{3}	1.4668×10^{3}	1.4185×10^{3}	1.3533×10^{3}
	std	3.8925×10^{3}	9.5119×10^{2}	5.6340×10^{1}	3.0894×10^{3}	5.3750×10^{1}	1.1738×10^{2}	8.6092×10^{1}	6.2598×10^{1}
F12	mean	3.1295×10^{10}	1.1064×10^{10}	1.8650×10^{6}	1.0328×10^{9}	1.9903×10^{6}	4.8427×10^{6}	2.9301×10^{6}	5.6288×10^{6}
	std	1.5432×10^{10}	5.7069×10^{9}	1.2302×10^{6}	2.2412×10^{8}	1.2650×10^{6}	2.9399×10^{6}	1.5640×10^{6}	1.9797×10^{6}
F13	mean	9.5359×10^{9}	2.6492×10^{9}	9.9551×10^{3}	6.4331×10^{7}	1.2909×10^{4}	3.0301×10^{4}	1.4754×10^{4}	1.6388×10^{4}
	std	8.9559×10^{9}	2.1321×10^{9}	6.4478×10^{3}	2.5275×10^{7}	7.3192×10^{3}	2.0204×10^{4}	8.4879×10^{3}	1.0682×10^{4}
F14	mean	8.6068×10^{6}	6.4390×10^{5}	3.6112×10^{4}	3.8147×10^{6}	1.9926×10^{3}	2.9897×10^{3}	2.7783×10^{3}	3.7747×10^{3}
	std	1.2775×10^{7}	1.3426×10^{6}	3.8934×10^{4}	1.6192×10^{6}	7.2118×10^{2}	3.0673×10^{3}	1.7768×10^{3}	1.1983×10^{3}
F15	mean	2.3076×10^{9}	1.7940×10^{8}	6.1390×10^{3}	8.1990×10^{6}	3.7896×10^{3}	6.3469×10^{3}	5.2779×10^{3}	1.7056×10^{4}
	std	1.0959×10^{9}	3.0048×10^{8}	6.9696×10^{3}	4.8859×10^{6}	2.3403×10^{3}	3.5743×10^{3}	2.7590×10^{3}	7.6003×10^{3}
F16	mean	5.2633×10^{3}	3.5140×10^{3}	3.1685×10^{3}	4.5867×10^{3}	3.3218×10^{3}	3.2019×10^{3}	3.4831×10^{3}	3.1105×10^{3}
	std	8.2670×10^{2}	4.5357×10^{2}	5.8538×10^{2}	1.7847×10^{2}	3.1923×10^{2}	3.6822×10^{2}	3.6402×10^{2}	3.4707×10^{2}
F17	mean	4.8161×10^{3}	3.1553×10^{3}	3.0079×10^{3}	3.6508×10^{3}	2.9160×10^{3}	2.8966×10^{3}	3.1376×10^{3}	2.8244×10^{3}
	std	9.4274×10^{2}	3.7566×10^{2}	3.3194×10^{2}	1.8767×10^{2}	1.9234×10^{2}	2.1369×10^{2}	2.2927×10^{2}	2.7948×10^{2}
F18	mean	6.0995×10^{7}	2.6772×10^{6}	7.6131×10^{5}	1.3302×10^{7}	4.6765×10^{4}	6.7016×10^{4}	7.6408×10^{4}	1.4274×10^{5}
	std	4.4414×10^{7}	4.6065×10^{6}	7.9664×10^{5}	5.4980×10^{6}	2.4159×10^{4}	6.8060×10^{4}	4.5358×10^{4}	1.9816×10^{5}
F19	mean	7.8875×10^{8}	2.5768×10^{7}	1.6933×10^{4}	1.5710×10^{6}	2.6731×10^{3}	6.2895×10^{3}	7.3391×10^{3}	1.3130×10^{4}
	std	5.5957×10^{8}	4.9328×10^{7}	1.2657×10^{4}	6.7330×10^{5}	1.8513×10^{3}	6.3910×10^{3}	7.3514×10^{3}	9.0738×10^{3}
F20	mean	3.3566×10^{3}	3.6699×10^{3}	3.3882×10^{3}	3.5801×10^{3}	3.2367×10^{3}	2.9608×10^{3}	3.4291×10^{3}	3.0214×10^{3}
	std	2.2943×10^{2}	3.1288×10^{2}	5.7311×10^{2}	1.8111×10^{2}	1.9690×10^{2}	2.1214×10^{2}	2.0773×10^{2}	2.4541×10^{2}
F21	mean	2.9198×10^{3}	2.6458×10^{3}	2.5239×10^{3}	2.7559×10^{3}	2.4620×10^{3}	2.4953×10^{3}	2.4947×10^{3}	2.4133×10^{3}
	std	6.0666×10^{1}	6.7601×10^{1}	4.5387×10^{1}	1.8568×10^{1}	2.2978×10^{1}	3.0413×10^{1}	2.4085×10^{1}	3.4811×10^{1}

Table 14. *Cont.*

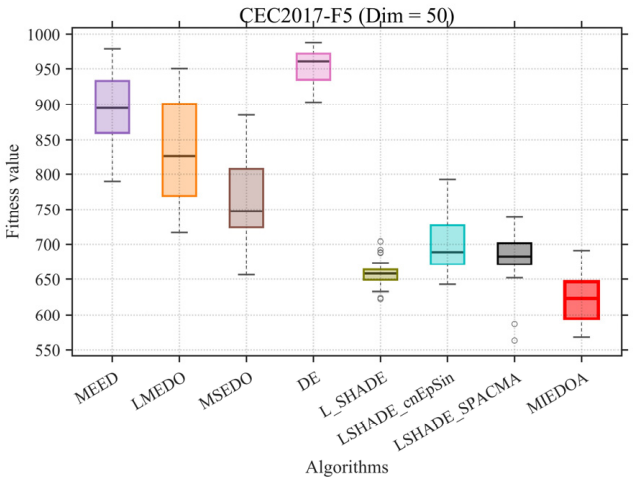
ID	Metric	MEED	LMEDO	MSEDO	DE	L_SHADE	LSHADE_cnEpSin	LSHADE_SPACMA	MIEDOA
F22	mean	1.1762×10^{4}	1.3135×10^{4}	1.5006×10^{4}	1.4595×10^{4}	9.9180×10^{3}	1.1056×10^{4}	1.0657×10^{4}	9.1114×10^{3}
	std	7.1116×10^{2}	2.8416×10^{3}	2.7218×10^{3}	3.4756×10^{2}	1.3376×10^{3}	1.2629×10^{3}	1.9803×10^{3}	1.0398×10^{3}
F23	mean	3.7795×10^{3}	3.4554×10^{3}	3.1235×10^{3}	3.1744×10^{3}	2.8984×10^{3}	2.9484×10^{3}	2.9391×10^{3}	2.8514×10^{3}
	std	1.6605×10^{2}	1.3573×10^{2}	9.0179×10^{1}	2.2286×10^{1}	2.3796×10^{1}	2.9634×10^{1}	2.9612×10^{1}	2.4858×10^{1}
F24	mean	3.9327×10^{3}	3.7015×10^{3}	3.2830×10^{3}	3.3907×10^{3}	3.0613×10^{3}	3.1176×10^{3}	3.1147×10^{3}	3.0141×10^{3}
	std	2.0485×10^{2}	1.4499×10^{2}	7.3418×10^{1}	1.6837×10^{1}	2.1529×10^{1}	4.1206×10^{1}	3.3771×10^{1}	2.8771×10^{1}
F25	mean	9.0570×10^{3}	6.4242×10^{3}	3.0837×10^{3}	3.6743×10^{3}	3.0650×10^{3}	3.0726×10^{3}	3.0868×10^{3}	3.0599×10^{3}
	std	1.4457×10^{3}	8.4391×10^{2}	3.3848×10^{1}	1.0246×10^{2}	2.7905×10^{1}	2.3680×10^{1}	3.4871×10^{1}	2.5281×10^{1}
F26	mean	1.5781×10^{4}	1.1511×10^{4}	7.7110×10^{3}	8.1936×10^{3}	5.2857×10^{3}	5.7555×10^{3}	5.7448×10^{3}	5.0813×10^{3}
	std	1.6353×10^{3}	8.5661×10^{2}	1.4804×10^{3}	1.9254×10^{2}	2.8402×10^{2}	4.2510×10^{2}	4.9076×10^{2}	3.1902×10^{2}
F27	mean	4.8883×10^{3}	4.3493×10^{3}	3.7104×10^{3}	3.5911×10^{3}	3.3695×10^{3}	3.4819×10^{3}	3.4005×10^{3}	3.4022×10^{3}
	std	7.2641×10^{2}	2.6821×10^{2}	1.6159×10^{2}	4.6143×10^{1}	7.0589×10^{1}	1.0135×10^{2}	6.9606×10^{1}	8.8368×10^{1}
F28	mean	8.4752×10^{3}	6.6460×10^{3}	3.3616×10^{3}	6.2534×10^{3}	3.3210×10^{3}	3.3714×10^{3}	3.3601×10^{3}	3.3236×10^{3}
	std	9.3344×10^{2}	7.7449×10^{2}	5.1067×10^{1}	3.7800×10^{2}	2.3449×10^{1}	4.4832×10^{1}	2.8653×10^{1}	1.5965×10^{1}
F29	mean	1.4945×10^{4}	6.2374×10^{3}	4.5162×10^{3}	5.2206×10^{3}	4.0733×10^{3}	4.0655×10^{3}	4.0224×10^{3}	4.2909×10^{3}
	std	8.4878×10^{3}	1.3479×10^{3}	3.6310×10^{2}	1.8344×10^{2}	2.4136×10^{2}	2.6971×10^{2}	2.6754×10^{2}	3.5781×10^{2}
F30	mean	2.0195×10^{9}	2.7250×10^{8}	2.1487×10^{6}	2.9147×10^{7}	1.4707×10^{6}	3.2574×10^{6}	1.9784×10^{6}	3.5505×10^{6}
	std	1.1013×10^{9}	1.6034×10^{8}	1.1725×10^{6}	1.0483×10^{7}	6.1243×10^{5}	1.6041×10^{6}	6.4497×10^{5}	9.0309×10^{5}

Table 15. Experimental Results Compared with EDOA Variants and the CEC Winner Algorithm on the CEC2017 Benchmark Functions (Dim = 100).

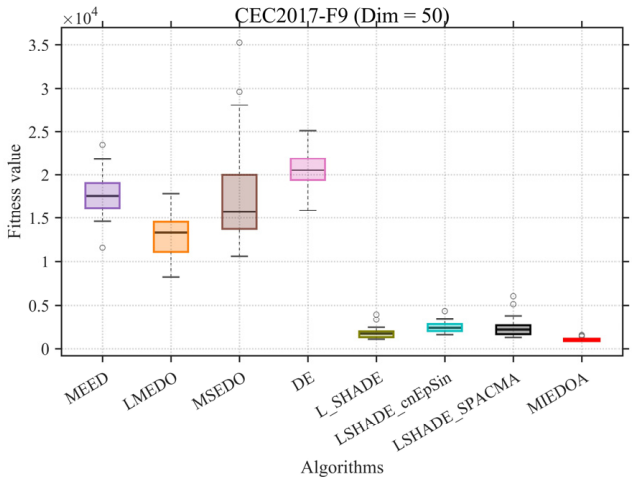
ID	Metric	MEED	LMEDO	MSEDO	DE	L_SHADE	LSHADE_cnEpSin	LSHADE_SPACMA	MIEDOA
F1	mean	1.8785×10^{11}	1.1440×10^{11}	1.2566×10^{9}	4.9673×10^{10}	7.1828×10^{8}	1.3980×10^{9}	1.7353×10^{9}	3.0542×10^{6}
	std	1.8162×10^{10}	1.7957×10^{10}	1.0801×10^{9}	4.2097×10^{9}	4.1830×10^{8}	4.5393×10^{8}	6.4425×10^{8}	1.1257×10^{6}
F2	mean	3.1913×10^{168}	7.2269×10^{144}	5.2812×10^{127}	1.8505×10^{153}	1.0000×10^{30}	1.0000×10^{30}	1.4250×10^{113}	4.7817×10^{97}
	std	6.5535×10^{4}	3.9582×10^{145}	2.8926×10^{128}	6.5535×10^{4}	1.4314×10^{14}	1.4314×10^{14}	7.8041×10^{113}	2.2299×10^{98}
F3	mean	4.5788×10^{5}	2.6013×10^{5}	3.2763×10^{5}	7.9729×10^{5}	3.4621×10^{5}	3.1231×10^{5}	3.4215×10^{5}	2.2516×10^{5}
	std	7.1671×10^{4}	1.9536×10^{4}	5.4329×10^{4}	6.1901×10^{4}	1.6698×10^{5}	1.0113×10^{5}	1.4895×10^{5}	2.7023×10^{4}
F4	mean	4.2728×10^{4}	2.0894×10^{4}	1.1837×10^{3}	8.5178×10^{3}	9.4651×10^{2}	1.1023×10^{3}	1.1246×10^{3}	8.1178×10^{2}
	std	1.0508×10^{4}	5.3401×10^{3}	2.2045×10^{2}	9.8911×10^{2}	7.2611×10^{1}	1.0171×10^{2}	1.0493×10^{2}	5.7534×10^{1}
F5	mean	1.7618×10^{3}	1.4843×10^{3}	1.1931×10^{3}	1.8150×10^{3}	1.1066×10^{3}	1.1951×10^{3}	1.1926×10^{3}	8.4872×10^{2}
	std	8.9494×10^{1}	1.3536×10^{2}	1.0539×10^{2}	3.3386×10^{1}	6.8225×10^{1}	5.4168×10^{1}	1.2780×10^{2}	4.9867×10^{1}
F6	mean	6.8379×10^{2}	6.7106×10^{2}	6.4759×10^{2}	6.5254×10^{2}	6.1823×10^{2}	6.2794×10^{2}	6.2043×10^{2}	6.1178×10^{2}
	std	5.2624×10^{0}	1.0192×10^{1}	6.0721×10^{0}	1.8185×10^{0}	4.8573×10^{0}	4.4313×10^{0}	3.5634×10^{0}	4.0377×10^{0}
F7	mean	3.6153×10^{3}	2.9879×10^{3}	3.0565×10^{3}	3.1846×10^{3}	1.8412×10^{3}	1.9628×10^{3}	1.8706×10^{3}	1.2826×10^{3}
	std	1.6327×10^{2}	2.0826×10^{2}	2.8394×10^{2}	1.0492×10^{2}	1.0372×10^{2}	1.4656×10^{2}	1.2141×10^{2}	7.8705×10^{1}
F8	mean	2.1663×10^{3}	1.8665×10^{3}	1.4779×10^{3}	2.0997×10^{3}	1.3720×10^{3}	1.4835×10^{3}	1.4611×10^{3}	1.1407×10^{3}
	std	1.0578×10^{2}	1.3510×10^{2}	1.0770×10^{2}	3.2946×10^{1}	8.5781×10^{1}	6.2775×10^{1}	7.6170×10^{1}	6.0454×10^{1}
F9	mean	4.8516×10^{4}	4.7620×10^{4}	6.3991×10^{4}	1.0457×10^{5}	1.3190×10^{4}	1.8707×10^{4}	1.8446×10^{4}	7.4659×10^{3}
	std	5.7803×10^{3}	4.9569×10^{3}	1.0406×10^{4}	7.2835×10^{3}	2.9144×10^{3}	4.7908×10^{3}	5.3973×10^{3}	2.0336×10^{3}

Table 15. *Cont.*

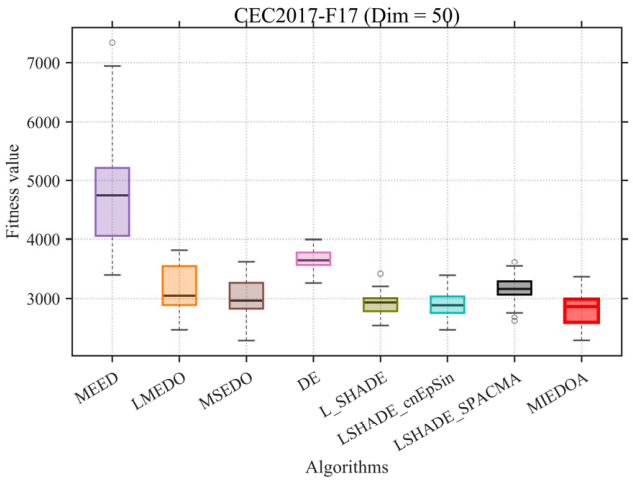
ID	Metric	MEED	LMEDO	MSEDO	DE	L_SHADE	LSHADE_cnEpSin	LSHADE_SPACMA	MIEDOA
F10	mean	2.3836×10^{4}	2.8460×10^{4}	3.1482×10^{4}	3.0349×10^{4}	2.1991×10^{4}	2.4022×10^{4}	2.3199×10^{4}	1.6341×10^{4}
	std	9.5430×10^{2}	8.2080×10^{2}	2.5593×10^{3}	3.5523×10^{2}	6.9864×10^{2}	2.9214×10^{3}	2.2481×10^{3}	1.6414×10^{3}
F11	mean	1.7760×10^{5}	2.2156×10^{4}	1.5980×10^{4}	1.6077×10^{5}	1.5472×10^{4}	2.2975×10^{4}	3.1109×10^{4}	2.5022×10^{4}
	std	4.4399×10^{4}	6.2801×10^{3}	7.0890×10^{3}	2.2417×10^{4}	2.3552×10^{4}	2.4464×10^{4}	3.5713×10^{4}	5.5280×10^{3}
F12	mean	1.0887×10^{11}	3.8528×10^{10}	8.0508×10^{7}	1.3348×10^{10}	5.1604×10^{7}	2.1239×10^{8}	1.5212×10^{8}	5.0755×10^{7}
	std	2.0766×10^{10}	8.8924×10^{9}	1.4392×10^{8}	1.5272×10^{9}	2.4250×10^{7}	1.3378×10^{8}	9.0584×10^{7}	1.9384×10^{7}
F13	mean	2.4160×10^{10}	4.7650×10^{9}	1.1202×10^{4}	2.1125×10^{8}	1.8853×10^{4}	6.1032×10^{4}	3.5942×10^{4}	7.5492×10^{3}
	std	4.0278×10^{9}	2.2784×10^{9}	7.1881×10^{3}	6.5829×10^{7}	7.7365×10^{3}	1.7416×10^{4}	1.0326×10^{4}	5.1346×10^{3}
F14	mean	2.6548×10^{7}	5.8420×10^{6}	7.3289×10^{5}	3.7126×10^{7}	2.4642×10^{5}	2.4819×10^{5}	2.4605×10^{5}	4.4593×10^{5}
	std	1.0410×10^{7}	5.3735×10^{6}	4.4924×10^{5}	9.4731×10^{6}	1.7917×10^{5}	1.6822×10^{5}	1.3151×10^{5}	2.3293×10^{5}
F15	mean	1.0308×10^{10}	8.3958×10^{8}	3.9243×10^{3}	3.7161×10^{7}	7.1610×10^{3}	2.0285×10^{4}	7.6912×10^{3}	4.7888×10^{3}
	std	2.7039×10^{9}	5.8249×10^{8}	1.9824×10^{3}	1.2077×10^{7}	4.7693×10^{3}	8.1313×10^{3}	2.9101×10^{3}	2.6149×10^{3}
F16	mean	1.5365×10^{4}	8.9605×10^{3}	5.5491×10^{3}	1.1326×10^{4}	7.0819×10^{3}	6.6869×10^{3}	7.3569×10^{3}	5.4896×10^{3}
	std	2.1561×10^{3}	1.4552×10^{3}	9.5718×10^{2}	3.8971×10^{2}	5.3353×10^{2}	5.4194×10^{2}	6.5170×10^{2}	6.6288×10^{2}
F17	mean	7.8074×10^{5}	1.0247×10^{4}	4.9442×10^{3}	8.3464×10^{3}	5.5722×10^{3}	5.3777×10^{3}	5.8640×10^{3}	4.8590×10^{3}
	std	8.3397×10^{5}	4.6522×10^{3}	8.2788×10^{2}	3.1464×10^{2}	3.8276×10^{2}	3.8467×10^{2}	5.6740×10^{2}	5.7589×10^{2}
F18	mean	2.8995×10^{7}	4.9803×10^{6}	2.5588×10^{6}	5.2640×10^{7}	4.3479×10^{5}	4.3642×10^{5}	3.9166×10^{5}	7.4686×10^{5}
	std	1.8448×10^{7}	5.7598×10^{6}	2.0927×10^{6}	1.7455×10^{7}	2.0514×10^{5}	2.0250×10^{5}	1.9404×10^{5}	4.0591×10^{5}
F19	mean	9.7852×10^{9}	8.6694×10^{8}	8.6910×10^{3}	6.4231×10^{7}	5.1946×10^{3}	3.5710×10^{4}	9.8610×10^{3}	6.7139×10^{3}
	std	3.3504×10^{9}	8.2864×10^{8}	1.1789×10^{4}	1.9618×10^{7}	4.0792×10^{3}	3.2859×10^{4}	1.0397×10^{4}	6.2932×10^{3}
F20	mean	6.4560×10^{3}	7.1451×10^{3}	6.7694×10^{3}	7.0179×10^{3}	6.1780×10^{3}	5.7648×10^{3}	6.7185×10^{3}	5.0637×10^{3}
	std	5.2528×10^{2}	2.5709×10^{2}	1.1938×10^{3}	2.1715×10^{2}	3.7974×10^{2}	3.4533×10^{2}	4.2603×10^{2}	5.4209×10^{2}
F21	mean	4.2442×10^{3}	3.6241×10^{3}	3.0982×10^{3}	3.6444×10^{3}	2.9223×10^{3}	3.0635×10^{3}	3.0436×10^{3}	2.6384×10^{3}
	std	2.4892×10^{2}	1.3200×10^{2}	1.1506×10^{2}	3.5036×10^{1}	7.3340×10^{1}	7.4660×10^{1}	9.0725×10^{1}	5.3075×10^{1}
F22	mean	2.7235×10^{4}	3.0819×10^{4}	3.3721×10^{4}	3.2278×10^{4}	2.4291×10^{4}	2.6575×10^{4}	2.6019×10^{4}	1.9101×10^{4}
	std	8.8203×10^{2}	2.3683×10^{3}	4.0106×10^{3}	5.8270×10^{2}	1.0039×10^{3}	2.2691×10^{3}	2.5869×10^{3}	1.8611×10^{3}
F23	mean	5.2662×10^{3}	4.8442×10^{3}	3.8535×10^{3}	3.8416×10^{3}	3.3911×10^{3}	3.5531×10^{3}	3.4975×10^{3}	3.1880×10^{3}
	std	5.2165×10^{2}	2.4311×10^{2}	1.5812×10^{2}	2.6638×10^{1}	6.8361×10^{1}	1.1196×10^{2}	6.9486×10^{1}	5.7972×10^{1}
F24	mean	6.4224×10^{3}	7.2801×10^{3}	4.9050×10^{3}	4.4390×10^{3}	3.9522×10^{3}	4.1507×10^{3}	4.0801×10^{3}	3.6830×10^{3}
	std	6.2437×10^{2}	6.0938×10^{2}	2.5847×10^{2}	2.8862×10^{1}	1.3126×10^{2}	1.5238×10^{2}	1.2961×10^{2}	6.4277×10^{1}
F25	mean	1.8393×10^{4}	1.2331×10^{4}	3.8699×10^{3}	1.5829×10^{4}	3.6697×10^{3}	3.8289×10^{3}	3.8316×10^{3}	3.4883×10^{3}
	std	2.3436×10^{3}	1.9862×10^{3}	1.7145×10^{2}	1.3991×10^{3}	7.6248×10^{1}	1.2325×10^{2}	1.3936×10^{2}	4.9523×10^{1}
F26	mean	4.3698×10^{4}	3.5091×10^{4}	2.0541×10^{4}	1.8218×10^{4}	1.1881×10^{4}	1.3979×10^{4}	1.3284×10^{4}	9.7951×10^{3}
	std	3.1174×10^{3}	3.3246×10^{3}	2.6158×10^{3}	3.7207×10^{2}	1.3019×10^{3}	1.5917×10^{3}	1.1289×10^{3}	6.5150×10^{2}
F27	mean	7.5503×10^{3}	6.8954×10^{3}	4.3333×10^{3}	4.4291×10^{3}	3.6466×10^{3}	3.8180×10^{3}	3.7489×10^{3}	3.5469×10^{3}
	std	2.2830×10^{3}	7.6135×10^{2}	3.0403×10^{2}	8.4968×10^{1}	1.0468×10^{2}	1.2439×10^{2}	1.2492×10^{2}	7.0500×10^{1}
F28	mean	2.2411×10^{4}	1.6367×10^{4}	4.3066×10^{3}	1.8462×10^{4}	3.8486×10^{3}	4.2133×10^{3}	4.2037×10^{3}	3.6288×10^{3}
	std	2.3665×10^{3}	2.1056×10^{3}	4.5930×10^{2}	5.3888×10^{2}	1.5246×10^{2}	3.2661×10^{2}	2.4646×10^{2}	5.2469×10^{1}
F29	mean	6.2254×10^{4}	1.4811×10^{4}	7.5573×10^{3}	1.0947×10^{4}	7.6710×10^{3}	7.1452×10^{3}	7.6661×10^{3}	7.2946×10^{3}
	std	3.2029×10^{4}	2.5330×10^{3}	6.8616×10^{2}	4.3223×10^{2}	5.3481×10^{2}	6.6419×10^{2}	5.1316×10^{2}	6.7544×10^{2}
F30	mean	2.2067×10^{10}	3.2876×10^{9}	2.5780×10^{6}	4.6555×10^{7}	2.0089×10^{5}	3.5339×10^{6}	1.1656×10^{6}	3.5857×10^{5}
	std	4.8643×10^{9}	1.7926×10^{9}	3.9722×10^{6}	8.7780×10^{6}	1.3217×10^{5}	2.0412×10^{6}	6.0445×10^{5}	1.7510×10^{5}



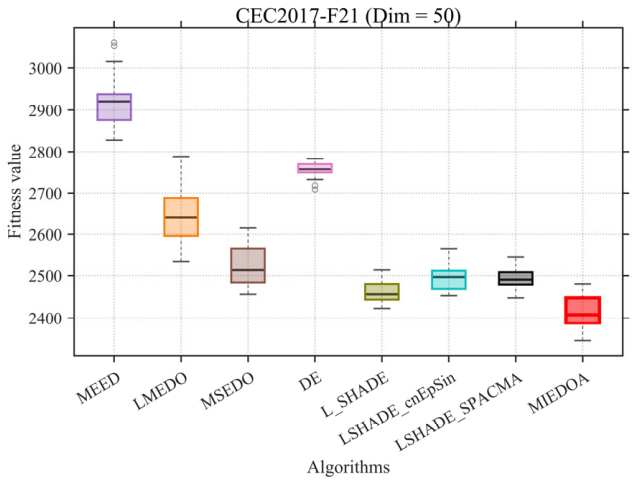
(**a**) CEC2017-F5 (Dim = 50)



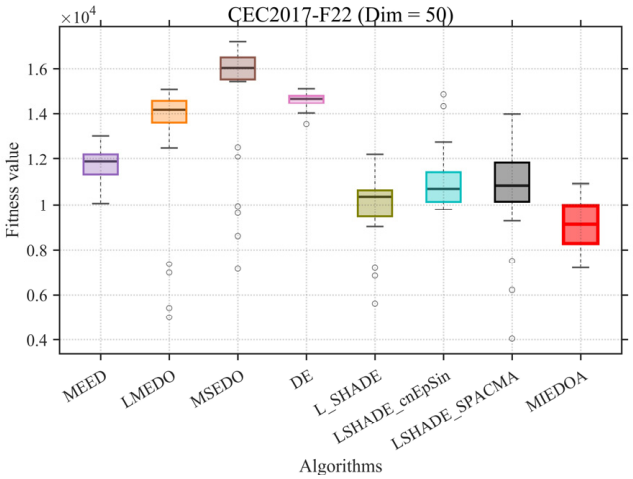
(**b**) CEC2017-F9 (Dim = 50)



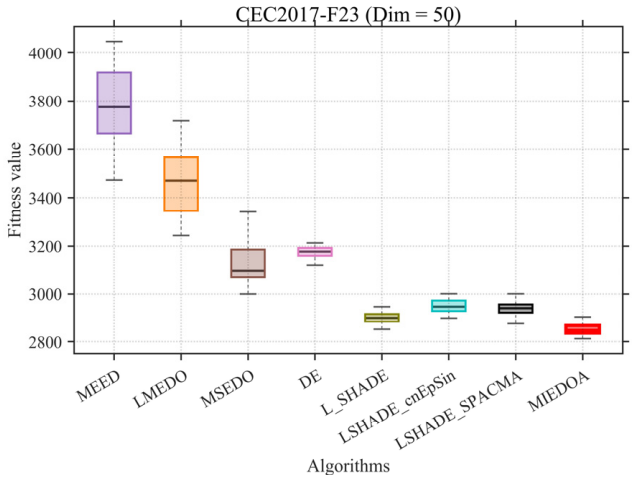
(**c**) CEC2017-F17 (Dim = 50)



(**d**) CEC2017-F21 (Dim = 50)

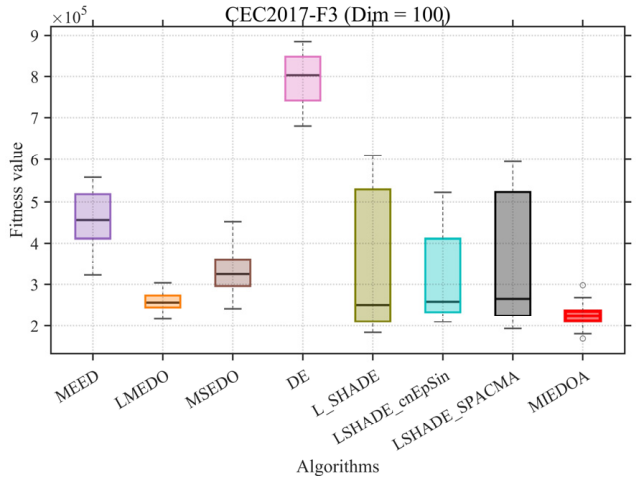


(**e**) CEC2017-F22 (Dim = 50)

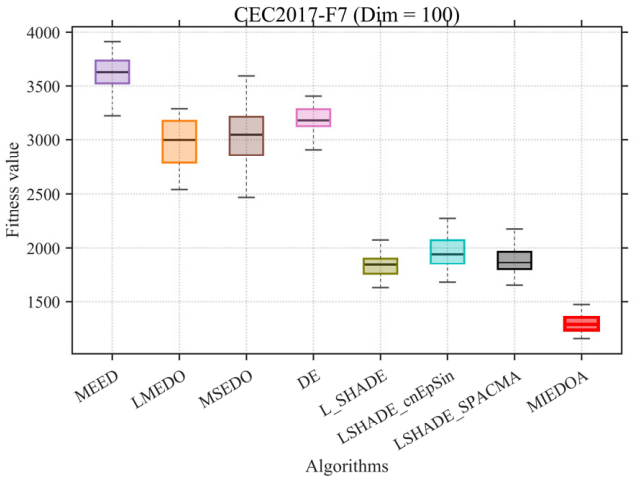


(**f**) CEC2017-F23 (Dim = 50)

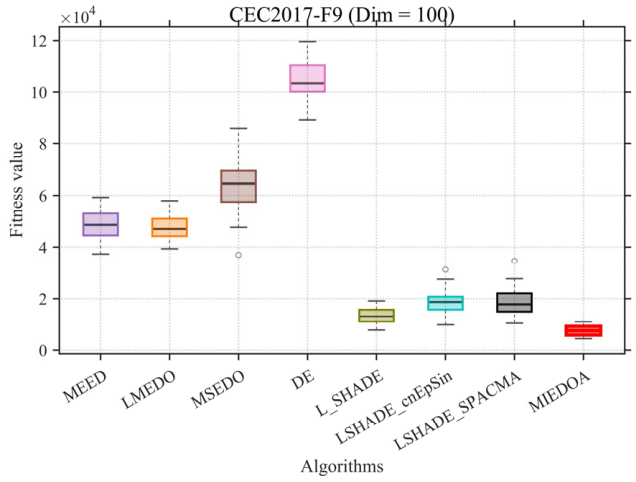
Figure 13. *Cont.*



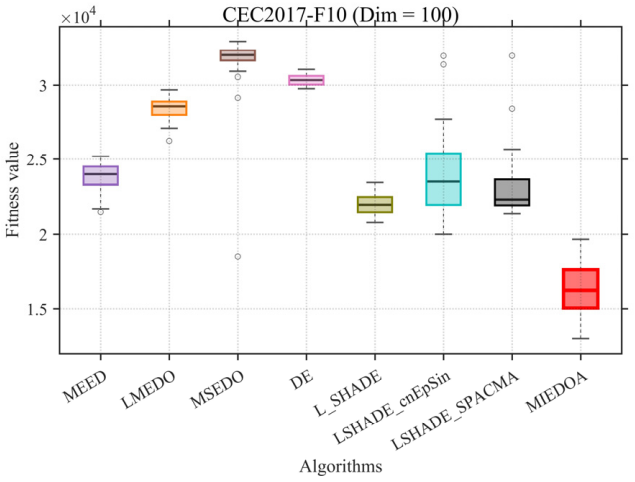
(**g**) CEC2017-F3 (Dim = 100)



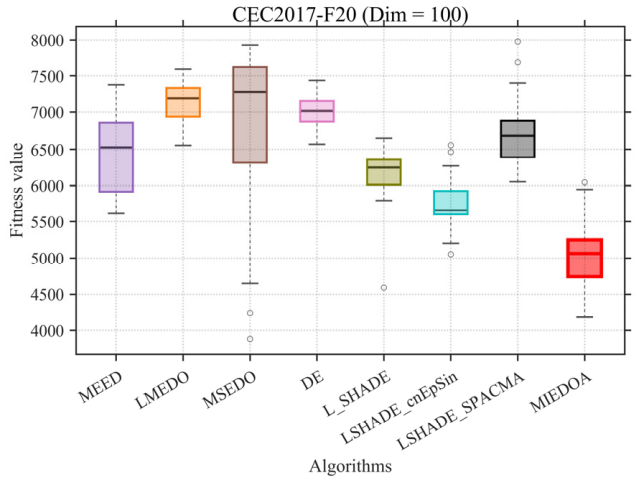
(**h**) CEC2017-F7 (Dim = 100)



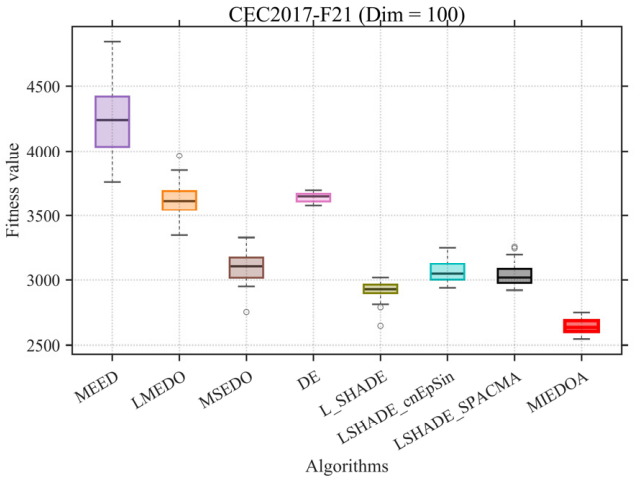
(**i**) CEC2017-F9 (Dim = 100)



(**j**) CEC2017-F10 (Dim = 100)



(**k**) CEC2017-F20 (Dim = 100)



(**l**) CEC2017-F21 (Dim = 100)

Figure 13. Box Plots Comparing EDOA Variants and the CEC Winner Algorithm.

4. MIEDOA for 3D Wireless Sensor Deployment

This section focuses on the application of the proposed MIEDOA to the three-dimensional wireless sensor network (3D WSN) deployment problem. First, a mathematical model of the 3D deployment scenario is established, including the system assumptions, coverage evaluation method, and optimization formulation. Then, a series of numerical experiments are conducted

to evaluate the effectiveness and robustness of MIEDOA under different network scales. The performance of the proposed algorithm is further validated through comparative analysis in terms of coverage quality, convergence behavior, and stability.

To focus on evaluating the optimization performance of MIEDOA in three-dimensional deployment problems, this study adopts a coverage-oriented deployment model that primarily considers sensing coverage while omitting several secondary network-layer constraints.

4.1. Three-Dimensional WSN Deployment Model

4.1.1. System Model

In practical applications such as underground monitoring, underwater exploration, and aerial surveillance, wireless sensor networks (WSNs) are often deployed in volumetric environments. Compared with conventional planar deployment models, three-dimensional (3D) deployment significantly increases the number of decision variables and introduces more complex spatial interactions, which greatly increases the difficulty of optimization [45–47].

In this study, the monitored region is modeled as a bounded cubic space in a 3D Cartesian coordinate system, defined as:

$$\Omega = \{(x, y, z) \mid x, y, z \in [0, L]\} \tag{16}$$

where L denotes the side length of the cube.

Assume that N homogeneous sensor nodes are deployed within Ω. Each sensor is equipped with an isotropic sensing device, and its sensing region can be approximated as a sphere with radius R. To focus on coverage performance, communication constraints among nodes are not considered in this model.

The position of the i-th sensor node in 3D space is represented as:

$$\boldsymbol{s}_i = [x_i, y_i, z_i],\ i = 1, 2, \ldots, N. \tag{17}$$

Thus, the deployment of all sensor nodes can be expressed by a $3N$-dimensional decision vector $\boldsymbol{X} = (x_1, \ldots, x_N, y_1, \ldots, y_N, z_1, \ldots, z_N)$. To ensure that the sensing region of each node is fully contained within the monitoring space, the following boundary constraints must be satisfied:

$$x_i, y_i, z_i \in [R, L - R], i = 1, 2, \ldots, N. \tag{18}$$

4.1.2. Volumetric Coverage Model

For any arbitrary point $\mathbf{p} = (x, y, z)$ in the monitored region Ω, the Euclidean distance between this point and the i-th sensor node is given by:

$$d_i(\mathbf{p}) = \| \mathbf{p} - \mathbf{s}_i \|_2 = \sqrt{(x - x_i)^2 + (y - y_i)^2 + (z - z_i)^2} \tag{19}$$

A point $\mathbf{p}$ is considered to be covered if at least one sensor satisfies $d_i(\mathbf{p}) \leq R$. Due to the high computational complexity of continuous volumetric integration, a discretization strategy is adopted. Specifically, the cubic region Ω is uniformly divided into L^3 grid points. For each grid point, a binary coverage indicator function is defined as:

$$M(x, y, z) = \begin{cases} 1, \text{if the point is covered by at least one sensor,} \\ 0, \text{otherwise} \end{cases} \tag{20}$$

Based on this discretization, the volumetric coverage ratio for a given deployment $\boldsymbol{X}$ can be calculated as:

$$C(\boldsymbol{X}) = \frac{1}{L^3} \sum_{x=1}^{L} \sum_{y=1}^{L} \sum_{z=1}^{L} M(x, y, z) \tag{21}$$

The value of $C(\boldsymbol{X})$ reflects the proportion of the monitored space that is effectively covered by the sensor network.

4.1.3. Optimization Formulation

The objective of the 3D WSN deployment problem is to determine the optimal spatial configuration of sensor nodes that maximizes the overall volumetric coverage. This can be formulated as:

$$\max_{\boldsymbol{X}} C(\boldsymbol{X}) \tag{22}$$

Subject to the boundary constraints of sensor positions.

Since most metaheuristic optimization algorithms are designed for minimization problems, the objective function is transformed into an equivalent form:

$$\min_{\boldsymbol{X}} f(\boldsymbol{X}) = \frac{1}{C(\boldsymbol{X})} \tag{23}$$

This transformation preserves the original optimization goal while allowing the problem to be efficiently solved using population-based optimization algorithms.

4.1.4. Experimental Settings

To evaluate the effectiveness of the proposed algorithm in solving 3D WSN deployment problems, simulations are conducted in a cubic monitoring space of size $50 \times 50 \times 50$. Two deployment scenarios with different network scales (e.g., $N = 30$ and $N = 50$) are considered to analyze scalability.

All algorithms were executed independently 30 times to mitigate the effects of randomness, and their average performance metrics were reported. A fixed maximum number of 500 iterations was adopted as the termination criterion. All algorithms utilized identical parameter settings to ensure fairness and reproducibility.

4.1.5. Limitations of the Simplified 3D WSN Deployment Model

It should be noted that the objective of this study is not to construct a fully realistic wireless sensor network deployment framework, but rather to provide a representative engineering optimization problem for evaluating the optimization capability of the proposed MIEDOA. Therefore, several practical factors commonly encountered in real-world WSN deployment scenarios are intentionally simplified.

Specifically, the current deployment model considers only sensing coverage optimization and assumes ideal spherical sensing regions. Communication constraints between sensor nodes, network connectivity requirements, energy consumption models, heterogeneous sensor characteristics, environmental obstacles, and terrain-induced signal attenuation are not explicitly incorporated into the formulation. Consequently, the optimization objective focuses exclusively on maximizing the coverage ratio of the monitored three-dimensional space.

Although the simplified model enables a clear evaluation of the search capability, convergence behavior, and deployment effectiveness of the proposed algorithm, future work will extend the current framework by incorporating communication connectivity constraints, energy-aware deployment mechanisms, obstacle-aware sensing models, and multi-objective optimization formulations to better reflect realistic wireless sensor network deployment scenarios.

4.2. Analysis of Experimental Results

In this subsection, we apply MIEDOA to the problem of 3D wireless sensor deployment in two scenarios—specifically, with 30 and 50 nodes—and present the analysis of the experimental results below.

4.2.1. Analysis of the 30-Node Deployment Experiment

In this subsection, a deployment scenario comprising 30 nodes is designed to evaluate the effectiveness of the proposed algorithm for coverage optimization in three-dimensional wireless sensor networks (WSNs). The sensor nodes are distributed within a predefined monitoring space and undergo position optimization to maximize volumetric coverage. To mitigate the influence of stochastic factors, each experiment was independently repeated 30 times, and the averaged results are reported herein. The detailed experimental results and corresponding analyses are presented below.

In terms of spatial distribution, Figure 14 illustrates the deployment structures generated by various algorithms under a 30-node configuration. It is readily apparent that the node distribution achieved by MIEDOA is more uniform and exhibits excellent spatial scalability; nodes maintain reasonable spacing relative to one another, thereby effectively preventing issues of excessive local clustering and coverage redundancy, while simultaneously significantly minimizing the presence of uncovered areas. This balanced distribution indicates that the algorithm effectively explores the solution space during the global search phase and demonstrates robust refinement capabilities during the local optimization phase, thereby yielding an optimal spatial coverage structure. In contrast, the node distributions produced by some of the benchmark algorithms exhibit significant spatial imbalance—manifesting as either localized clustering or sparse distribution—which ultimately leads to diminished coverage efficiency.

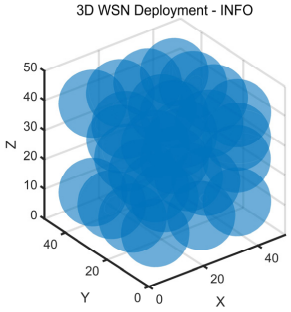
In terms of convergence performance, Figure 15 illustrates the convergence curves of the various algorithms for the 30-node deployment problem. It can be observed that MIEDOA exhibits a rapid downward trend during the early stages of iteration, indicating its strong global exploration capability and its ability to quickly approach regions containing high-quality solutions. During the middle to late stages, its convergence curve continues to decline steadily, without displaying significant oscillations or premature stagnation; this demonstrates excellent local exploitation capability and convergence stability. In contrast, some algorithms exhibit premature convergence or oscillatory behavior during the iterative process, suggesting that they are prone to becoming trapped in local optima or lack the capacity for sustained optimization.

In terms of quantitative performance, Table 16 presents a statistical analysis of the experimental results obtained by each algorithm in the 30-node deployment task. As indicated in the table, MIEDOA achieved optimal or near-optimal results across metrics such as “Best” and “Mean”; furthermore, its relatively low standard deviation (Std) values demonstrate that the algorithm exhibits high stability and robustness across multiple independent runs. Additionally, its attainment of the top rank in the Friedman test further validates that its overall performance surpasses that of the other comparative algorithms.

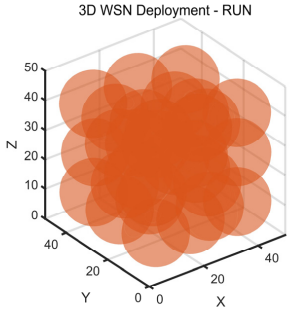
Taken together, the spatial distribution results in Figure 14, the convergence behavior in Figure 15, and the statistical metrics in Table 16 mutually corroborate one another, conclusively demonstrating that MIEDOA possesses significant advantages in the 30-node 3D sensor deployment problem. Its enhanced performance is primarily attributable to a multi-strategy collaborative mechanism: diversified initialization improves the distributional quality of the initial solutions; the collaborative learning mechanism enhances search directionality; and feedback-based adaptive regulation further establishes a dynamic balance between exploration and exploitation—thereby exhibiting superiority in terms of coverage performance, convergence speed, and result stability.

Table 16. Experimental Results of the 30-Node Deployment.

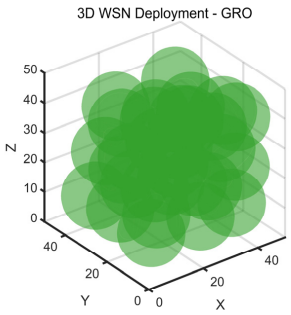
Algorithm	Best	Worst	Mean	Median	Std	Friedman Rank
INFO	76.3352	71.9768	75.2015	75.3212	0.9666	3.57
RUN	74.0456	67.0728	71.9427	72.4392	1.5773	7.40
GRO	68.8248	63.0200	65.8248	65.6856	1.1779	10.43
ESC	75.1248	72.5408	73.8970	73.8228	0.6562	5.33
RIME	73.3176	69.7304	71.3884	71.3800	0.8958	8.20
GKSO	75.1480	70.6336	73.0297	73.0172	0.9628	6.40
RTH	76.5944	74.9584	75.9793	75.9632	0.4763	2.43
FTO	74.8168	69.3240	72.1264	72.1356	1.3861	7.30
BBO	76.1184	74.0296	75.3902	75.6588	0.6660	3.00
IGWO	70.3376	63.1040	65.1234	64.7212	1.7331	10.63
EDOA	67.2936	58.7816	60.5172	60.1464	1.6184	11.93
MIEDOA	76.6536	75.3	76.2847	76.462	0.4287	1.37



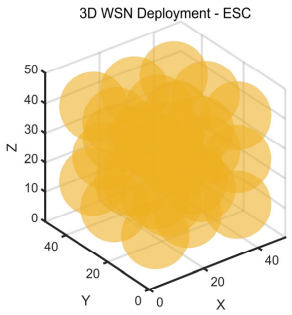
(**a**) 3D WSN Deployment—INFO



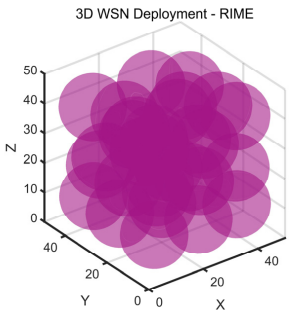
(**b**) 3D WSN Deployment—RUN



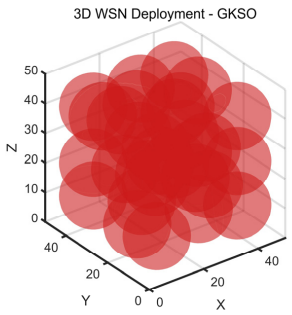
(**c**) 3D WSN Deployment—GRO



(**d**) 3D WSN Deployment—ESC

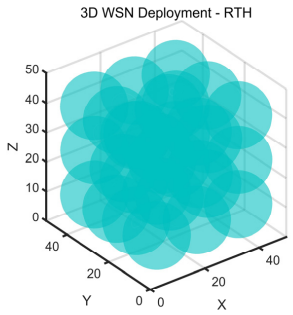


(**e**) 3D WSN Deployment—RIME

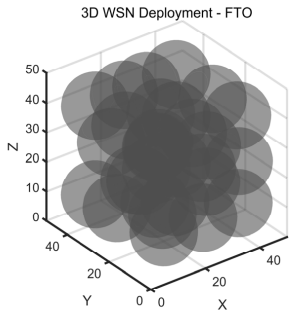


(**f**) 3D WSN Deployment—GKSO

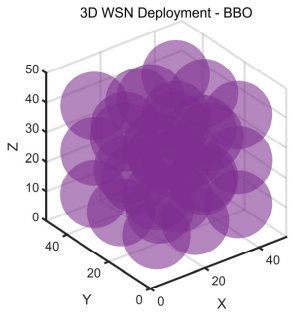
Figure 14. *Cont.*



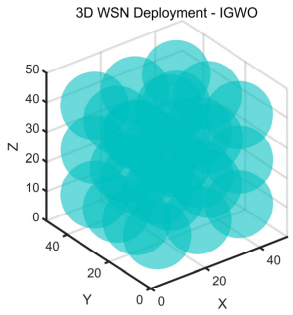
(**g**) 3D WSN Deployment—RTH



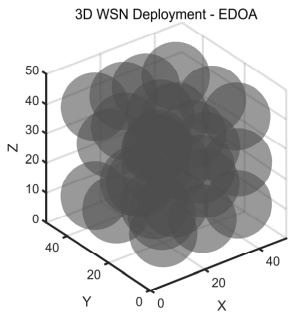
(**h**) 3D WSN Deployment—FTO



(**i**) 3D WSN Deployment—BBO



(**j**) 3D WSN Deployment—IGWO



(**k**) 3D WSN Deployment—EDOA



(**l**) 3D WSN Deployment—MIEDOA

Figure 14. 30-Node Deployment Diagram.

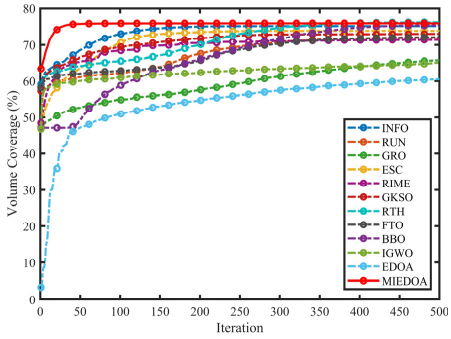
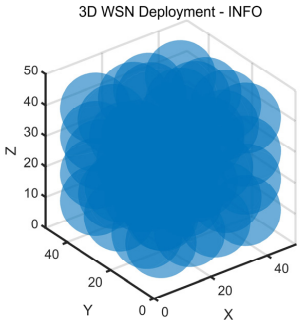


Figure 15. 30-Node Deployment Convergence Curve.

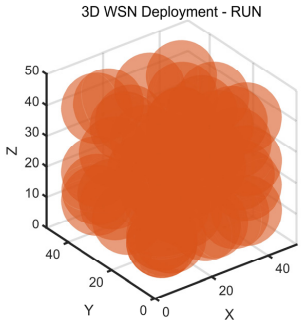
4.2.2. Analysis of the 50-Node Deployment Experiment

In this subsection, a deployment scenario comprising 50 nodes is designed to evaluate the effectiveness of the proposed algorithm for coverage optimization in three-dimensional wireless sensor networks (WSNs). The sensor nodes are distributed within a predefined monitoring space and undergo position optimization to maximize volumetric coverage. To mitigate the influence of stochastic factors, each experiment was independently repeated 30 times, and the averaged results are reported herein. The detailed experimental results and corresponding analyses are presented below.

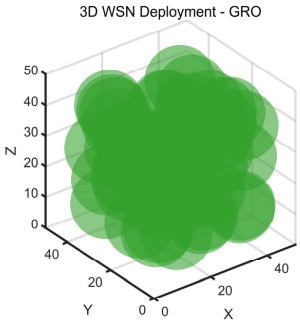
In terms of spatial distribution, Figure 16 illustrates the deployment structures of the various algorithms at a scale of 50 nodes. As the number of nodes increases, the complexity of the search space rises significantly; however, MIEDOA continues to maintain a relatively uniform spatial distribution. The nodes demonstrate excellent scalability and coverage continuity within the three-dimensional region, effectively filling potential coverage gaps while simultaneously minimizing redundant coverage. This indicates that the algorithm retains robust global search capabilities and spatial adaptability even within complex, high-dimensional scenarios. In contrast, some of the comparison algorithms are more prone to issues of local clustering or uneven distribution under high-node-density conditions—leading to diminished coverage efficiency—thereby highlighting their insufficient adaptability in complex environments.



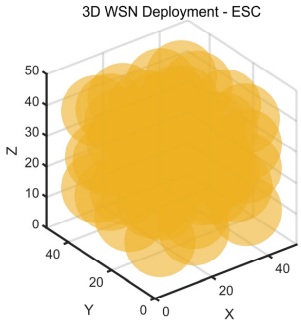
(**a**) 3D WSN Deployment—INFO



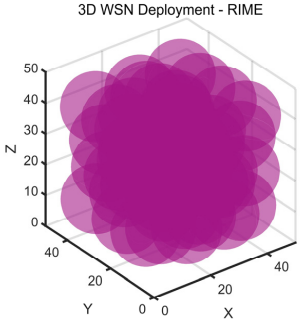
(**b**) 3D WSN Deployment—RUN



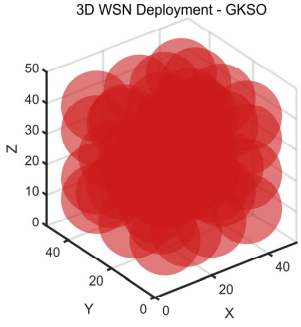
(**c**) 3D WSN Deployment—GRO



(**d**) 3D WSN Deployment—ESC

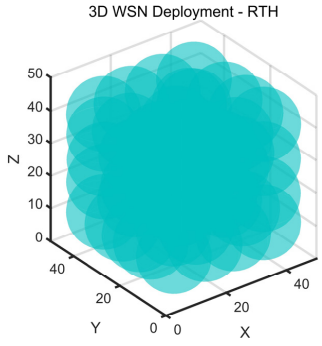


(**e**) 3D WSN Deployment—RIME

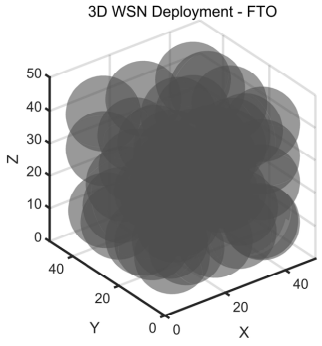


(**f**) 3D WSN Deployment—GKSO

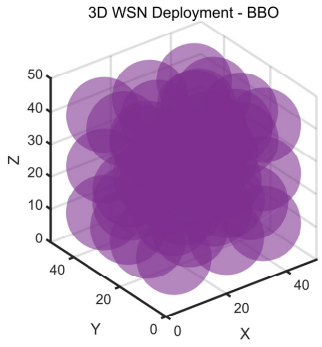
Figure 16. *Cont.*



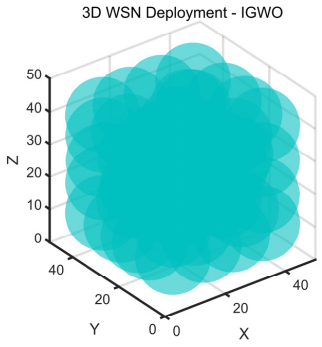
(**g**) 3D WSN Deployment—RTH



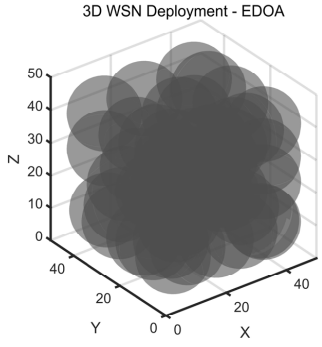
(**h**) 3D WSN Deployment—FTO



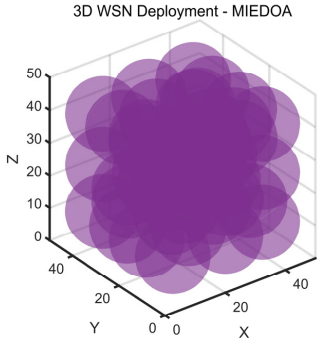
(**i**) 3D WSN Deployment—BBO



(**j**) 3D WSN Deployment—IGWO



(**k**) 3D WSN Deployment—EDOA



(**l**) 3D WSN Deployment—MIEDOA

Figure 16. 50-Node Deployment Diagram.

Regarding convergence performance, Figure 17 presents the convergence curves for a 50-node deployment problem. It can be observed that MIEDOA maintains a rapid convergence rate during the initial iterations, indicating that its multi-strategy initialization and global exploration mechanisms enable it to quickly locate regions containing high-quality solutions. In the mid-to-late stages, the convergence process becomes smoother and continues to descend steadily, exhibiting neither significant oscillations nor premature convergence; this demonstrates its robust local exploitation capabilities and stability. In contrast, some of the comparison algorithms experience a marked slowdown in convergence speed—or even stagnation and oscillation—in this high-dimensional scenario, revealing deficiencies in their ability to balance exploration and exploitation.

In terms of quantitative performance, Table 17 presents a statistical analysis of the experimental results obtained by each algorithm in the 50-node deployment task. Based on the overall results, MIEDOA continues to achieve optimal or near-optimal performance across both the "Best" and "Mean" metrics; moreover, its low standard deviation (Std) values indicate a high degree of stability and consistency across multiple independent runs. Furthermore, it maintains a leading position in the Friedman ranking, thereby further validating its superiority

in addressing complex, high-dimensional optimization problems. Compared to the 30-node scenario—despite the increased overall optimization difficulty—MIEDOA exhibited only a minimal decline in performance, thereby demonstrating excellent scalability and robustness.

Taken together, the spatial distribution results in Figure 16, the convergence behavior in Figure 17, and the statistical analysis in Table 17 mutually corroborate one another, demonstrating that MIEDOA maintains superior performance even in highly complex 3D deployment problems involving 50 nodes. Its advantages stem primarily from the effective operation of a multi-strategy collaborative mechanism across different stages: diversified initialization enhances the quality of initial solutions, collaborative learning improves search directionality, and an adaptive feedback regulation mechanism dynamically balances exploration and exploitation—thereby enabling the algorithm to outperform its counterparts in terms of coverage performance, convergence speed, and stability.

Table 17. Experimental Results of the 50-Node Deployment.

Algorithm	Best	Worst	Mean	Median	Std	Friedman Rank
INFO	82.5872	81.3480	82.1030	82.1240	0.2914	2.83
RUN	80.2928	77.8304	79.0926	79.1556	0.6055	7.40
GRO	75.8496	71.3144	73.6423	73.7588	1.1795	10.20
ESC	81.3368	79.1000	80.1499	80.1348	0.5459	5.63
RIME	78.8480	76.6664	77.7168	77.7236	0.5749	8.97
GKSO	81.0928	78.8536	80.3156	80.3336	0.4771	5.27
RTH	83.3824	81.2464	82.4867	82.5220	0.4966	2.03
FTO	80.3992	78.0760	79.4443	79.4664	0.4981	7.10
BBO	81.1896	79.5840	80.6253	80.6580	0.4133	4.63
IGWO	75.5440	67.3744	71.6146	71.4732	2.0100	11.07
EDOA	73.5048	64.7288	69.4103	70.2340	2.2250	11.73
MIEDOA	83.4264	82.6168	83.0241	83.0660	0.2220	1.13

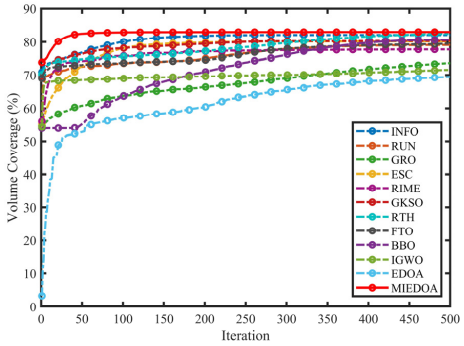


Figure 17. 50-Node Deployment Convergence Curve.

5. Conclusions

This paper proposed a Multi-Strategy Improved Enterprise Development Optimization Algorithm (MIEDOA) to address several limitations of the original EDOA, including insufficient population diversity, weak search guidance, and limited adaptability in balancing exploration and exploitation. To improve the optimization capability of EDOA, three complementary strategies were developed, namely Strategic Diversification Initialization (SDI), Organizational Synergy Learning (OSL), and Adaptive Governance with Feedback Regulation (AGFR). These strategies aim to improve the initial population distribution, enhance collaborative search guidance, and adaptively regulate the search process throughout the optimization procedure.

To evaluate the performance of the proposed algorithm, extensive experiments were conducted on the CEC2017 and CEC2020 benchmark suites. The experimental results indicate that MIEDOA generally achieves competitive optimization performance in terms of convergence accuracy, convergence behavior, and robustness when compared with the considered algorithms. The boxplot analysis further suggests that MIEDOA exhibits

relatively stable performance across multiple independent runs. In addition, the strategy effectiveness analysis indicates that the proposed mechanisms contribute positively to the overall optimization process, while the Wilcoxon signed-rank test, Friedman mean rank test, Holm post hoc test, and effect size analysis provide statistical evidence supporting the observed performance differences.

Furthermore, MIEDOA was applied to a three-dimensional wireless sensor network deployment problem to investigate its engineering applicability. The experimental results under different node scales suggest that MIEDOA can generate relatively uniform deployment solutions, achieve competitive coverage performance, and maintain stable convergence behavior throughout the optimization process. These findings indicate that the proposed algorithm can be applied to both numerical optimization problems and representative deployment optimization tasks.

Despite the encouraging results obtained in this study, several limitations should be acknowledged. First, although the effectiveness of MIEDOA has been evaluated through extensive benchmark experiments and engineering applications, a rigorous theoretical convergence proof has not been established and remains an important topic for future research. Second, the wireless sensor network deployment model adopted in this work is a simplified coverage-oriented model that does not explicitly consider communication connectivity, energy consumption, environmental obstacles, heterogeneous sensing characteristics, or other practical network constraints. Third, the performance of MIEDOA may be influenced by the selection of control parameters. Although parameter sensitivity analysis has been conducted, more advanced self-adaptive parameter adjustment mechanisms deserve further investigation. In addition, the engineering validation is currently limited to a representative wireless sensor network deployment problem, and additional real-world optimization scenarios are required to further assess the general applicability of the proposed algorithm. Furthermore, while comparisons were conducted with representative EDOA variants and several CEC winner algorithms, there remain other highly competitive evolutionary and swarm intelligence algorithms that could be considered in future studies. Finally, the additional search mechanisms introduced in MIEDOA inevitably increase the computational overhead to some extent, particularly when dealing with high-dimensional optimization problems or computationally expensive objective functions.

Future work will focus on establishing a more rigorous theoretical foundation for MIEDOA, extending the algorithm to dynamic, constrained, large-scale, and multi-objective optimization problems, and incorporating more realistic practical constraints into engineering deployment scenarios. In addition, adaptive parameter control, surrogate-assisted optimization, and hybridization with machine learning techniques will be explored to further improve the generalization capability and computational efficiency of the proposed algorithm.

Author Contributions: Conceptualization, L.D. and A.L.; methodology, L.D. and A.L.; software, L.D. and A.L.; validation, L.D. and A.L.; formal analysis, L.D. and A.L.; investigation, L.D. and A.L.; resources, L.D. and A.L.; data curation, L.D. and A.L.; writing—original draft preparation, L.D. and A.L.; writing—review and editing, L.D. and A.L.; visualization, L.D. and A.L.; supervision, L.D.; funding acquisition, L.D. All authors have read and agreed to the published version of the manuscript.

Funding: This research received no external funding.

Data Availability Statement: Data are contained within the article.

Conflicts of Interest: The authors declare no conflicts of interest.

Appendix A

Table A1. P_holm-values for various algorithms on the CEC 2017 (dim = 30).

Item	INFO	RUN	GRO	ESC	RIME	GKSO	RTH	FTO	BBO	IGWO	EDOA
F1	1.0000×10^{0}	5.8741×10^{-2}	1.9078×10^{-5}	1.0000×10^{0}	1.9078×10^{-5}	1.0000×10^{0}	1.0000×10^{0}	1.9078×10^{-5}	1.9078×10^{-5}	1.9078×10^{-5}	1.9078×10^{-5}
F2	1.9078×10^{-5}	1.9078×10^{-5}	1.9078×10^{-5}	1.9078×10^{-5}	1.9078×10^{-5}	1.0454×10^{-3}	6.3207×10^{-2}	1.9078×10^{-5}	2.0589×10^{-1}	1.9078×10^{-5}	6.3158×10^{-3}
F3	1.9078×10^{-5}	4.8969×10^{-4}	1.9078×10^{-5}	1.9078×10^{-5}	1.9078×10^{-5}	1.0614×10^{-4}	1.9078×10^{-5}	1.9078×10^{-5}	1.9078×10^{-5}	1.9078×10^{-5}	1.9078×10^{-5}
F4	1.8462×10^{-1}	1.9588×10^{-3}	2.8637×10^{-5}	4.4374×10^{-5}	3.8571×10^{-5}	1.7129×10^{-1}	3.8571×10^{-5}	2.8637×10^{-5}	1.7129×10^{-1}	8.9614×10^{-5}	2.6535×10^{-4}
F5	1.9078×10^{-5}	1.9078×10^{-5}	1.9078×10^{-5}	1.9078×10^{-5}	1.9078×10^{-5}	1.9078×10^{-5}	1.9078×10^{-5}	2.7202×10^{-5}	2.5398×10^{-5}	4.5336×10^{-4}	1.9078×10^{-5}
F6	1.9078×10^{-5}	1.9078×10^{-5}	1.9078×10^{-5}	1.9078×10^{-5}	1.9078×10^{-5}	1.9078×10^{-5}	1.9078×10^{-5}	1.9078×10^{-5}	1.9078×10^{-5}	1.9078×10^{-5}	1.9078×10^{-5}
F7	1.9078×10^{-5}	1.9078×10^{-5}	1.9078×10^{-5}	1.9078×10^{-5}	1.9078×10^{-5}	1.9078×10^{-5}	1.9078×10^{-5}	1.9078×10^{-5}	1.9078×10^{-5}	1.9078×10^{-5}	1.9078×10^{-5}
F8	1.9078×10^{-5}	1.9078×10^{-5}	1.9078×10^{-5}	1.9078×10^{-5}	1.9078×10^{-5}	1.9078×10^{-5}	1.9078×10^{-5}	5.2269×10^{-4}	5.3965×10^{-5}	7.1889×10^{-1}	1.9078×10^{-5}
F9	1.9078×10^{-5}	1.9078×10^{-5}	1.9078×10^{-5}	7.8647×10^{-2}	1.9078×10^{-5}	1.9078×10^{-5}	1.9078×10^{-5}	1.9078×10^{-5}	1.9078×10^{-5}	1.9078×10^{-5}	1.9078×10^{-5}
F10	1.0000×10^{0}	1.0511×10^{-1}	1.0000×10^{0}	1.9078×10^{-5}	6.0222×10^{-1}	1.0000×10^{0}	1.0000×10^{0}	1.1149×10^{-2}	8.0499×10^{-3}	7.5137×10^{-4}	8.0499×10^{-3}
F11	4.1427×10^{-3}	7.0018×10^{-2}	2.1130×10^{-5}	5.1705×10^{-1}	3.1817×10^{-5}	8.1569×10^{-4}	3.3196×10^{-3}	6.1527×10^{-5}	7.3987×10^{-4}	4.1427×10^{-3}	5.7052×10^{-5}
F12	2.8278×10^{-1}	1.9078×10^{-5}	1.9078×10^{-5}	9.9518×10^{-4}	1.9078×10^{-5}	3.0861×10^{-1}	1.9078×10^{-5}	1.9078×10^{-5}	1.9078×10^{-5}	1.9078×10^{-5}	1.9078×10^{-5}
F13	1.3531×10^{-2}	9.2595×10^{-2}	1.1394×10^{-1}	1.5128×10^{-3}	4.2857×10^{-5}	4.2857×10^{-5}	1.9816×10^{-3}	6.9869×10^{-1}	7.8126×10^{-1}	2.1130×10^{-5}	4.4112×10^{-1}
F14	1.9078×10^{-5}	1.9078×10^{-5}	1.9078×10^{-5}	1.9078×10^{-5}	1.9078×10^{-5}	1.9078×10^{-5}	1.9078×10^{-5}	1.9078×10^{-5}	1.9078×10^{-5}	1.9078×10^{-5}	1.9078×10^{-5}
F15	2.1228×10^{-4}	1.9078×10^{-5}	2.1228×10^{-4}	1.4839×10^{-3}	1.9078×10^{-5}	2.1228×10^{-4}	2.0358×10^{-4}	3.4510×10^{-5}	1.9078×10^{-5}	1.9078×10^{-5}	1.9078×10^{-5}
F16	4.2563×10^{-5}	2.1130×10^{-5}	2.0589×10^{-1}	1.5043×10^{-1}	4.2563×10^{-5}	6.5210×10^{-5}	6.7592×10^{-5}	1.9966×10^{-2}	9.8647×10^{-5}	3.9583×10^{-2}	2.1130×10^{-5}
F17	1.9078×10^{-5}	1.9078×10^{-5}	1.0000×10^{0}	1.6281×10^{-1}	1.9078×10^{-5}	3.1299×10^{-5}	1.9078×10^{-5}	1.0000×10^{0}	1.5005×10^{-1}	4.2417×10^{-1}	1.9078×10^{-5}
F18	1.9078×10^{-5}	1.9078×10^{-5}	1.9078×10^{-5}	1.9078×10^{-5}	1.9078×10^{-5}	1.9078×10^{-5}	5.4463×10^{-2}	1.9078×10^{-5}	1.9078×10^{-5}	1.9078×10^{-5}	1.9078×10^{-5}
F19	5.9743×10^{-5}	1.9078×10^{-5}	2.3646×10^{-5}	5.9743×10^{-5}	1.9078×10^{-5}	5.9743×10^{-5}	1.2506×10^{-4}	1.9078×10^{-5}	1.9078×10^{-5}	1.9078×10^{-5}	1.9078×10^{-5}
F20	1.9209×10^{-5}	6.2528×10^{-4}	6.7654×10^{-3}	1.0000×10^{0}	3.1145×10^{-4}	2.5907×10^{-5}	2.5907×10^{-5}	8.8993×10^{-4}	4.5082×10^{-4}	1.0000×10^{0}	1.9078×10^{-5}
F21	4.6145×10^{-5}	3.4285×10^{-5}	3.3228×10^{-3}	3.4285×10^{-5}	5.1232×10^{-5}	1.9078×10^{-5}	1.9078×10^{-5}	1.2044×10^{-1}	1.5462×10^{-2}	1.4975×10^{-2}	1.9078×10^{-5}
F22	6.2802×10^{-1}	4.0427×10^{-1}	1.0000×10^{0}	1.0000×10^{0}	6.0171×10^{-1}	1.0000×10^{0}	1.0000×10^{0}	3.0650×10^{-3}	1.0000×10^{0}	1.0000×10^{0}	1.3619×10^{-4}
F23	1.9078×10^{-5}	1.9078×10^{-5}	2.8758×10^{-5}	1.3785×10^{-4}	1.9078×10^{-5}	1.9078×10^{-5}	1.9078×10^{-5}	7.8918×10^{-5}	9.3369×10^{-5}	9.3676×10^{-2}	1.9078×10^{-5}
F24	1.9078×10^{-5}	5.6327×10^{-5}	1.6286×10^{-4}	1.9078×10^{-5}	1.9090×10^{-5}	1.9078×10^{-5}	1.9078×10^{-5}	1.6286×10^{-4}	8.1405×10^{-2}	6.4352×10^{-1}	1.9078×10^{-5}
F25	4.4318×10^{-4}	2.4429×10^{-4}	1.9078×10^{-5}	1.9253×10^{-3}	1.9078×10^{-5}	2.4429×10^{-4}	2.5637×10^{-2}	1.9078×10^{-5}	3.8844×10^{-4}	1.9078×10^{-5}	1.9078×10^{-5}
F26	1.3601×10^{-4}	1.8177×10^{-4}	3.9109×10^{-1}	1.0000×10^{0}	1.5005×10^{-1}	2.1657×10^{-2}	1.7757×10^{-4}	1.7757×10^{-4}	1.0000×10^{0}	1.0000×10^{0}	8.4599×10^{-5}
F27	1.9078×10^{-5}	1.9078×10^{-5}	1.9078×10^{-5}	8.1405×10^{-2}	8.6521×10^{-5}	1.9078×10^{-5}	1.9078×10^{-5}	1.9078×10^{-5}	1.5921×10^{-4}	2.0589×10^{-1}	1.9078×10^{-5}
F28	1.0000×10^{0}	1.0000×10^{0}	1.9078×10^{-5}	4.5082×10^{-4}	2.1266×10^{-5}	3.0175×10^{-2}	4.4374×10^{-5}	2.1266×10^{-5}	1.0000×10^{0}	3.0175×10^{-2}	3.7834×10^{-5}
F29	1.9209×10^{-5}	1.9209×10^{-5}	1.7797×10^{-4}	1.8735×10^{-1}	1.9209×10^{-5}	1.9209×10^{-5}	1.9209×10^{-5}	1.9209×10^{-5}	3.5920×10^{-3}	2.5364×10^{-1}	1.9078×10^{-5}
F30	1.9078×10^{-5}	4.2278×10^{-4}	3.1603×10^{-2}	1.9078×10^{-5}	1.9078×10^{-5}	1.6433×10^{-2}	1.9078×10^{-5}	6.8006×10^{-5}	4.2278×10^{-4}	1.9078×10^{-5}	1.9078×10^{-5}

Table A2. P_holm-values for various algorithms on the CEC 2017 (dim = 50).

Item	INFO	RUN	GRO	ESC	RIME	GKSO	RTH	FTO	BBO	IGWO	EDOA
F1	1.9078×10^{-5}	1.9078×10^{-5}	1.9078×10^{-5}	1.6614×10^{-3}	1.9078×10^{-5}	1.9078×10^{-5}	7.1903×10^{-2}	1.9078×10^{-5}	1.9078×10^{-5}	1.9078×10^{-5}	1.9078×10^{-5}
F2	1.9078×10^{-5}	1.9078×10^{-5}	1.9078×10^{-5}	1.9078×10^{-5}	2.3646×10^{-5}	7.2354×10^{-4}	6.2683×10^{-2}	1.9078×10^{-5}	7.2354×10^{-4}	1.9078×10^{-5}	5.9091×10^{-4}
F3	1.0000×10^{0}	4.1354×10^{-4}	1.9078×10^{-5}	1.9078×10^{-5}	1.9078×10^{-5}	6.7654×10^{-3}	1.9078×10^{-5}	2.8532×10^{-3}	1.0000×10^{0}	5.9357×10^{-3}	7.1724×10^{-5}
F4	1.4849×10^{-1}	1.4849×10^{-1}	1.9078×10^{-5}	1.1476×10^{-4}	1.1838×10^{-4}	1.1838×10^{-4}	3.5675×10^{-4}	1.9078×10^{-5}	3.3886×10^{-1}	3.1637×10^{-5}	3.4285×10^{-5}

Table A2. *Cont.*

Item	INFO	RUN	GRO	ESC	RIME	GKSO	RTH	FTO	BBO	IGWO	EDOA
F5	1.9078×10^{-5}	1.9078×10^{-5}	1.9078×10^{-5}	1.9078×10^{-5}	1.9078×10^{-5}	1.9078×10^{-5}	1.9078×10^{-5}	1.9078×10^{-5}	1.9078×10^{-5}	4.8603×10^{-5}	1.9078×10^{-5}
F6	1.9078×10^{-5}	1.9078×10^{-5}	1.9078×10^{-5}	3.8811×10^{-4}	1.9078×10^{-5}	1.9078×10^{-5}	1.9078×10^{-5}	1.9078×10^{-5}	1.9078×10^{-5}	1.9078×10^{-5}	1.9078×10^{-5}
F7	1.9078×10^{-5}	1.9078×10^{-5}	1.9078×10^{-5}	1.9078×10^{-5}	1.9078×10^{-5}	1.9078×10^{-5}	1.9078×10^{-5}	1.9078×10^{-5}	1.9078×10^{-5}	1.9078×10^{-5}	1.9078×10^{-5}
F8	1.9078×10^{-5}	1.9078×10^{-5}	1.9078×10^{-5}	1.9078×10^{-5}	1.9078×10^{-5}	1.9078×10^{-5}	1.9078×10^{-5}	1.9078×10^{-5}	6.2246×10^{-5}	7.5137×10^{-5}	1.9078×10^{-5}
F9	1.9078×10^{-5}	1.9078×10^{-5}	1.9078×10^{-5}	9.7539×10^{-1}	1.9078×10^{-5}	1.9078×10^{-5}	1.9078×10^{-5}	1.9078×10^{-5}	1.9078×10^{-5}	1.9078×10^{-5}	1.9078×10^{-5}
F10	1.0000×10^{0}	1.0000×10^{0}	1.5786×10^{-2}	1.9078×10^{-5}	1.0000×10^{0}	1.0000×10^{0}	1.0000×10^{0}	7.6909×10^{-5}	2.9794×10^{-4}	2.1334×10^{-4}	1.9961×10^{-1}
F11	1.9966×10^{-2}	1.4787×10^{-2}	1.9078×10^{-5}	1.9078×10^{-5}	1.9078×10^{-5}	1.0000×10^{0}	1.0000×10^{0}	4.6145×10^{-5}	1.0000×10^{0}	1.9078×10^{-5}	1.9078×10^{-5}
F12	5.7165×10^{-1}	6.9691×10^{-4}	1.9078×10^{-5}	2.3947×10^{-3}	1.9078×10^{-5}	7.2354×10^{-4}	1.9078×10^{-5}	1.9078×10^{-5}	6.7974×10^{-4}	1.9078×10^{-5}	1.9078×10^{-5}
F13	7.6552×10^{-1}	1.5325×10^{-3}	1.9078×10^{-5}	4.2672×10^{-1}	1.9078×10^{-5}	4.4552×10^{-3}	4.4552×10^{-3}	1.9078×10^{-5}	1.9078×10^{-5}	1.9078×10^{-5}	1.9078×10^{-5}
F14	1.9078×10^{-5}	1.9078×10^{-5}	1.9078×10^{-5}	1.9078×10^{-5}	1.9078×10^{-5}	1.9078×10^{-5}	4.0715×10^{-5}	1.9078×10^{-5}	1.9078×10^{-5}	1.9078×10^{-5}	1.9078×10^{-5}
F15	1.0995×10^{-2}	2.5088×10^{-1}	1.0995×10^{-2}	5.1765×10^{-5}	1.9078×10^{-5}	1.0387×10^{-2}	1.1048×10^{-1}	6.1431×10^{-1}	3.9175×10^{-3}	1.9078×10^{-5}	2.9084×10^{-2}
F16	2.9855×10^{-3}	6.6457×10^{-3}	9.0561×10^{-1}	1.7092×10^{-1}	2.4118×10^{-3}	2.5266×10^{-2}	2.4749×10^{-1}	9.0561×10^{-1}	5.3372×10^{-1}	3.0085×10^{-1}	2.5888×10^{-5}
F17	7.6195×10^{-5}	4.6273×10^{-3}	4.1178×10^{-1}	3.7631×10^{-1}	3.2572×10^{-4}	3.2572×10^{-4}	2.5888×10^{-5}	2.4749×10^{-1}	5.3044×10^{-1}	2.4749×10^{-1}	6.3391×10^{-5}
F18	3.8599×10^{-3}	9.9179×10^{-1}	1.9078×10^{-5}	1.9078×10^{-5}	1.9078×10^{-5}	1.4355×10^{-3}	1.1334×10^{-2}	2.1428×10^{-5}	1.9078×10^{-5}	1.9078×10^{-5}	1.9078×10^{-5}
F19	4.7657×10^{-1}	1.9078×10^{-5}	7.8583×10^{-3}	4.7657×10^{-1}	1.9078×10^{-5}	5.9867×10^{-3}	4.7657×10^{-1}	1.9078×10^{-5}	5.5894×10^{-5}	1.9078×10^{-5}	1.9078×10^{-5}
F20	9.5787×10^{-3}	2.7485×10^{-1}	2.7485×10^{-1}	7.9165×10^{-2}	1.2154×10^{-1}	9.6743×10^{-3}	2.0023×10^{-3}	1.3595×10^{-3}	4.9080×10^{-1}	2.7485×10^{-1}	2.8564×10^{-4}
F21	1.9078×10^{-5}	1.9078×10^{-5}	1.9078×10^{-5}	1.9078×10^{-5}	1.9078×10^{-5}	1.9078×10^{-5}	1.9078×10^{-5}	1.9078×10^{-5}	1.9078×10^{-5}	1.9078×10^{-5}	1.9078×10^{-5}
F22	2.3125×10^{-2}	1.0000×10^{0}	7.9444×10^{-1}	1.9078×10^{-5}	1.0000×10^{0}	1.0000×10^{0}	5.8741×10^{-2}	6.9838×10^{-5}	9.0064×10^{-3}	1.9294×10^{-3}	2.3370×10^{-4}
F23	1.9078×10^{-5}	1.9078×10^{-5}	1.9078×10^{-5}	1.9078×10^{-5}	1.9078×10^{-5}	1.9078×10^{-5}	1.9078×10^{-5}	1.9078×10^{-5}	1.9078×10^{-5}	5.2872×10^{-4}	1.9078×10^{-5}
F24	1.9078×10^{-5}	1.9078×10^{-5}	1.9078×10^{-5}	1.9078×10^{-5}	1.9078×10^{-5}	1.9078×10^{-5}	1.9078×10^{-5}	1.9078×10^{-5}	1.9078×10^{-5}	3.8723×10^{-2}	1.9078×10^{-5}
F25	1.9078×10^{-5}	1.9078×10^{-5}	1.9078×10^{-5}	1.9078×10^{-5}	1.9078×10^{-5}	2.5398×10^{-5}	7.0356×10^{-1}	1.9078×10^{-5}	8.8987×10^{-5}	1.9078×10^{-5}	1.9078×10^{-5}
F26	1.9078×10^{-5}	1.9078×10^{-5}	1.9078×10^{-5}	6.5578×10^{-5}	1.9078×10^{-5}	8.8987×10^{-5}	6.5578×10^{-5}	1.9078×10^{-5}	6.1904×10^{-5}	8.8987×10^{-5}	1.9078×10^{-5}
F27	1.9078×10^{-5}	1.9078×10^{-5}	1.9078×10^{-5}	6.5480×10^{-2}	2.1428×10^{-5}	1.9078×10^{-5}	2.5357×10^{-5}	1.9078×10^{-5}	7.6552×10^{-1}	1.1419×10^{-1}	1.9078×10^{-5}
F28	7.4485×10^{-5}	2.3646×10^{-5}	1.9078×10^{-5}	1.9078×10^{-5}	1.9090×10^{-5}	5.9188×10^{-5}	2.3646×10^{-5}	1.9078×10^{-5}	1.7088×10^{-3}	1.9078×10^{-5}	1.9078×10^{-5}
F29	2.8122×10^{-5}	2.1181×10^{-5}	1.4542×10^{-2}	5.2848×10^{-4}	1.1838×10^{-4}	1.9078×10^{-5}	1.1476×10^{-4}	1.9918×10^{-3}	1.9152×10^{-1}	8.8993×10^{-4}	1.9078×10^{-5}
F30	1.9078×10^{-5}	1.9078×10^{-5}	8.1878×10^{-5}	1.9078×10^{-5}	1.9078×10^{-5}	1.9078×10^{-5}	1.9078×10^{-5}	1.9078×10^{-5}	1.9078×10^{-5}	1.9078×10^{-5}	1.9078×10^{-5}

Table A3. P_holm-values for various algorithms on the CEC 2017 (dim = 100).

Item	INFO	RUN	GRO	ESC	RIME	GKSO	RTH	FTO	BBO	IGWO	EDOA
F1	1.9078×10^{-5}	1.9078×10^{-5}	1.9078×10^{-5}	1.9078×10^{-5}	1.9078×10^{-5}	1.9078×10^{-5}	1.9078×10^{-5}	1.9078×10^{-5}	1.9078×10^{-5}	1.9078×10^{-5}	1.9078×10^{-5}
F2	1.9078×10^{-5}	1.9078×10^{-5}	1.9078×10^{-5}	1.9078×10^{-5}	1.9078×10^{-5}	1.9078×10^{-5}	3.1854×10^{-3}	1.9078×10^{-5}	3.1854×10^{-3}	4.4807×10^{-5}	1.9078×10^{-5}
F3	3.3796×10^{-5}	3.3796×10^{-5}	1.9078×10^{-5}	1.9078×10^{-5}	1.9078×10^{-5}	9.8421×10^{-3}	1.9078×10^{-5}	1.9078×10^{-5}	1.9078×10^{-5}	1.9078×10^{-5}	1.9078×10^{-5}
F4	1.9078×10^{-5}	1.9078×10^{-5}	1.9078×10^{-5}	1.9078×10^{-5}	1.9078×10^{-5}	1.9078×10^{-5}	2.9871×10^{-5}	1.9078×10^{-5}	6.5833×10^{-1}	1.9078×10^{-5}	1.9078×10^{-5}
F5	1.9078×10^{-5}	1.9078×10^{-5}	1.9078×10^{-5}	1.9078×10^{-5}	1.9078×10^{-5}	1.9078×10^{-5}	1.9078×10^{-5}	1.9078×10^{-5}	1.9078×10^{-5}	1.9078×10^{-5}	1.9078×10^{-5}
F6	1.9078×10^{-5}	1.9078×10^{-5}	1.9078×10^{-5}	1.9078×10^{-5}	1.9078×10^{-5}	1.9078×10^{-5}	1.9078×10^{-5}	1.9078×10^{-5}	1.9078×10^{-5}	1.9078×10^{-5}	1.9078×10^{-5}
F7	1.9078×10^{-5}	1.9078×10^{-5}	1.9078×10^{-5}	1.9078×10^{-5}	1.9078×10^{-5}	1.9078×10^{-5}	1.9078×10^{-5}	1.9078×10^{-5}	1.9078×10^{-5}	1.9078×10^{-5}	1.9078×10^{-5}
F8	1.9078×10^{-5}	1.9078×10^{-5}	1.9078×10^{-5}	1.9078×10^{-5}	1.9078×10^{-5}	1.9078×10^{-5}	1.9078×10^{-5}	1.9078×10^{-5}	1.9078×10^{-5}	1.9078×10^{-5}	1.9078×10^{-5}
F9	1.9078×10^{-5}	1.9078×10^{-5}	1.9078×10^{-5}	8.4508×10^{-1}	1.9078×10^{-5}	1.9078×10^{-5}	1.9078×10^{-5}	1.9078×10^{-5}	1.9078×10^{-5}	1.9078×10^{-5}	1.9078×10^{-5}

Table A3. *Cont.*

Item	INFO	RUN	GRO	ESC	RIME	GKSO	RTH	FTO	BBO	IGWO	EDOA
F10	7.8277×10^{-2}	1.0000×10^{0}	1.9078×10^{-5}	1.9078×10^{-5}	2.5453×10^{-5}	1.0000×10^{0}	1.0000×10^{0}	1.9078×10^{-5}	9.1629×10^{-3}	3.0000×10^{-5}	6.7592×10^{-5}
F11	1.9078×10^{-5}	1.9078×10^{-5}	1.9078×10^{-5}	1.9078×10^{-5}	2.4519×10^{-1}	1.9078×10^{-5}	1.9078×10^{-5}	4.6076×10^{-2}	1.9078×10^{-5}	1.9966×10^{-2}	3.1333×10^{-2}
F12	1.9078×10^{-5}	1.9078×10^{-5}	1.9078×10^{-5}	1.9078×10^{-5}	1.9078×10^{-5}	1.9078×10^{-5}	1.9078×10^{-5}	1.9078×10^{-5}	1.9078×10^{-5}	1.9078×10^{-5}	1.9078×10^{-5}
F13	1.9078×10^{-5}	1.9078×10^{-5}	1.9078×10^{-5}	1.9078×10^{-5}	1.9078×10^{-5}	1.9078×10^{-5}	1.7791×10^{-1}	1.9078×10^{-5}	1.9078×10^{-5}	1.9078×10^{-5}	1.9078×10^{-5}
F14	2.7641×10^{-3}	3.7517×10^{-4}	1.9078×10^{-5}	1.9078×10^{-5}	1.9078×10^{-5}	2.4519×10^{-1}	1.9078×10^{-5}	1.9078×10^{-5}	1.9078×10^{-5}	1.9078×10^{-5}	1.9078×10^{-5}
F15	7.7622×10^{-4}	1.9078×10^{-5}	1.9078×10^{-5}	1.9078×10^{-5}	1.9078×10^{-5}	1.9078×10^{-5}	1.3059×10^{-1}	1.9078×10^{-5}	1.9078×10^{-5}	1.9078×10^{-5}	1.9078×10^{-5}
F16	9.0205×10^{-3}	3.7919×10^{-4}	4.6013×10^{-5}	1.9209×10^{-5}	3.1637×10^{-5}	3.7919×10^{-4}	4.1924×10^{-2}	1.1476×10^{-4}	4.2672×10^{-1}	8.1302×10^{-1}	1.9078×10^{-5}
F17	3.1145×10^{-4}	2.7242×10^{-4}	1.0000×10^{0}	3.8668×10^{-5}	1.1143×10^{-4}	2.0978×10^{-3}	4.5082×10^{-4}	4.6992×10^{-2}	1.0000×10^{0}	4.6992×10^{-2}	3.8668×10^{-5}
F18	9.5899×10^{-1}	4.9183×10^{-5}	1.9078×10^{-5}	1.9078×10^{-5}	1.9078×10^{-5}	3.6924×10^{-1}	3.3864×10^{-5}	1.9078×10^{-5}	2.6082×10^{-5}	1.9078×10^{-5}	1.9078×10^{-5}
F19	1.9684×10^{-2}	1.9078×10^{-5}	1.9078×10^{-5}	1.9078×10^{-5}	1.9078×10^{-5}	1.9078×10^{-5}	5.4401×10^{-1}	1.9078×10^{-5}	1.9078×10^{-5}	1.9078×10^{-5}	1.9078×10^{-5}
F20	8.7168×10^{-2}	9.3057×10^{-1}	9.9393×10^{-2}	4.7143×10^{-5}	2.4749×10^{-1}	7.1081×10^{-1}	9.3057×10^{-1}	5.8168×10^{-2}	2.4749×10^{-1}	1.2438×10^{-2}	8.9187×10^{-4}
F21	1.9078×10^{-5}	1.9078×10^{-5}	1.9078×10^{-5}	1.9078×10^{-5}	1.9078×10^{-5}	1.9078×10^{-5}	1.9078×10^{-5}	1.9078×10^{-5}	1.9078×10^{-5}	1.9078×10^{-5}	1.9078×10^{-5}
F22	1.5562×10^{-4}	4.2278×10^{-4}	4.6145×10^{-5}	1.9078×10^{-5}	1.9078×10^{-5}	4.1461×10^{-3}	1.1419×10^{-1}	1.9078×10^{-5}	6.4352×10^{-1}	3.4285×10^{-5}	4.0262×10^{-5}
F23	1.9078×10^{-5}	1.9078×10^{-5}	1.9078×10^{-5}	2.7029×10^{-2}	1.9078×10^{-5}	1.9078×10^{-5}	1.9078×10^{-5}	1.9078×10^{-5}	1.9078×10^{-5}	1.9078×10^{-5}	1.9078×10^{-5}
F24	1.9078×10^{-5}	1.9078×10^{-5}	1.9078×10^{-5}	1.9078×10^{-5}	1.9078×10^{-5}	1.9078×10^{-5}	1.9078×10^{-5}	1.9078×10^{-5}	1.9078×10^{-5}	1.9078×10^{-5}	1.9078×10^{-5}
F25	1.9078×10^{-5}	1.9078×10^{-5}	1.9078×10^{-5}	1.9078×10^{-5}	1.9078×10^{-5}	1.9078×10^{-5}	1.9078×10^{-5}	1.9078×10^{-5}	2.2888×10^{-1}	1.9078×10^{-5}	1.9078×10^{-5}
F26	1.9078×10^{-5}	1.9078×10^{-5}	1.9078×10^{-5}	1.9078×10^{-5}	1.9078×10^{-5}	1.9078×10^{-5}	1.9078×10^{-5}	1.9078×10^{-5}	1.9078×10^{-5}	1.9078×10^{-5}	1.9078×10^{-5}
F27	1.9078×10^{-5}	1.9078×10^{-5}	1.9078×10^{-5}	1.9078×10^{-5}	1.9078×10^{-5}	1.9078×10^{-5}	1.9078×10^{-5}	1.9078×10^{-5}	8.1430×10^{-5}	6.1564×10^{-4}	1.9078×10^{-5}
F28	1.9078×10^{-5}	1.9078×10^{-5}	1.9078×10^{-5}	1.9078×10^{-5}	1.9078×10^{-5}	1.9078×10^{-5}	1.9078×10^{-5}	1.9078×10^{-5}	9.7110×10^{-5}	1.9078×10^{-5}	1.9078×10^{-5}
F29	3.1696×10^{-5}	1.9078×10^{-5}	1.9078×10^{-5}	2.8278×10^{-1}	1.9078×10^{-5}	1.9078×10^{-5}	8.4508×10^{-1}	1.9078×10^{-5}	8.4210×10^{-3}	3.7358×10^{-2}	1.9078×10^{-5}
F30	1.9078×10^{-5}	1.9078×10^{-5}	1.9078×10^{-5}	1.9078×10^{-5}	1.9078×10^{-5}	1.9078×10^{-5}	1.9078×10^{-5}	1.9078×10^{-5}	1.9078×10^{-5}	1.9078×10^{-5}	1.9078×10^{-5}

Table A4. P_holm-values for various algorithms on the CEC 2020 (dim = 10).

Item	INFO	RUN	GRO	ESC	RIME	GKSO	RTH	FTO	BBO	IGWO	EDOA
F1	1.9078×10^{-5}	1.9078×10^{-5}	1.9078×10^{-5}	1.9078×10^{-5}	1.9078×10^{-5}	1.9078×10^{-5}	9.7110×10^{-5}	1.9078×10^{-5}	1.9078×10^{-5}	1.9078×10^{-5}	1.9078×10^{-5}
F2	1.6412×10^{-3}	2.7201×10^{-3}	1.0000×10^{0}	1.0000×10^{0}	1.0000×10^{0}	7.6195×10^{-5}	3.8668×10^{-5}	1.9816×10^{-3}	3.9323×10^{-1}	1.0000×10^{0}	4.7292×10^{-5}
F3	1.9209×10^{-5}	1.9078×10^{-5}	7.7622×10^{-4}	5.4463×10^{-2}	2.6535×10^{-4}	4.1732×10^{-5}	1.9209×10^{-5}	5.9263×10^{-5}	5.9091×10^{-4}	6.1546×10^{-4}	7.4285×10^{-5}
F4	2.3193×10^{-2}	4.6948×10^{-5}	1.0000×10^{0}	9.9046×10^{-5}	1.7061×10^{-4}	1.0338×10^{-2}	2.6033×10^{-5}	3.8561×10^{-3}	1.0000×10^{0}	1.9078×10^{-5}	9.9046×10^{-5}
F5	1.9078×10^{-5}	1.9078×10^{-5}	1.9078×10^{-5}	1.9078×10^{-5}	1.9078×10^{-5}	1.9078×10^{-5}	1.9078×10^{-5}	1.9078×10^{-5}	1.9078×10^{-5}	1.9078×10^{-5}	1.9078×10^{-5}
F6	1.9078×10^{-5}	2.0150×10^{-5}	7.4485×10^{-5}	7.4987×10^{-1}	2.1091×10^{-5}	2.3073×10^{-5}	1.9078×10^{-5}	2.1091×10^{-5}	2.1091×10^{-5}	1.9078×10^{-5}	1.9078×10^{-5}
F7	1.9078×10^{-5}	1.9078×10^{-5}	1.9078×10^{-5}	1.9078×10^{-5}	1.9078×10^{-5}	3.3173×10^{-4}	1.9078×10^{-5}	1.9078×10^{-5}	1.9078×10^{-5}	1.9078×10^{-5}	1.9078×10^{-5}
F8	2.3430×10^{-5}	1.3811×10^{-4}	1.4381×10^{-1}	9.5899×10^{-1}	3.1070×10^{-3}	1.3811×10^{-4}	3.0849×10^{-3}	1.9406×10^{-3}	2.3430×10^{-5}	1.9078×10^{-5}	2.1266×10^{-5}
F9	2.8434×10^{-4}	1.9318×10^{-2}	1.8413×10^{-1}	1.0000×10^{0}	1.8034×10^{-4}	5.2237×10^{-1}	2.3521×10^{-3}	2.2132×10^{-2}	1.0000×10^{0}	1.0000×10^{0}	2.6338×10^{-2}
F10	1.3601×10^{-4}	6.4186×10^{-4}	5.9149×10^{-3}	1.3601×10^{-4}	4.8246×10^{-4}	6.9730×10^{-5}	6.4186×10^{-4}	3.5595×10^{-4}	4.8555×10^{-4}	1.8462×10^{-1}	4.8246×10^{-4}

Table A5. P_holm-values for various algorithms on the CEC 2020 (dim = 20).

Item	INFO	RUN	GRO	ESC	RIME	GKSO	RTH	FTO	BBO	IGWO	EDOA
F1	1.9078×10^{-5}	2.4147×10^{-3}	1.9078×10^{-5}	5.4404×10^{-5}	1.9078×10^{-5}	5.4404×10^{-5}	5.4404×10^{-5}	1.9078×10^{-5}	1.9078×10^{-5}	1.9078×10^{-5}	1.9078×10^{-5}
F2	9.3057×10^{-1}	4.8886×10^{-1}	9.3057×10^{-1}	3.2678×10^{-1}	3.5595×10^{-4}	2.8011×10^{-4}	9.6743×10^{-3}	4.8886×10^{-1}	6.4007×10^{-1}	5.7381×10^{-5}	5.7381×10^{-5}
F3	1.9078×10^{-5}	1.9078×10^{-5}	1.9078×10^{-5}	5.4463×10^{-2}	1.9078×10^{-5}	1.9078×10^{-5}	1.9078×10^{-5}	1.9078×10^{-5}	1.9078×10^{-5}	1.0614×10^{-4}	1.9078×10^{-5}
F4	3.0000×10^{-5}	1.9078×10^{-5}	8.4924×10^{-4}	5.2848×10^{-4}	6.9691×10^{-4}	4.9127×10^{-4}	1.9078×10^{-5}	3.1317×10^{-2}	1.0201×10^{-1}	1.9078×10^{-5}	1.9078×10^{-5}
F5	1.9078×10^{-5}	1.9078×10^{-5}	1.9078×10^{-5}	1.9078×10^{-5}	1.9078×10^{-5}	1.9078×10^{-5}	1.9078×10^{-5}	1.9078×10^{-5}	1.9078×10^{-5}	1.9078×10^{-5}	1.9078×10^{-5}
F6	1.7061×10^{-4}	3.6515×10^{-5}	2.5846×10^{-3}	1.7889×10^{-3}	5.9091×10^{-4}	2.3029×10^{-5}	1.9078×10^{-5}	5.9091×10^{-4}	2.1181×10^{-5}	2.0358×10^{-4}	1.9078×10^{-5}
F7	1.9078×10^{-5}	1.9078×10^{-5}	1.9078×10^{-5}	1.9078×10^{-5}	1.9078×10^{-5}	1.9078×10^{-5}	3.0861×10^{-1}	1.9078×10^{-5}	1.9078×10^{-5}	1.9078×10^{-5}	1.9078×10^{-5}
F8	1.2313×10^{-3}	1.9078×10^{-5}	1.9078×10^{-5}	1.9078×10^{-5}	1.9078×10^{-5}	1.9078×10^{-5}	1.2313×10^{-3}	1.9078×10^{-5}	1.9078×10^{-5}	1.9078×10^{-5}	1.9078×10^{-5}
F9	1.9078×10^{-5}	8.1971×10^{-5}	1.0000×10^{0}	8.1971×10^{-5}	8.1971×10^{-5}	1.9078×10^{-5}	1.9078×10^{-5}	1.3515×10^{-2}	1.0000×10^{0}	1.0000×10^{0}	1.5325×10^{-3}
F10	1.2978×10^{-4}	2.5453×10^{-5}	2.1181×10^{-5}	8.1302×10^{-1}	3.1070×10^{-3}	2.0358×10^{-4}	1.1476×10^{-4}	1.9078×10^{-5}	3.0055×10^{-4}	3.9292×10^{-3}	1.9078×10^{-5}

Table A6. EffectSize-values for various algorithms on the CEC 2017 (dim = 30).

Item	INFO	RUN	GRO	ESC	RIME	GKSO	RTH	FTO	BBO	IGWO	EDOA
F1	-2.0000×10^{-1}	-5.2688×10^{-1}	-1.0000×10^{0}	-1.6559×10^{-1}	-1.0000×10^{0}	2.1720×10^{-1}	7.0968×10^{-2}	-1.0000×10^{0}	-9.8280×10^{-1}	-1.0000×10^{0}	-1.0000×10^{0}
F2	-9.9140×10^{-1}	-9.9570×10^{-1}	-1.0000×10^{0}	-1.0000×10^{0}	-9.9140×10^{-1}	-7.6344×10^{-1}	-4.4946×10^{-1}	-1.0000×10^{0}	2.6452×10^{-1}	-1.0000×10^{0}	-6.4301×10^{-1}
F3	-1.0000×10^{0}	-7.2903×10^{-1}	-1.0000×10^{0}	-1.0000×10^{0}	-1.0000×10^{0}	-8.4516×10^{-1}	1.0000×10^{0}	-1.0000×10^{0}	-1.0000×10^{0}	-1.0000×10^{0}	-1.0000×10^{0}
F4	-2.7742×10^{-1}	-7.2903×10^{-1}	-9.8280×10^{-1}	-9.4409×10^{-1}	-9.5699×10^{-1}	-3.8925×10^{-1}	9.6129×10^{-1}	-9.8280×10^{-1}	-3.9785×10^{-1}	-9.0538×10^{-1}	-8.4516×10^{-1}
F5	-1.0000×10^{0}	-1.0000×10^{0}	-1.0000×10^{0}	-1.0000×10^{0}	-9.9140×10^{-1}	-1.0000×10^{0}	-1.0000×10^{0}	-9.0968×10^{-1}	-9.3118×10^{-1}	-7.3333×10^{-1}	-1.0000×10^{0}
F6	-1.0000×10^{0}	-1.0000×10^{0}	-1.0000×10^{0}	1.0000×10^{0}	-1.0000×10^{0}	-1.0000×10^{0}	-1.0000×10^{0}	-1.0000×10^{0}	-1.0000×10^{0}	-1.0000×10^{0}	-1.0000×10^{0}
F7	-1.0000×10^{0}	-1.0000×10^{0}	-9.7419×10^{-1}	-9.9570×10^{-1}	-1.0000×10^{0}	-1.0000×10^{0}	-1.0000×10^{0}	-9.9140×10^{-1}	-1.0000×10^{0}	-1.0000×10^{0}	-1.0000×10^{0}
F8	-1.0000×10^{0}	-1.0000×10^{0}	-9.6989×10^{-1}	-1.0000×10^{0}	-1.0000×10^{0}	-1.0000×10^{0}	-1.0000×10^{0}	-7.6344×10^{-1}	-8.9677×10^{-1}	7.5269×10^{-2}	-1.0000×10^{0}
F9	-1.0000×10^{0}	-1.0000×10^{0}	-1.0000×10^{0}	-3.6774×10^{-1}	-1.0000×10^{0}	-1.0000×10^{0}	-1.0000×10^{0}	-1.0000×10^{0}	-1.0000×10^{0}	-1.0000×10^{0}	-1.0000×10^{0}
F10	-4.5161×10^{-2}	-4.9677×10^{-1}	2.1720×10^{-1}	-1.0000×10^{0}	3.2473×10^{-1}	3.2258×10^{-2}	-2.3441×10^{-1}	-6.6022×10^{-1}	6.9032×10^{-1}	-8.2796×10^{-1}	-6.9462×10^{-1}
F11	-6.8602×10^{-1}	-4.4086×10^{-1}	-9.9570×10^{-1}	1.3548×10^{-1}	-9.7419×10^{-1}	-7.9785×10^{-1}	-7.1183×10^{-1}	-9.3548×10^{-1}	-8.1075×10^{-1}	-6.8602×10^{-1}	-9.4409×10^{-1}
F12	3.0753×10^{-1}	-1.0000×10^{0}	-9.9570×10^{-1}	-7.5054×10^{-1}	-1.0000×10^{0}	-2.1290×10^{-1}	1.0000×10^{0}	-9.8710×10^{-1}	-9.6989×10^{-1}	-9.7849×10^{-1}	-1.0000×10^{0}
F13	6.3871×10^{-1}	4.9247×10^{-1}	4.5806×10^{-1}	7.8065×10^{-1}	-9.6129×10^{-1}	9.5699×10^{-1}	7.5914×10^{-1}	1.9570×10^{-1}	5.8065×10^{-2}	-9.9570×10^{-1}	-3.0323×10^{-1}
F14	-1.0000×10^{0}	-9.9140×10^{-1}	-1.0000×10^{0}	-1.0000×10^{0}	-1.0000×10^{0}	-1.0000×10^{0}	-9.7849×10^{-1}	-1.0000×10^{0}	-1.0000×10^{0}	-1.0000×10^{0}	-1.0000×10^{0}
F15	-8.4516×10^{-1}	-1.0000×10^{0}	-8.3656×10^{-1}	-6.6452×10^{-1}	-1.0000×10^{0}	-8.1505×10^{-1}	-8.5806×10^{-1}	-9.4839×10^{-1}	-1.0000×10^{0}	-1.0000×10^{0}	-1.0000×10^{0}
F16	-9.5699×10^{-1}	-9.9570×10^{-1}	-2.6452×10^{-1}	-3.7204×10^{-1}	-9.5269×10^{-1}	-9.2688×10^{-1}	-9.1828×10^{-1}	-5.8710×10^{-1}	-8.9247×10^{-1}	-5.1828×10^{-1}	-9.9570×10^{-1}
F17	-9.8710×10^{-1}	-9.9570×10^{-1}	-1.9355×10^{-2}	4.2796×10^{-1}	-9.8710×10^{-1}	-9.5269×10^{-1}	-1.0000×10^{0}	-4.5161×10^{-2}	-4.5376×10^{-1}	3.0753×10^{-1}	-1.0000×10^{0}
F18	-9.9570×10^{-1}	-1.0000×10^{0}	-1.0000×10^{0}	-1.0000×10^{0}	-1.0000×10^{0}	-1.0000×10^{0}	-4.0215×10^{-1}	-1.0000×10^{0}	-1.0000×10^{0}	-1.0000×10^{0}	-1.0000×10^{0}
F19	-8.9247×10^{-1}	-1.0000×10^{0}	-9.5699×10^{-1}	-9.0538×10^{-1}	-9.9570×10^{-1}	-9.0108×10^{-1}	-8.0215×10^{-1}	-1.0000×10^{0}	-1.0000×10^{0}	-1.0000×10^{0}	-1.0000×10^{0}
F20	-9.9570×10^{-1}	-8.0215×10^{-1}	-6.3871×10^{-1}	1.9355×10^{-2}	-8.5376×10^{-1}	-9.7849×10^{-1}	-9.7849×10^{-1}	-7.7204×10^{-1}	-8.2796×10^{-1}	7.0968×10^{-2}	-1.0000×10^{0}
F21	-9.3548×10^{-1}	-9.6129×10^{-1}	-6.9892×10^{-1}	-9.6129×10^{-1}	-9.2258×10^{-1}	-1.0000×10^{0}	-1.0000×10^{0}	-3.2473×10^{-1}	-5.5699×10^{-1}	-5.8710×10^{-1}	-1.0000×10^{0}
F22	-3.5484×10^{-1}	-4.1935×10^{-1}	6.4516×10^{-3}	-2.7312×10^{-1}	-3.7204×10^{-1}	-2.3656×10^{-2}	-2.0000×10^{-1}	-7.5484×10^{-1}	-1.2258×10^{-1}	-7.5269×10^{-2}	-9.1398×10^{-1}
F23	-1.0000×10^{0}	-1.0000×10^{0}	-9.4839×10^{-1}	-8.3226×10^{-1}	-9.8280×10^{-1}	-1.0000×10^{0}	-1.0000×10^{0}	-8.9247×10^{-1}	-8.7097×10^{-1}	-3.5054×10^{-1}	-1.0000×10^{0}
F24	-9.9570×10^{-1}	-9.1828×10^{-1}	-8.5806×10^{-1}	-9.9140×10^{-1}	-9.7419×10^{-1}	-1.0000×10^{0}	-1.0000×10^{0}	-8.4516×10^{-1}	-4.2796×10^{-1}	9.6774×10^{-2}	-1.0000×10^{0}
F25	-7.9355×10^{-1}	-8.4946×10^{-1}	-1.0000×10^{0}	-6.9032×10^{-1}	-9.8280×10^{-1}	-8.5806×10^{-1}	-4.6667×10^{-1}	-1.0000×10^{0}	-8.1505×10^{-1}	-1.0000×10^{0}	-1.0000×10^{0}
F26	-9.0968×10^{-1}	-8.7957×10^{-1}	3.4624×10^{-1}	-1.6559×10^{-1}	-4.5376×10^{-1}	-6.0860×10^{-1}	-8.8817×10^{-1}	-8.9247×10^{-1}	-4.0860×10^{-2}	7.0968×10^{-2}	-9.3548×10^{-1}
F27	-9.8710×10^{-1}	-9.9570×10^{-1}	-9.8710×10^{-1}	-4.2796×10^{-1}	-8.8817×10^{-1}	-1.0000×10^{0}	-1.0000×10^{0}	-9.9570×10^{-1}	-8.4516×10^{-1}	2.6452×10^{-1}	-1.0000×10^{0}
F28	-1.6989×10^{-1}	1.6129×10^{-1}	-1.0000×10^{0}	-8.2796×10^{-1}	-9.8710×10^{-1}	-5.7419×10^{-1}	9.4409×10^{-1}	-9.9140×10^{-1}	-1.9570×10^{-1}	-5.6989×10^{-1}	-9.5699×10^{-1}
F29	-9.7849×10^{-1}	-9.9140×10^{-1}	-8.5376×10^{-1}	3.5054×10^{-1}	-9.9570×10^{-1}	-9.8280×10^{-1}	-9.6989×10^{-1}	-9.9140×10^{-1}	-6.7742×10^{-1}	2.3871×10^{-1}	-1.0000×10^{0}
F30	9.8280×10^{-1}	-8.1075×10^{-1}	-4.4946×10^{-1}	9.9570×10^{-1}	-1.0000×10^{0}	5.5269×10^{-1}	1.0000×10^{0}	-9.0968×10^{-1}	-8.0215×10^{-1}	-9.9570×10^{-1}	-1.0000×10^{0}

Table A7. EffectSize-values for various algorithms on the CEC 2017 (dim = 50).

Item	INFO	RUN	GRO	ESC	RIME	GKSO	RTH	FTO	BBO	IGWO	EDOA
F1	-1.0000×10^{0}	-1.0000×10^{0}	-1.0000×10^{0}	-6.9892×10^{-1}	-1.0000×10^{0}	-1.0000×10^{0}	3.7634×10^{-1}	-1.0000×10^{0}	-1.0000×10^{0}	-1.0000×10^{0}	-1.0000×10^{0}
F2	-1.0000×10^{0}	-1.0000×10^{0}	-1.0000×10^{0}	-1.0000×10^{0}	-9.5699×10^{-1}	-7.6344×10^{-1}	3.8925×10^{-1}	-1.0000×10^{0}	7.6774×10^{-1}	-1.0000×10^{0}	-7.9355×10^{-1}
F3	1.3978×10^{-1}	8.3226×10^{-1}	-1.0000×10^{0}	-1.0000×10^{0}	-1.0000×10^{0}	6.3871×10^{-1}	1.0000×10^{0}	-7.2043×10^{-1}	-1.3548×10^{-1}	-6.6452×10^{-1}	-9.2258×10^{-1}
F4	-4.1075×10^{-1}	4.0645×10^{-1}	-1.0000×10^{0}	-9.0108×10^{-1}	-8.8817×10^{-1}	-8.9247×10^{-1}	8.1935×10^{-1}	-1.0000×10^{0}	-2.0000×10^{-1}	-9.6989×10^{-1}	-9.6129×10^{-1}
F5	-1.0000×10^{0}	-1.0000×10^{0}	-1.0000×10^{0}	-9.9570×10^{-1}	-9.8710×10^{-1}	-1.0000×10^{0}	-1.0000×10^{0}	-9.6559×10^{-1}	-9.8710×10^{-1}	-8.4946×10^{-1}	-1.0000×10^{0}
F6	-1.0000×10^{0}	-1.0000×10^{0}	-1.0000×10^{0}	7.4194×10^{-1}	-1.0000×10^{0}	-1.0000×10^{0}	-1.0000×10^{0}	-1.0000×10^{0}	-1.0000×10^{0}	-1.0000×10^{0}	-1.0000×10^{0}
F7	-1.0000×10^{0}	-1.0000×10^{0}	-1.0000×10^{0}	-1.0000×10^{0}	-1.0000×10^{0}	-1.0000×10^{0}	-1.0000×10^{0}	-1.0000×10^{0}	-9.9570×10^{-1}	-9.9570×10^{-1}	-1.0000×10^{0}
F8	-1.0000×10^{0}	-1.0000×10^{0}	-1.0000×10^{0}	-1.0000×10^{0}	-1.0000×10^{0}	-1.0000×10^{0}	-1.0000×10^{0}	-9.9570×10^{-1}	-8.7097×10^{-1}	-8.2796×10^{-1}	-1.0000×10^{0}
F9	-1.0000×10^{0}	-1.0000×10^{0}	-1.0000×10^{0}	6.4516×10^{-3}	-1.0000×10^{0}	-1.0000×10^{0}	-1.0000×10^{0}	-1.0000×10^{0}	-1.0000×10^{0}	-1.0000×10^{0}	-1.0000×10^{0}
F10	-2.5161×10^{-1}	2.0430×10^{-1}	-6.3871×10^{-1}	-1.0000×10^{0}	2.3441×10^{-1}	1.6559×10^{-1}	2.0860×10^{-1}	-9.3548×10^{-1}	8.6237×10^{-1}	-8.8387×10^{-1}	-4.4516×10^{-1}
F11	-5.8710×10^{-1}	6.2151×10^{-1}	-1.0000×10^{0}	-9.9570×10^{-1}	-1.0000×10^{0}	-1.4839×10^{-1}	2.1505×10^{-3}	-9.3548×10^{-1}	-1.6559×10^{-1}	-1.0000×10^{0}	-1.0000×10^{0}
F12	1.1828×10^{-1}	-7.8495×10^{-1}	-1.0000×10^{0}	-6.7742×10^{-1}	-1.0000×10^{0}	-7.6774×10^{-1}	1.0000×10^{0}	-1.0000×10^{0}	-7.9785×10^{-1}	-1.0000×10^{0}	-1.0000×10^{0}
F13	6.2366×10^{-2}	-7.5484×10^{-1}	-1.0000×10^{0}	2.6022×10^{-1}	-1.0000×10^{0}	-6.8172×10^{-1}	6.7312×10^{-1}	-9.9570×10^{-1}	-9.9570×10^{-1}	-1.0000×10^{0}	-9.9140×10^{-1}
F14	-1.0000×10^{0}	-1.0000×10^{0}	-1.0000×10^{0}	-1.0000×10^{0}	-1.0000×10^{0}	-9.8710×10^{-1}	-8.5806×10^{-1}	-1.0000×10^{0}	-1.0000×10^{0}	-1.0000×10^{0}	-1.0000×10^{0}
F15	6.5161×10^{-1}	-3.2043×10^{-1}	6.5161×10^{-1}	9.4839×10^{-1}	-1.0000×10^{0}	6.6452×10^{-1}	4.3656×10^{-1}	-1.0538×10^{-1}	-7.2903×10^{-1}	-1.0000×10^{0}	-5.6129×10^{-1}
F16	-7.5054×10^{-1}	-6.9892×10^{-1}	1.5699×10^{-1}	-4.5806×10^{-1}	-7.6774×10^{-1}	-6.0860×10^{-1}	-4.1075×10^{-1}	-5.3763×10^{-2}	2.8172×10^{-1}	3.7204×10^{-1}	-9.8710×10^{-1}
F17	-9.3118×10^{-1}	-7.0323×10^{-1}	2.6452×10^{-1}	-3.2043×10^{-1}	-8.5376×10^{-1}	-8.5806×10^{-1}	-9.8710×10^{-1}	-4.1075×10^{-1}	-1.3118×10^{-1}	-3.9785×10^{-1}	-9.4409×10^{-1}
F18	-6.7312×10^{-1}	2.1505×10^{-3}	-1.0000×10^{0}	-1.0000×10^{0}	-1.0000×10^{0}	-7.4624×10^{-1}	5.7849×10^{-1}	-9.6129×10^{-1}	-1.0000×10^{0}	-9.8710×10^{-1}	-1.0000×10^{0}
F19	-2.6452×10^{-1}	-9.9140×10^{-1}	-6.4731×10^{-1}	-2.9462×10^{-1}	-9.9570×10^{-1}	-6.7742×10^{-1}	-2.4301×10^{-1}	-9.9570×10^{-1}	-9.2688×10^{-1}	-1.0000×10^{0}	-1.0000×10^{0}
F20	-6.7742×10^{-1}	-3.8065×10^{-1}	3.7204×10^{-1}	-5.1828×10^{-1}	-4.7097×10^{-1}	-6.6882×10^{-1}	-7.7204×10^{-1}	-7.9785×10^{-1}	-1.4409×10^{-1}	-3.3333×10^{-1}	-8.7957×10^{-1}
F21	-1.0000×10^{0}	-1.0000×10^{0}	-1.0000×10^{0}	-1.0000×10^{0}	-1.0000×10^{0}	-1.0000×10^{0}	-1.0000×10^{0}	-9.8280×10^{-1}	-9.9140×10^{-1}	-9.6559×10^{-1}	-1.0000×10^{0}
F22	-6.0430×10^{-1}	5.8065×10^{-2}	2.6882×10^{-1}	-1.0000×10^{0}	-2.0000×10^{-1}	-3.6559×10^{-2}	-5.2688×10^{-1}	-9.3978×10^{-1}	6.7312×10^{-1}	-7.6774×10^{-1}	-8.7957×10^{-1}
F23	-1.0000×10^{0}	-1.0000×10^{0}	-1.0000×10^{0}	-1.0000×10^{0}	-1.0000×10^{0}	-1.0000×10^{0}	-1.0000×10^{0}	-1.0000×10^{0}	-1.0000×10^{0}	-7.2473×10^{-1}	-1.0000×10^{0}
F24	-1.0000×10^{0}	-1.0000×10^{0}	-1.0000×10^{0}	-1.0000×10^{0}	-1.0000×10^{0}	-1.0000×10^{0}	-1.0000×10^{0}	-1.0000×10^{0}	-9.7849×10^{-1}	-4.3226×10^{-1}	-1.0000×10^{0}
F25	-1.0000×10^{0}	-9.8280×10^{-1}	-1.0000×10^{0}	-1.0000×10^{0}	-9.8280×10^{-1}	-9.3118×10^{-1}	7.9570×10^{-2}	-1.0000×10^{0}	-8.5376×10^{-1}	-1.0000×10^{0}	-1.0000×10^{0}
F26	-1.0000×10^{0}	-1.0000×10^{0}	-1.0000×10^{0}	-8.9677×10^{-1}	-1.0000×10^{0}	-8.5376×10^{-1}	-9.0108×10^{-1}	-1.0000×10^{0}	-9.1398×10^{-1}	-8.4086×10^{-1}	-1.0000×10^{0}
F27	-9.9570×10^{-1}	-1.0000×10^{0}	-1.0000×10^{0}	-4.7957×10^{-1}	-9.6129×10^{-1}	-1.0000×10^{0}	-9.4409×10^{-1}	-1.0000×10^{0}	-6.2366×10^{-2}	3.9785×10^{-1}	-1.0000×10^{0}
F28	-8.6237×10^{-1}	-9.4839×10^{-1}	-1.0000×10^{0}	-1.0000×10^{0}	-9.7419×10^{-1}	-8.9247×10^{-1}	9.5699×10^{-1}	-1.0000×10^{0}	-6.5591×10^{-1}	-1.0000×10^{0}	-9.9570×10^{-1}
F29	-9.6989×10^{-1}	-9.8710×10^{-1}	-5.6129×10^{-1}	8.1075×10^{-1}	-8.9247×10^{-1}	-1.0000×10^{0}	-9.0108×10^{-1}	-7.1183×10^{-1}	-2.7312×10^{-1}	7.7204×10^{-1}	-1.0000×10^{0}
F30	1.0000×10^{0}	-1.0000×10^{0}	-8.2366×10^{-1}	1.0000×10^{0}	-1.0000×10^{0}	-1.0000×10^{0}	1.0000×10^{0}	-1.0000×10^{0}	-1.0000×10^{0}	-1.0000×10^{0}	-1.0000×10^{0}

Table A8. EffectSize-values for various algorithms on the CEC 2017 (dim = 100).

Item	INFO	RUN	GRO	ESC	RIME	GKSO	RTH	FTO	BBO	IGWO	EDOA
F1	-1.0000×10^{0}	-1.0000×10^{0}	-1.0000×10^{0}	-1.0000×10^{0}	-1.0000×10^{0}	-1.0000×10^{0}	1.0000×10^{0}	-1.0000×10^{0}	-1.0000×10^{0}	-1.0000×10^{0}	-1.0000×10^{0}
F2	-1.0000×10^{0}	-1.0000×10^{0}	-1.0000×10^{0}	-1.0000×10^{0}	-1.0000×10^{0}	-9.7419×10^{-1}	6.2581×10^{-1}	-1.0000×10^{0}	6.6022×10^{-1}	-9.0538×10^{-1}	-1.0000×10^{0}
F3	-9.1828×10^{-1}	-9.1398×10^{-1}	-1.0000×10^{0}	-1.0000×10^{0}	-1.0000×10^{0}	-5.3978×10^{-1}	1.0000×10^{0}	-1.0000×10^{0}	-1.0000×10^{0}	-1.0000×10^{0}	-1.0000×10^{0}
F4	-1.0000×10^{0}	-9.9140×10^{-1}	-1.0000×10^{0}	-1.0000×10^{0}	-9.9570×10^{-1}	-9.8280×10^{-1}	9.0538×10^{-1}	-1.0000×10^{0}	-9.2473×10^{-2}	-1.0000×10^{0}	-1.0000×10^{0}
F5	-1.0000×10^{0}	-1.0000×10^{0}	-1.0000×10^{0}	-1.0000×10^{0}	-1.0000×10^{0}	-1.0000×10^{0}	-1.0000×10^{0}	-1.0000×10^{0}	-1.0000×10^{0}	-1.0000×10^{0}	-1.0000×10^{0}
F6	-1.0000×10^{0}	-1.0000×10^{0}	-1.0000×10^{0}	9.1828×10^{-1}	-1.0000×10^{0}	-1.0000×10^{0}	-1.0000×10^{0}	-1.0000×10^{0}	-1.0000×10^{0}	-9.3548×10^{-1}	-1.0000×10^{0}
F7	-1.0000×10^{0}	-1.0000×10^{0}	-1.0000×10^{0}	-1.0000×10^{0}	-1.0000×10^{0}	-1.0000×10^{0}	-1.0000×10^{0}	-1.0000×10^{0}	-1.0000×10^{0}	-9.8710×10^{-1}	-1.0000×10^{0}
F8	-1.0000×10^{0}	-1.0000×10^{0}	-1.0000×10^{0}	-1.0000×10^{0}	-1.0000×10^{0}	-1.0000×10^{0}	-1.0000×10^{0}	-1.0000×10^{0}	-1.0000×10^{0}	-9.9570×10^{-1}	-1.0000×10^{0}
F9	-1.0000×10^{0}	-1.0000×10^{0}	-1.0000×10^{0}	-4.0860×10^{-2}	-1.0000×10^{0}	-1.0000×10^{0}	-1.0000×10^{0}	-1.0000×10^{0}	-1.0000×10^{0}	-1.0000×10^{0}	-1.0000×10^{0}
F10	-4.8817×10^{-1}	1.9140×10^{-1}	-1.0000×10^{0}	-1.0000×10^{0}	-9.7419×10^{-1}	-1.9140×10^{-1}	-7.9570×10^{-2}	-1.0000×10^{0}	6.5161×10^{-1}	-9.6129×10^{-1}	-9.1828×10^{-1}
F11	9.8710×10^{-1}	1.0000×10^{0}	-1.0000×10^{0}	-1.0000×10^{0}	2.4301×10^{-1}	1.0000×10^{0}	1.0000×10^{0}	4.7527×10^{-1}	1.0000×10^{0}	5.8710×10^{-1}	5.3548×10^{-1}
F12	-9.4839×10^{-1}	-1.0000×10^{0}	-1.0000×10^{0}	-1.0000×10^{0}	-1.0000×10^{0}	-1.0000×10^{0}	1.0000×10^{0}	-1.0000×10^{0}	-9.9570×10^{-1}	-1.0000×10^{0}	-1.0000×10^{0}
F13	-1.0000×10^{0}	-1.0000×10^{0}	-1.0000×10^{0}	-1.0000×10^{0}	-1.0000×10^{0}	-1.0000×10^{0}	-2.8172×10^{-1}	-1.0000×10^{0}	-1.0000×10^{0}	-1.0000×10^{0}	-1.0000×10^{0}

Table A8. *Cont.*

Item	INFO	RUN	GRO	ESC	RIME	GKSO	RTH	FTO	BBO	IGWO	EDOA
F14	-6.6882×10^{-1}	8.0215×10^{-1}	-1.0000×10^{0}	-1.0000×10^{0}	-1.0000×10^{0}	2.4301×10^{-1}	1.0000×10^{0}	-9.6559×10^{-1}	-1.0000×10^{0}	-9.8710×10^{-1}	-1.0000×10^{0}
F15	-7.4194×10^{-1}	-1.0000×10^{0}	-1.0000×10^{0}	-9.8710×10^{-1}	-1.0000×10^{0}	-9.9570×10^{-1}	-3.1613×10^{-1}	-1.0000×10^{0}	-1.0000×10^{0}	-1.0000×10^{0}	-1.0000×10^{0}
F16	-6.3871×10^{-1}	-8.2796×10^{-1}	-9.4839×10^{-1}	-9.9570×10^{-1}	-9.6989×10^{-1}	-8.3656×10^{-1}	-5.1398×10^{-1}	-9.0108×10^{-1}	-2.6022×10^{-1}	4.9462×10^{-2}	-1.0000×10^{0}
F17	-8.5376×10^{-1}	-8.6667×10^{-1}	-1.0108×10^{-1}	-9.6989×10^{-1}	-9.1398×10^{-1}	-7.3763×10^{-1}	-8.2796×10^{-1}	-5.1398×10^{-1}	5.3763×10^{-2}	5.2688×10^{-1}	-9.6989×10^{-1}
F18	-1.0753×10^{-2}	9.0108×10^{-1}	-1.0000×10^{0}	-1.0000×10^{0}	-1.0000×10^{0}	2.7742×10^{-1}	9.3118×10^{-1}	-1.0000×10^{0}	-9.5269×10^{-1}	-9.7849×10^{-1}	-1.0000×10^{0}
F19	-5.3978×10^{-1}	-1.0000×10^{0}	-1.0000×10^{0}	-9.8280×10^{-1}	-1.0000×10^{0}	-1.0000×10^{0}	1.2688×10^{-1}	-1.0000×10^{0}	-1.0000×10^{0}	-1.0000×10^{0}	-1.0000×10^{0}
F20	-5.2258×10^{-1}	1.3978×10^{-1}	5.0108×10^{-1}	-9.6129×10^{-1}	-4.0215×10^{-1}	-2.4731×10^{-1}	-1.5269×10^{-1}	-5.6129×10^{-1}	4.1075×10^{-1}	-6.6882×10^{-1}	-8.1935×10^{-1}
F21	-1.0000×10^{0}	-1.0000×10^{0}	-1.0000×10^{0}	-1.0000×10^{0}	-1.0000×10^{0}	-1.0000×10^{0}	-1.0000×10^{0}	-9.9570×10^{-1}	-9.9140×10^{-1}	-1.0000×10^{0}	-1.0000×10^{0}
F22	-8.7097×10^{-1}	-8.1075×10^{-1}	-9.3548×10^{-1}	-1.0000×10^{0}	-1.0000×10^{0}	-6.6882×10^{-1}	-3.9785×10^{-1}	-1.0000×10^{0}	-9.6774×10^{-2}	-9.6129×10^{-1}	-9.4839×10^{-1}
F23	-1.0000×10^{0}	-1.0000×10^{0}	-1.0000×10^{0}	-4.6237×10^{-1}	-1.0000×10^{0}	-1.0000×10^{0}	-1.0000×10^{0}	-1.0000×10^{0}	-1.0000×10^{0}	-9.7849×10^{-1}	-1.0000×10^{0}
F24	-1.0000×10^{0}	-1.0000×10^{0}	-1.0000×10^{0}	-1.0000×10^{0}	-1.0000×10^{0}	-1.0000×10^{0}	-1.0000×10^{0}	-1.0000×10^{0}	-1.0000×10^{0}	-9.4839×10^{-1}	-1.0000×10^{0}
F25	-1.0000×10^{0}	-1.0000×10^{0}	-1.0000×10^{0}	-1.0000×10^{0}	-1.0000×10^{0}	-1.0000×10^{0}	9.7419×10^{-1}	-1.0000×10^{0}	2.5161×10^{-1}	-1.0000×10^{0}	-1.0000×10^{0}
F26	-1.0000×10^{0}	-1.0000×10^{0}	-1.0000×10^{0}	-9.9140×10^{-1}	-1.0000×10^{0}	-1.0000×10^{0}	-1.0000×10^{0}	-1.0000×10^{0}	-9.1828×10^{-1}	-9.9140×10^{-1}	-1.0000×10^{0}
F27	-1.0000×10^{0}	-1.0000×10^{0}	-1.0000×10^{0}	-9.6989×10^{-1}	-9.9570×10^{-1}	-1.0000×10^{0}	-9.9570×10^{-1}	-1.0000×10^{0}	-8.5806×10^{-1}	-7.1613×10^{-1}	-1.0000×10^{0}
F28	-1.0000×10^{0}	-9.8710×10^{-1}	-1.0000×10^{0}	-1.0000×10^{0}	-1.0000×10^{0}	-9.2688×10^{-1}	1.0000×10^{0}	-1.0000×10^{0}	8.1505×10^{-1}	-1.0000×10^{0}	-1.0000×10^{0}
F29	-9.4409×10^{-1}	-1.0000×10^{0}	-9.9570×10^{-1}	-3.0753×10^{-1}	-1.0000×10^{0}	-1.0000×10^{0}	-4.0860×10^{-2}	-9.9570×10^{-1}	-6.4301×10^{-1}	5.2258×10^{-1}	-1.0000×10^{0}
F30	-9.3978×10^{-1}	-1.0000×10^{0}	-1.0000×10^{0}	-1.0000×10^{0}	-1.0000×10^{0}	-1.0000×10^{0}	1.0000×10^{0}	-1.0000×10^{0}	-1.0000×10^{0}	-1.0000×10^{0}	-1.0000×10^{0}

Table A9. EffectSize-values for various algorithms on the CEC 2020 (dim = 10).

Item	INFO	RUN	GRO	ESC	RIME	GKSO	RTH	FTO	BBO	IGWO	EDOA
F1	1.0000×10^{0}	-9.9570×10^{-1}	-1.0000×10^{0}	-9.6559×10^{-1}	-1.0000×10^{0}	-9.9570×10^{-1}	-8.1505×10^{-1}	-1.0000×10^{0}	-9.7849×10^{-1}	-1.0000×10^{0}	-1.0000×10^{0}
F2	-7.7634×10^{-1}	-7.3333×10^{-1}	-2.0430×10^{-1}	1.2688×10^{-1}	1.3548×10^{-1}	-9.3118×10^{-1}	-9.6989×10^{-1}	-7.5914×10^{-1}	-3.6774×10^{-1}	-6.4516×10^{-3}	-9.5699×10^{-1}
F3	-9.9140×10^{-1}	-1.0000×10^{0}	-7.4194×10^{-1}	-4.0215×10^{-1}	-8.4516×10^{-1}	-9.5269×10^{-1}	-9.9570×10^{-1}	-9.3118×10^{-1}	-7.9355×10^{-1}	-7.7634×10^{-1}	-9.1398×10^{-1}
F4	-5.5699×10^{-1}	-9.5269×10^{-1}	1.9355×10^{-2}	-9.1398×10^{-1}	-8.7527×10^{-1}	-6.3011×10^{-1}	-9.8280×10^{-1}	-7.0323×10^{-1}	1.0753×10^{-2}	-1.0000×10^{0}	-9.1398×10^{-1}
F5	-9.9140×10^{-1}	-1.0000×10^{0}	-1.0000×10^{0}	-1.0000×10^{0}	-1.0000×10^{0}	-9.8280×10^{-1}	-9.8710×10^{-1}	-9.9570×10^{-1}	-1.0000×10^{0}	-1.0000×10^{0}	-1.0000×10^{0}
F6	-9.8710×10^{-1}	-9.7849×10^{-1}	-8.6237×10^{-1}	-6.6667×10^{-2}	-9.5699×10^{-1}	-9.3548×10^{-1}	-1.0000×10^{0}	-9.6989×10^{-1}	-9.6989×10^{-1}	-1.0000×10^{0}	-1.0000×10^{0}
F7	-9.4409×10^{-1}	-9.9140×10^{-1}	-1.0000×10^{0}	-9.7419×10^{-1}	-9.9570×10^{-1}	-7.5054×10^{-1}	-9.8280×10^{-1}	-9.9140×10^{-1}	-1.0000×10^{0}	-1.0000×10^{0}	-1.0000×10^{0}
F8	-9.7849×10^{-1}	-8.9247×10^{-1}	-3.7634×10^{-1}	-1.0753×10^{-2}	-6.8602×10^{-1}	-8.8817×10^{-1}	-7.0323×10^{-1}	-7.4194×10^{-1}	-9.8280×10^{-1}	-1.0000×10^{0}	-9.9140×10^{-1}
F9	-8.7527×10^{-1}	-6.3441×10^{-1}	4.3656×10^{-1}	-8.8172×10^{-2}	-9.0108×10^{-1}	-3.1613×10^{-1}	-7.6344×10^{-1}	-6.1720×10^{-1}	4.5161×10^{-2}	-1.0753×10^{-2}	-5.9570×10^{-1}
F10	-9.0968×10^{-1}	-7.8925×10^{-1}	-6.2151×10^{-1}	-9.0968×10^{-1}	-8.2796×10^{-1}	-9.4409×10^{-1}	-7.8925×10^{-1}	-8.5376×10^{-1}	-8.1505×10^{-1}	2.7742×10^{-1}	-8.3226×10^{-1}

Table A10. EffectSize-values for various algorithms on the CEC 2020 (dim = 20).

Item	INFO	RUN	GRO	ESC	RIME	GKSO	RTH	FTO	BBO	IGWO	EDOA
F1	1.0000×10^{0}	-6.3441×10^{-1}	-1.0000×10^{0}	-9.0538×10^{-1}	-1.0000×10^{0}	-9.0968×10^{-1}	-8.8387×10^{-1}	-1.0000×10^{0}	-1.0000×10^{0}	-1.0000×10^{0}	-1.0000×10^{0}
F2	-1.1828×10^{-1}	3.4624×10^{-1}	1.5269×10^{-1}	4.0215×10^{-1}	8.5376×10^{-1}	-8.7097×10^{-1}	-6.6882×10^{-1}	3.3763×10^{-1}	2.6022×10^{-1}	-9.5269×10^{-1}	-9.5269×10^{-1}
F3	-1.0000×10^{0}	-1.0000×10^{0}	-1.0000×10^{0}	-4.0215×10^{-1}	-9.9570×10^{-1}	-1.0000×10^{0}	-1.0000×10^{0}	-1.0000×10^{0}	-9.8710×10^{-1}	-8.4516×10^{-1}	-1.0000×10^{0}
F4	-9.6129×10^{-1}	-1.0000×10^{0}	-7.5914×10^{-1}	-8.1075×10^{-1}	-7.8495×10^{-1}	-8.2366×10^{-1}	-1.0000×10^{0}	-5.0538×10^{-1}	3.4194×10^{-1}	-1.0000×10^{0}	-1.0000×10^{0}
F5	-9.9140×10^{-1}	-1.0000×10^{0}	-1.0000×10^{0}	-1.0000×10^{0}	-1.0000×10^{0}	-9.8710×10^{-1}	-9.2688×10^{-1}	-1.0000×10^{0}	-1.0000×10^{0}	-1.0000×10^{0}	-1.0000×10^{0}
F6	-8.7527×10^{-1}	-9.5269×10^{-1}	-6.3011×10^{-1}	6.9462×10^{-1}	-7.8065×10^{-1}	-9.7849×10^{-1}	-1.0000×10^{0}	-7.9355×10^{-1}	-9.8710×10^{-1}	-8.5806×10^{-1}	-1.0000×10^{0}
F7	-9.3118×10^{-1}	-1.0000×10^{0}	-1.0000×10^{0}	-1.0000×10^{0}	-1.0000×10^{0}	-1.0000×10^{0}	-2.1290×10^{-1}	-9.9570×10^{-1}	-1.0000×10^{0}	-1.0000×10^{0}	-1.0000×10^{0}
F8	-7.1613×10^{-1}	-1.0000×10^{0}	-1.0000×10^{0}	-1.0000×10^{0}	-1.0000×10^{0}	-9.9140×10^{-1}	-7.1613×10^{-1}	-1.0000×10^{0}	-1.0000×10^{0}	-1.0000×10^{0}	-1.0000×10^{0}
F9	-1.0000×10^{0}	-9.1828×10^{-1}	-1.7849×10^{-1}	-9.0968×10^{-1}	-9.2258×10^{-1}	-9.9570×10^{-1}	-1.0000×10^{0}	-6.1290×10^{-1}	-1.1828×10^{-1}	1.2258×10^{-1}	-7.5484×10^{-1}
F10	-8.8817×10^{-1}	-9.7419×10^{-1}	-9.8710×10^{-1}	4.9462×10^{-2}	-6.8602×10^{-1}	-8.5806×10^{-1}	-9.0108×10^{-1}	-1.0000×10^{0}	-8.2796×10^{-1}	-6.4731×10^{-1}	-1.0000×10^{0}

References

1. Abualigah, L.; Elaziz, M.A.; Khasawneh, A.M.; Alshinwan, M.; Ibrahim, R.A.; Al-Qaness, M.A.; Mirjalili, S.; Sumari, P.; Gandomi, A.H. Meta-Heuristic Optimization Algorithms for Solving Real-World Mechanical Engineering Design Problems: A Comprehensive Survey, Applications, Comparative Analysis, and Results. *Neural Comput. Appl.* **2022**, *34*, 4081–4110.
2. Guo, Y.; Zhang, W.; Qin, Q.; Chen, K.; Wei, Y. Intelligent Manufacturing Management System Based on Data Mining in Artificial Intelligence Energy-Saving Resources. *Soft Comput.* **2023**, *27*, 4061–4076.
3. Liu, Y.-F.; Chang, T.-H.; Hong, M.; Wu, Z.; So, A.M.-C.; Jorswieck, E.A.; Yu, W. A Survey of Recent Advances in Optimization Methods for Wireless Communications. *IEEE J. Sel. Areas Commun.* **2024**, *42*, 2992–3031. [CrossRef]
4. Thirunavukkarasu, G.S.; Seyedmahmoudian, M.; Jamei, E.; Horan, B.; Mekhilef, S.; Stojcevski, A. Role of Optimization Techniques in Microgrid Energy Management Systems—A Review. *Energy Strategy Rev.* **2022**, *43*, 100899. [CrossRef]
5. Chinchanikar, S.; Shaikh, A.A. A Review on Machine Learning, Big Data Analytics, and Design for Additive Manufacturing for Aerospace Applications. *J. Mater. Eng. Perform.* **2022**, *31*, 6112–6130. [CrossRef]
6. Abdulkadirov, R.; Lyakhov, P.; Nagornov, N. Survey of Optimization Algorithms in Modern Neural Networks. *Mathematics* **2023**, *11*, 2466. [CrossRef]
7. Sumiea, E.H.; Abdulkadir, S.J.; Alhussian, H.S.; Al-Selwi, S.M.; Alqushaibi, A.; Ragab, M.G.; Fati, S.M. Deep Deterministic Policy Gradient Algorithm: A Systematic Review. *Heliyon* **2024**, *10*, e30697. [CrossRef] [PubMed]
8. Sharma, V.; Tripathi, A.K. A Systematic Review of Meta-Heuristic Algorithms in IoT Based Application. *Array* **2022**, *14*, 100164.
9. Yu, M.; Xu, J.; Liang, W.; Qiu, Y.; Bao, S.; Tang, L. Improved Multi-Strategy Adaptive Grey Wolf Optimization for Practical Engineering Applications and High-Dimensional Problem Solving. *Artif. Intell. Rev.* **2024**, *57*, 277. [CrossRef]
10. Braik, M.; Ryalat, M.H.; Al-Zoubi, H. A Novel Meta-Heuristic Algorithm for Solving Numerical Optimization Problems: Ali Baba and the Forty Thieves. *Neural Comput. Appl.* **2022**, *34*, 409–455.
11. El-Kenawy, E.-S.M.; Mirjalili, S.; Alassery, F.; Zhang, Y.-D.; Eid, M.M.; El-Mashad, S.Y.; Aloyaydi, B.A.; Ibrahim, A.; Abdelhamid, A.A. Novel Meta-Heuristic Algorithm for Feature Selection, Unconstrained Functions and Engineering Problems. *IEEE Access* **2022**, *10*, 40536–40555. [CrossRef]
12. Yu, M.; Zhang, J.; Yu, L.; Yang, H.; Lu, H.; Wei, X.; Xu, J. Alzheimer's Disease Brain Image Segmentation Using Multi-Feature Fusion in 3D Rényi Entropy Model and Quantum Hybrid Optimization. *Artif. Intell. Rev.* **2026**, *59*, 95. [CrossRef]
13. Zhao, F.; Song, L.; Jiang, T.; Wang, L.; Dong, C. A Policy-Based Meta-Heuristic Algorithm for Energy-Aware Distributed No-Wait Flow-Shop Scheduling in Heterogeneous Factory Systems. *IEEE Trans. Syst. Man. Cybern. Syst.* **2024**, *55*, 620–634.
14. Yu, M.; Du, J.; Xu, X.; Xu, J.; Jiang, F.; Fu, S.; Zhang, J.; Liang, A. A Multi-Strategy Enhanced Dung Beetle Optimization for Real-World Engineering Problems and UAV Path Planning. *Alex. Eng. J.* **2025**, *118*, 406–434. [CrossRef]
15. Xie, M.; Pi, D.; Dai, C.; Xu, Y. A Metaheuristic-Based Algorithm for Optimizing Node Deployment in Wireless Sensor Network. *Neural Comput. Appl.* **2024**, *36*, 13027–13049. [CrossRef]
16. Kennedy, J.; Eberhart, R. Particle Swarm Optimization. In *Proceedings of the ICNN'95—International Conference on Neural Networks, Perth, WA, Australia, 27 November–1 December 1995*; IEEE: Piscataway, NJ, USA, 1995; Volume 4, pp. 1942–1948.
17. Mathew, T.V. Genetic Algorithm. *Rep. Submitt. IIT Bombay* **2012**, *53*, 18–19.
18. Dorigo, M.; Birattari, M.; Stutzle, T. Ant Colony Optimization. *IEEE Comput. Intell. Mag.* **2006**, *1*, 28–39. [CrossRef]
19. Mirjalili, S.; Mirjalili, S.M.; Lewis, A. Grey Wolf Optimizer. *Adv. Eng. Softw.* **2014**, *69*, 46–61. [CrossRef]
20. Yu, M.; Yang, H.; Zhang, J.; Ouyang, K.; Fu, S.; Tan, P.; Jiang, F.; Xu, J. Bounty Hunter Optimizer: A Novel Metaheuristic with an Application to Multi-UAV Mobile Edge Computing and Path Planning. *Knowl.-Based Syst.* **2026**, *341*, 115836. [CrossRef]
21. Cheng, J.; De Waele, W. Detective Behavior Algorithm (DBA): A New Metaheuristic for Design and Engineering Optimization. *Knowl.-Based Syst.* **2026**, *338*, 115434. [CrossRef]
22. Taheri, A.; RahimiZadeh, K.; Baumbach, J.; Beheshti, A.; Zolotareva, O.; Al-Betar, M.A.; Mirjalili, S.; Gandomi, A.H. Farthest Better or Nearest Worse Optimizer: A Novel Metaheuristic Algorithm. *Artif. Intell. Rev.* **2026**, *59*, 79. [CrossRef]
23. Braik, M.; Al-Hiary, H.; Alzoubi, H.; Hammouri, A.; Azmi Al-Betar, M.; Awadallah, M.A. Tornado Optimizer with Coriolis Force: A Novel Bio-Inspired Meta-Heuristic Algorithm for Solving Engineering Problems. *Artif. Intell. Rev.* **2025**, *58*, 123. [CrossRef]
24. Xiao, Y.; Cui, H.; Khurma, R.A.; Castillo, P.A. Artificial Lemming Algorithm: A Novel Bionic Meta-Heuristic Technique for Solving Real-World Engineering Optimization Problems. *Artif. Intell. Rev.* **2025**, *58*, 84.
25. Yu, M.; Yang, H.; Wei, X.; Fu, S.; Xu, J.; Zhang, J. Carbon Footprint Efficiency Ratio: A Unified Indicator for Green Evaluation of Evolutionary Algorithms. *IEEE Trans. Emerg. Top. Comput. Intell.* **2026**, 1–14. [CrossRef]
26. Xie, C.; Li, S.; Qin, X.; Fu, S.; Zhang, X. Multiple Elite Strategy Enhanced RIME Algorithm for 3D UAV Path Planning. *Sci. Rep.* **2024**, *14*, 21734. [CrossRef] [PubMed]
27. Lu, Z.; Wang, C.; Wang, P.; Xu, W. 3D Deployment Optimization of Wireless Sensor Networks for Heterogeneous Functional Nodes. *Sensors* **2025**, *25*, 1366. [CrossRef] [PubMed]
28. Truong, D.-N.; Chou, J.-S. Metaheuristic Algorithm Inspired by Enterprise Development for Global Optimization and Structural Engineering Problems with Frequency Constraints. *Eng. Struct.* **2024**, *318*, 118679. [CrossRef]

29. Zhao, D.; Feng, L.; Wang, Y.; Cai, X.; Liu, X. An Improved Enterprise Development Optimizer Based on Labor Migration for Numerical Optimization. *Sci. Rep.* **2025**, *15*, 26227. [CrossRef] [PubMed]
30. Cai, X.; Wang, W.; Wang, Y. Multi-Strategy Enterprise Development Optimizer for Numerical Optimization and Constrained Problems. *Sci. Rep.* **2025**, *15*, 10538. [CrossRef] [PubMed]
31. Li, Z.; Liao, Y.; Zhou, H. Improved Enterprise Development Optimization with Historical Trend Updating for High-Precision Photovoltaic Model Parameter Estimation. *Mathematics* **2026**, *14*, 121. [CrossRef]
32. Wu, G.; Mallipeddi, R.; Suganthan, P.N. *Problem Definitions and Evaluation Criteria for the CEC 2017 Competition on Constrained Real-Parameter Optimization*; Technical Report; National University of Defense Technology: Changsha, China; Kyungpook National University: Daegu, Republic of Korea; Nanyang Technological University: Singapore, 2017; Volume 9, pp. 1–16.
33. Mohamed, A.W.; Hadi, A.A.; Mohamed, A.K.; Awad, N.H. *Evaluating the Performance of Adaptive Gainingsharing Knowledge Based Algorithm on CEC 2020 Benchmark Problems*; IEEE: Piscataway, NJ, USA, 2020; pp. 1–8.
34. Ahmadianfar, I.; Heidari, A.A.; Noshadian, S.; Chen, H.; Gandomi, A.H. INFO: An Efficient Optimization Algorithm Based on Weighted Mean of Vectors. *Expert Syst. Appl.* **2022**, *195*, 116516. [CrossRef]
35. Ahmadianfar, I.; Heidari, A.A.; Gandomi, A.H.; Chu, X.; Chen, H. RUN beyond the Metaphor: An Efficient Optimization Algorithm Based on Runge Kutta Method. *Expert Syst. Appl.* **2021**, *181*, 115079. [CrossRef]
36. Zolfi, K. Gold Rush Optimizer: A New Population-Based Metaheuristic Algorithm. *Oper. Res. Decis.* **2023**, *33*, 113–150. [CrossRef]
37. Ouyang, K.; Fu, S.; Chen, Y.; Cai, Q.; Heidari, A.A.; Chen, H. Escape: An Optimization Method Based on Crowd Evacuation Behaviors. *Artif. Intell. Rev.* **2024**, *58*, 19. [CrossRef]
38. Su, H.; Zhao, D.; Heidari, A.A.; Liu, L.; Zhang, X.; Mafarja, M.; Chen, H. RIME: A Physics-Based Optimization. *Neurocomputing* **2023**, *532*, 183–214. [CrossRef]
39. Hu, G.; Guo, Y.; Wei, G.; Abualigah, L. Genghis Khan Shark Optimizer: A Novel Nature-Inspired Algorithm for Engineering Optimization. *Adv. Eng. Inform.* **2023**, *58*, 102210. [CrossRef]
40. Ferahtia, S.; Houari, A.; Rezk, H.; Djerioui, A.; Machmoum, M.; Motahhir, S.; Ait-Ahmed, M. Red-Tailed Hawk Algorithm for Numerical Optimization and Real-World Problems. *Sci. Rep.* **2023**, *13*, 12950. [PubMed]
41. Saad, M.R.; Emam, M.M.; Hosney, M.E.; Samee, N.A.; Alkanhel, R.I.; Houssein, E.H. Fourier Transform Optimizer: A Novel Physics-Inspired Metaheuristic Algorithm for Optimization Problems. *Knowl.-Based Syst.* **2026**, *340*, 115651. [CrossRef]
42. Ouyang, K.; Wei, D.; Sha, X.; Yu, J.; Zhao, Y.; Qiu, M.; Fu, S.; Heidari, A.A.; Chen, H. Beaver Behavior Optimizer: A Novel Metaheuristic Algorithm for Solar PV Parameter Identification and Engineering Problems. *J. Adv. Res.* **2026**, *84*, 525–555. [CrossRef] [PubMed]
43. Nadimi-Shahraki, M.H.; Taghian, S.; Mirjalili, S. An Improved Grey Wolf Optimizer for Solving Engineering Problems. *Expert Syst. Appl.* **2021**, *166*, 113917. [CrossRef]
44. Okoye, K.; Hosseini, S. Wilcoxon Statistics in R: Signed-Rank Test and Rank-Sum Test. In *R Programming: Statistical Data Analysis in Research*; Springer: Berlin/Heidelberg, Germany, 2024; pp. 279–303.
45. Cao, T.; Yang, F.; Fan, C.; Han, R.; Yang, X.; Shu, L. A Survey of Three-Dimensional Wireless Sensor Networks Deployment Techniques. *J. Sens. Actuator Netw.* **2025**, *14*, 94. [CrossRef]
46. Tan, L.; Liu, Y.; Zhang, H.; Yuan, T.; Shang, Z.; Jiang, X. 3dSN-SSA: Wireless Sensor Network Deployment of 3D Surface Based on Improved Sparrow Search Algorithm. *Wirel. Netw.* **2025**, *31*, 4637–4648.
47. Muthusamy, S.; Ruby, E.D.K.; Arunachalam, R.; Chinnappa, K. An Improved Distance Vector Hop Algorithm and A* Algorithm with Modified Supernova Optimizer for 3-Dimensional Localization in Wireless Sensor Networks. *Wirel. Netw.* **2025**, *31*, 2827–2846. [CrossRef]

Disclaimer/Publisher's Note: The statements, opinions and data contained in all publications are solely those of the individual author(s) and contributor(s) and not of MDPI and/or the editor(s). MDPI and/or the editor(s) disclaim responsibility for any injury to people or property resulting from any ideas, methods, instructions or products referred to in the content.